



Flexible Hydrogen Production

*A Comprehensive Study on Optimizing Cost-Efficient Combinations of
Production and Storage Capacity to Exploit Electricity Price Fluctuations*

Lars Skaugen Strømholm and Raag August Sandal Rolfsen

Supervisor: Endre Bjørndal and Mette Bjørndal

Master thesis, Economics and Business Administration

Major: Business Analytics

NORWEGIAN SCHOOL OF ECONOMICS

This thesis was written as a part of the Master of Science in Economics and Business Administration at NHH. Please note that neither the institution nor the examiners are responsible – through the approval of this thesis – for the theories and methods used, or results and conclusions drawn in this work.

Acknowledgements

This thesis was written as part of our master's degree at the Norwegian School of Economics (NHH). It has been an exciting and educational process, and we would like to thank those who helped us along the way.

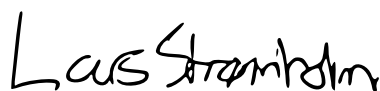
We want to start by dedicating a special thanks to our supervisors – Endre Bjørndal and Mette Bjørndal, for helping us throughout the process of writing our thesis. First, for guiding us in the choice of an exciting research question in which the possibilities for new findings seemed endless. Second, for advising us through the structuring of the thesis. Third, for helping us by sharing their deep understanding both within the fields of energy analysis and decision modeling.

We would also like to give a major thanks to Daniel Janzen from Greensight AS for developing the research question and dedicating several weekends to enhance our understanding of the complex details in hydrogen production and how it relates to the electricity price markets.

Thank you.

Norwegian School of Economics

Bergen, February 2021



Lars Skaguen Strømholm



Raag August Sandal Rolfsen

Abstract

Due to the high costs related to green hydrogen, most of the world's hydrogen today is supplied from grey hydrogen, resulting in a substantial carbon footprint. However, with decreasing capital costs, and the possibility to exploit electricity price fluctuations to reduce production costs, green hydrogen could prove to become a competitive alternative.

This thesis focuses on evaluating the potential to reduce the total cost of hydrogen production stemming from alkaline water electrolysis. The method is based on exploiting electricity price fluctuations through excess production capacity combined with hydrogen storage. A mathematical, multi-period decision model was developed to find the most cost-efficient, long-term production schedule for an on-site, grid-connected production plant. Model results stem from various scenarios representing different horizons and storage options to determine the optimally combined capacities for production and storage. Thus, the effects of plant cost reductions, increased electricity price fluctuations, innovative storage solutions, and improving efficiencies are explored in regard to hydrogen production.

The main findings show that it is costly to exploit electricity price fluctuations to reduce hydrogen costs when obligated to satisfy a required demand. In most cases, the cost of additional production and storage equipment counteracts the benefit of producing in hours of low-cost electricity. However, under certain circumstances, mainly very volatile electricity prices and underground hydrogen storage, hydrogen costs can be reduced through investments in excess production capacity. Additionally, under a special cost structure for grid fees, capacity expansions became substantially more attractive, in which an optimal solution pushed the determined limit for production capacity. In a future scenario, a 36% increase in daily production capacity was observed to be the economically preferred option, which resulted in a production cost reduction of 8.86% and an overall decrease in the levelized cost of hydrogen.

Keywords – Hydrogen, alkaline water electrolysis, flexibility, multi-period optimization, MILP, time series aggregation, electricity price fluctuations, production scheduling

Abbreviations

AEL	Alkaline electrolyzer
AMPL	A Mathematical Programming Language
API	Application programming interface
CAPEX	Capital expenditure
CH₃OH	Methanol
CO₂	Carbon dioxide
e⁻	Electron
EU ETS	European Union Emission Trading System
GW	Gigawatt
H⁺	Proton
HHV	Higher heating value
H₂	Hydrogen
H₂O	Water
kW	Kilowatt
kWh	Kilowatt hours
LaNi₅	Lanthanum-nickel alloy
LCOH	Levelized cost of hydrogen
LH₂	Liquid hydrogen
LHV	Lower heating value
MILP	Mixed-integer linear programming
MINLP	Mixed-integer non-linear programming
MJ	Mega-joule
MW	Megawatt
MWh	Megawatt hours
NO2	Nord Pool region 2, Kristiansand
OPEX	Operational expenditure
O₂	Oxygen
PEM	Polymer electrolyte membrane
SOEC	Solid oxide electrolyzer
WACC	Weighted average cost of capital

Other key elements

Today	A time-horizon starting in 2020.
Medium-term	A time-horizon starting in 2030.
Long-term	A time-horizon starting in 2040.
EURO/NOK	1 EUR to NOK = 10.87.
EURO/USD	1 EUR to USD = 1.176.

Contents

1	Introduction	1
1.1	Background and motivation	2
1.2	Literature review	4
1.3	Scope of the thesis	5
2	Hydrogen	7
2.1	How hydrogen is produced	7
2.2	Water electrolysis technologies	9
2.2.1	Alkaline electrolysis (AEL)	9
2.2.2	Polymer electrolyte membrane electrolysis (PEM)	10
2.2.3	System comparison	11
2.3	Compression, liquefaction, and storage	11
2.3.1	Compression of hydrogen	12
2.3.2	Liquefaction of hydrogen	13
2.3.3	Storage of hydrogen	13
2.4	Applications of hydrogen	15
2.4.1	Material-based hydrogen applications	15
2.4.2	Energy-based hydrogen applications	16
3	Alkaline electrolysis production process	19
3.1	Process overview	19
3.2	Power supply	20
3.3	Water electrolysis	21
3.4	Oxygen and hydrogen separation	22
3.5	Compression	22
3.6	Purification	22
3.7	Storage and application	23
3.8	Production process assumptions	23
4	Data	25
4.1	Electricity price data	25
4.1.1	Raw electricity prices	25
4.1.2	Time series aggregation of electricity price data	27
4.1.3	Data sampling	31
4.2	Plant costs	34
4.2.1	Electrolyzer CAPEX	35
4.2.2	Storage CAPEX	37
4.2.3	Electrolyzer OPEX	39
4.2.4	Storage OPEX	39
4.2.5	Cell-stack replacement	39
4.2.6	Grid fees	40
4.2.7	Electricity consumption	40
4.2.8	Utilization	41
4.2.9	Cold starts and standby	42
4.2.10	Discount rate	42

5	Model	44
5.1	Model introduction	44
5.2	Sets and parameters	46
5.3	Decision variables	49
5.4	Objective function	50
5.4.1	Electrolyzer CAPEX	51
5.4.2	Storage CAPEX	52
5.4.3	Electrolyzer OPEX	52
5.4.4	Storage OPEX	52
5.4.5	Cell-stack replacement	53
5.4.6	Grid fees	53
5.4.7	Production cost	54
5.4.8	Standby costs	55
5.4.9	Cold starts	56
5.4.10	Total costs	56
5.5	Constraints	57
5.5.1	Capacity	57
5.5.2	Storage and inventory balance	58
5.5.3	Production	61
5.5.4	Cold start	62
5.5.5	Non-negativity	64
6	Results	65
6.1	Metrics	65
6.2	Scenario overview	66
6.3	Scenario results	68
6.3.1	Scenario 1	68
6.3.2	Scenario 2	71
6.3.3	Scenario 3	73
6.3.4	Scenario 4	76
6.3.5	Scenario 5	78
6.4	The effect of grid fees on water electrolysis	82
7	Discussion	87
7.1	Limitations and external validity	87
7.2	Further work	89
8	Conclusion	92
	References	93
	Appendix	99
A1	Figures	99
A1.1	Statnett mentions	99
A2	Data	100
A2.1	Statnett estimates	100
A2.2	NVE estimates	100
A3	Parameter comparison	101
A4	CAPEX specifications in scenarios 1-5	104

A4.1	Scenario 1	104
A4.2	Scenario 2	104
A4.3	Scenario 3	105
A4.4	Scenario 4	106
A4.5	Scenario 5	106
A5	LCOH when neglecting grid fees in scenarios 1-5	107
A5.1	Scenario 1	107
A5.2	Scenario 2	107
A5.3	Scenario 3	108
A5.4	Scenario 4	108
A5.5	Scenario 5	108

List of Figures

1.1	Day-ahead prices for NO ₂ on the 10th of December 2020.	3
2.1	Overview of different hydrogen production methods (Shiva Kumar and Himabindu, 2019).	7
2.2	Energy losses for different steps in the hydrogen production chain and transformation back to electricity.	8
2.3	Graphical illustration of AEL (Ziazi et al., 2017).	9
2.4	Graphical illustration of PEM electrolysis (Ziazi et al., 2017).	10
2.5	Gravimetric and volumetric density of different fuels (Mazloomi and Gomes, 2012; Dagdougui et al., 2018).	12
2.6	Illustration of underground hydrogen storage (Tarkowski, 2019).	14
3.1	Illustration of the hydrogen production process using alkaline water electrolysis (NEL, 2019).	19
4.1	Hourly average of electricity prices for Nord Pool NO ₂ region (2013-2019).	28
4.2	Hourly average, filtered by day of the week, of electricity prices for Nord Pool NO ₂ region (2013-2019).	29
4.3	Hourly average, filtered by season, of electricity prices for Nord Pool NO ₂ region (2013-2019).	30
4.4	Representative weeks for winter, spring, summer and fall 2019 for Nord Pool NO ₂ region.	30
4.5	Transformation of the data from original mean to zero mean.	32
4.6	20 year aggregated electricity price scenarios for different time horizons. Top: today. Middle: medium-term (2030). Bottom: long-term (2040).	33
4.7	Economies of scale for an AEL system using Equation 4.1. Based on CAPEX of 750 €/kW for a 2 MW stack, specific energy consumption of 50 kWh/kg, and scaling exponent of 0.85.	37
4.8	Storage CAPEX for different capacities.	38
5.1	Graphical illustration of a case when the storage fills up during a representative period.	60
6.1	LCOH and production cost for different production capacities in scenario 1, given a storage capacity of 3,000 kg.	70
6.2	LCOH and production cost for different production and storage capacities in scenario 2.	72
6.3	LCOH and production cost for different production and storage capacities in scenario 3.	74
6.4	Illustrating the average change in storage during different seasons.	76
6.5	A comparison of LCOH and production costs between scenario 2 and 4.	77
6.6	LCOH and production cost for different production capacities in scenario 5, given a storage capacity of 500,000 kg.	79
6.7	Hourly, weekly average, production schedule and electricity prices in scenario 5.	80
6.8	Stacked LCOH for optimal cases in scenarios 1-5 with and without grid fees.	85
6.9	Left: Number of hours the modeled plant has operated in standby-mode. Right: Number of cold starts performed over the modeled plants lifetime.	86
A1.1	Greensight AS' overview of mentions in Statnett reports.	99
A4.1	Electrolyzer and storage CAPEX based on system size in scenario 1.	104
A4.2	Electrolyzer and storage CAPEX based on system size in scenario 2.	105
A4.3	Electrolyzer and storage CAPEX based on system size in scenario 3.	105

A4.4 Electrolyzer CAPEX based on system size in scenario 4.	106
A4.5 Electrolyzer CAPEX based on system size in scenario 5.	106

List of Tables

4.1	Data structure for electricity prices in 2019.	26
4.2	Summary statistics of electricity prices (€/MWh) for Nord Pool NO2 region in real 2019-values (2013-2019).	27
4.3	Future electricity prices estimates for Southwestern Norway (NO2) from Statnett and NVE (Statnett, 2020; NVE, 2020a).	31
4.4	Summary statistics of electricity price scenarios (€/MWh).	33
5.1	Model sets.	47
5.2	Model parameters.	47
5.3	Continuation of Table 5.2	48
5.4	Continuation of Table 5.2 and Table 5.3.	49
5.5	Model decision variables.	50
6.1	Summary of scenario parameters.	67
6.2	LCOH (€/kg) in scenario 1. Each column represent production capacity (tonne) while each row represent storage capacity (kg).	69
6.3	LCOH (€/kg) in scenario 2. Each column represent production capacity (tonne) while each row represent storage capacity (kg).	71
6.4	LCOH (€/kg) in scenario 3. Each column represent production capacity (tonne) while each row represent storage capacity (kg).	73
6.5	LCOH (€/kg) and production cost (€/kg) in scenario 4 for different production capacities and storage capacity of 500,000 kg.	76
6.6	LCOH (€/kg) and production cost (€/kg) in scenario 5 for different production capacities and storage capacity of 500,000 kg.	78
6.7	Optimal production capacity (tonnes), storage capacity (kg), LCOH (€/kg) and production cost (€/kg) in scenarios 1-5 with and without grid fees.	84
A2.1	Statnett estimations for future electricity price in Nordic regions. Published 26.10.2020 in Statnetts's long term market analysis.	100
A2.2	NVE estimations for future electricity price in Nordic regions. Published 28.10.2020 in NVE's long term power market analysis.	100
A3.1	Overview of alkaline water electrolysis costs and parameters drawn from different studies, reports and organisations. Published year is used in cases where year of estimation is not specified.	101
A3.2	Continuation of Table A3.1.	102
A3.3	Continuation of Table A3.2.	103
A5.1	LCOH (€/kg) in scenario 1 (neglecting grid fees).	107
A5.2	LCOH (€/kg) in scenario 2 (neglecting grid fees).	107
A5.3	LCOH (€/kg) in scenario 3 (neglecting grid fees).	108
A5.4	LCOH (€/kg) in scenario 4 (neglecting grid fees).	108
A5.5	LCOH (€/kg) in scenario 5 (neglecting grid fees).	108

1 Introduction

In efforts to combat climate change, nations all over the world are encouraged to act immediately. The shift towards a sustainable energy mix requires us to identify key roles for renewables. In need of decarbonization, clean hydrogen has received vast attention in recent years for its possible contribution to reducing power production from fossil fuels. In fact, mentions of the word hydrogen have increased 18-fold in Statnett's long-term market analysis over the last two years (Statnett, 2020)¹. Nonetheless, the clean, widespread use of hydrogen still faces many challenges as we stand in front of a transition. One of these remains to be high production costs for green and blue hydrogen². With the price of electricity being one of the most prominent costs in water electrolysis, this will be an important parameter to study. The implementation of renewable energy sources has historically led to increased local electricity price volatility, with inexpensive hours during periods with a high degree of renewable impacts and vice versa. Today, researchers have a widespread understanding that electricity price fluctuations could be exploited to achieve lower production costs for hydrogen from water electrolysis by producing during off-peak hours. Going forward, the increased introduction of renewables into the energy mix is expected to cause even more fluctuations. Due to this, it is necessarily better to understand the combined benefits of water electrolysis and storage.

We intend to explore if electricity price savings, through the use of excess production capacity and storage, can exceed the associated investment costs.

Consequently, we hypothesize that the levelized cost of hydrogen (LCOH) can be reduced by investing in excess production capacity and storage. To test the hypothesis, we use mathematical programming to develop a multi-period optimization model. By aggregating electricity prices to capture seasonal effects in a minimal amount of data, we can determine an optimal production schedule over an extensive time-horizon of 20 years. We intend to explore the combination of alkaline water electrolysis and storage to minimize the overall

¹Statnett is the system operator in the Norwegian energy system. Figure A1.1 illustrates the increasing trend for hydrogen.

²Green hydrogen is produced from water electrolysis with renewable power, and blue hydrogen is produced from natural gas with CCS (carbon capture and storage).

cost of hydrogen production, subject to current and future electricity prices, current and future electrolyzer costs, current and future operational costs, current and future hydrogen storage costs, grid fees, and hydrogen demand.

We examine several publications and peer-reviewed articles from journals, organizations, and agencies to obtain an extensive overview of today's water electrolysis costs. A decision model is developed, taking relevant costs and adjusted electricity prices for Kristiansand into account. The location is chosen due to the possibility of subsurface storage in the North Sea Basin. Initial results are compared to findings in literature, reports, and official publications to validate our model. Next, we explore realistic scenarios based on future projections from recognized agencies and manufacturers regarding estimated plant costs and electricity prices. Thus, our model seeks to illustrate and quantify the current and future possible benefits of investing in excess production and storage capacities. This can allow for over-production during inexpensive periods, such that production can cease during more expensive periods while still meeting the required demand in each period.

1.1 Background and motivation

In a recent report, NVE (2020a) mentions that the amount of electricity generated from dispatchable sources will decrease substantially in the coming years. Thus, the need for flexible industries that can use electricity during periods of overproduction and reduce electricity consumption during periods of underproduction becomes apparent. Due to the special properties of hydrogen, mainly its ability to hold energy without substantial leakage, it is considered suitable for energy storage over longer periods of time and can even provide balance to the grid. The EU Commission (2020) has developed a comprehensive strategic plan for the deployment of hydrogen in Europe to reach climate neutrality. One step in reaching that goal is to reduce the cost of hydrogen production from fossil fuels combined with carbon capture in the short term and from electricity in the long term. To achieve this, the EU Commission has kick-started the European Renewable Hydrogen Alliance, whose purpose is to support hydrogen technology investments to develop a full-fledged hydrogen eco-system, thus implying a substantial role for hydrogen in the development of renewable energy sources in the EU.

With the increased attention for hydrogen, Greensight AS reached out and proposed to

investigate the opportunity to exploit the increasing volatility in electricity prices through hydrogen production by investing in excess production capacity and storage options, and whether doing so can reduce the total cost of hydrogen production from water electrolysis.

On the 10th of December 2020, the extreme curve shown in Figure 1.1 was observed in the Nord Pool NO2 region.

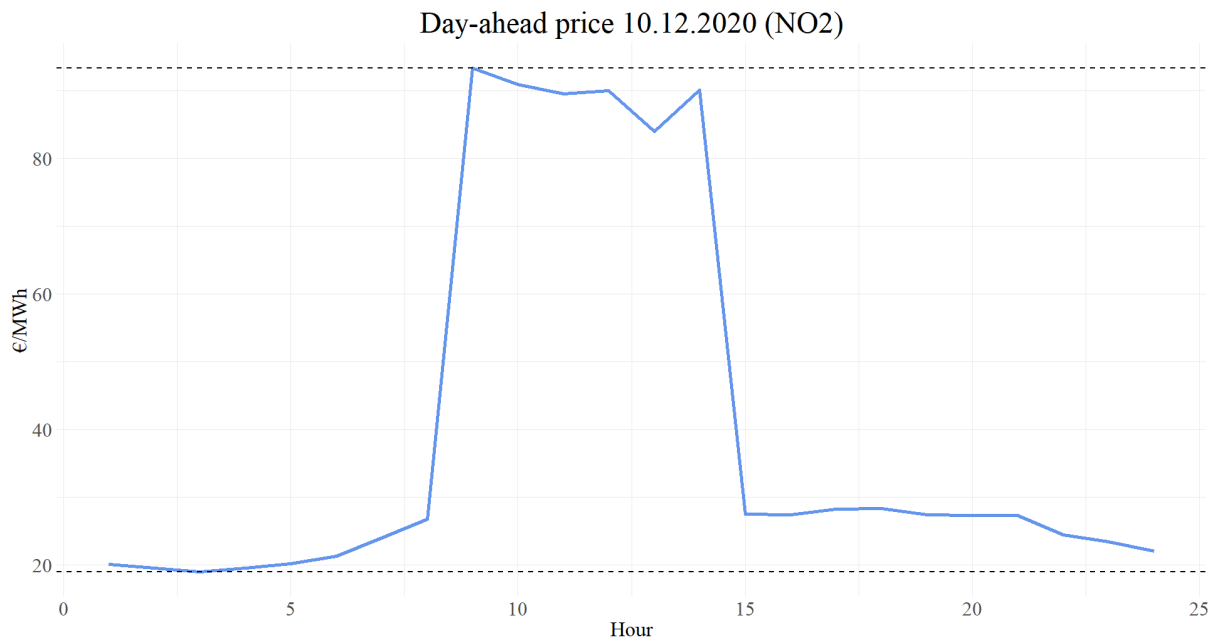


Figure 1.1: Day-ahead prices for NO2 on the 10th of December 2020.

With the prices within a single day ranging from below 20 €/MWh, to over 90 €/MWh, it is clear that there is potential for cost savings for flexible, power demanding industries. Through production planning, one can reduce the electricity cost of hydrogen from water electrolysis. Also, if the future electricity generation is to be performed by an increasing amount of renewable, non-dispatchable generators, these curves may occur more frequently. Thus, the need for industries that can counteract these effects become prominent. A proposed solution is to produce hydrogen during off-peak hours and use that hydrogen to provide more power during on-peak hours. Doing so can be beneficial for several stakeholders, for instance, providing balance to the grid or exploiting surplus energy from renewable sources that otherwise would be lost.

1.2 Literature review

There are substantial amounts of research performed on the subject of hydrogen production, possibly due to the vast increase in the attention it has received over the last decades as a contribution to solve the climate problem. Hydrogen production from water electrolysis has been highlighted as the best long-term production method by the EU Commission (2020), and several researchers have explored this technique of hydrogen production. Nguyen et al. (2019) presented a techno-economic analysis of grid-connected hydrogen production from large-scale electrolysis and used a cut-off technique to separate between hours when production should occur and not. In some cases, they managed to reduce production costs substantially. However, they stated the need to optimize the trade-off between reduced production costs and increased investment costs. Yates et al. (2020) used a Monte Carlo simulation to establish the most important cost drivers for green hydrogen and calculate realistic intervals for LCOH today. Kuckshinrichs et al. (2017) presented a study for alkaline water electrolysis technology, focusing on financial metrics, projection of key performance parameters, and further financial and tax parameters. The study uses a cash flow analysis to determine the levelized cost of hydrogen, net present value to determine attractiveness, and variable cost elasticity for market flexibility analysis. Many studies have in common that they seek to estimate hydrogen costs from average measures and not explore real possibilities of cost reductions through production scheduling and optimization.

When developing the HyOpt model, Kaut et al. (2019) used a method of mathematical optimization to fully exploit the limits for hydrogen production capacities and storage to minimize costs. They divide the time periods into strategic and operational periods. If the strategic period is one year, and the operational period covers one week of operation, the costs and revenues from the one week are repeated 52 times to represent the cash flows across the whole period. Their model is fascinating but does not include the important long-term, seasonal variations in electricity prices, thus overlooking the effect that seasonality could play in reducing hydrogen costs from water electrolysis. Matute et al. (2020) also pursued a mathematical model to investigate the profit of hydrogen from electrolysis. However, they focus on a more technical approach when establishing the relationship between profits and the different states the electrolyzer equipment can

operate in. Another approach for mathematical modeling is presented by Michalski et al. (2017), though focusing on micro and macroeconomic analysis. An interesting aspect of this study focuses on underground hydrogen storage, which allows for large quantities of hydrogen storage over longer periods of time. Several other researchers also focused on the possibilities and/or economics of underground hydrogen storage (Kruck et al., 2013; Lord et al., 2014; Crotofino, 2016; Le Duigou et al., 2017; Tarkowski, 2019).

This thesis is fundamentally based on the work of Nguyen et al. (2019), Yates et al. (2020), and Kuckshinrichs et al. (2017), who identified and established the most important parameters to include when modeling hydrogen production from water electrolysis. Using their findings, we seek to explore further steps in developing a long-term production schedule to clarify whether reductions in LCOH can be achieved through flexible production scheduling. Moreover, we implement different aspects from other mathematical optimization models and incorporate the most important ones found by each researcher. Kaut et al. (2019) has inspired us in many smaller details, including how we model the deterioration of the equipment. Additionally, they point out the importance of establishing long-term seasonal variations in electricity prices as a future improvement to their model – an aspect we aim to achieve. From Matute et al. (2019), we include the option for the electrolyzer equipment to be operated in different states that determine the current equipment’s production capabilities. Michalski et al. (2017) illustrated the possibilities to reduce costs through the use of large-scale, underground storage, which we also include in some model scenarios. Thus, we seek to incorporate several important aspects from earlier research and explore the possible improvements to earlier methods. With a slightly less technical perspective than some literature, though with an increased aspect of economic detail compared to some, we seek to shed light on the possibilities of cost savings through flexible hydrogen production by focusing on overproduction and storage to exploit the volatility in electricity markets.

1.3 Scope of the thesis

This thesis’ model provides a general framework to determine optimal production and storage capacity for a hydrogen production plant. We apply our model to electricity price data from the Nord Pool NO2 region and focus on grid-connected hydrogen production

instead of using renewable sources such as wind, hydro, or solar. It is not inconceivable that large-scale plants may require additional investments in grid capacity. However, this is considered unproblematic for plants with less power off-take than 0.5 GW (DNV GL, 2019). Furthermore, the model is intended for an on-site hydrogen production plant, meaning that transportation costs are disregarded. We find this assumption reasonable considering that water electrolysis is suitable for localized production purposes because it only needs water and power as resources. Lastly, our model is currently limited to hydrogen production using alkaline electrolysis technology, which is the most mature electrolyzer technology today. Other options are polymer electrolyte membrane (PEM) electrolysis and solid oxide electrolyzer cells (SOEC). We will discuss the differences between electrolyzer technologies in Section 2.2.

Software and application

The optimization model and data in this thesis are implemented and solved in AMPL (A Mathematical Programming Language), using the Gurobi solver. However, running models through other software is made possible through the AMPL application programming interface (API). AMPL API provides an object-oriented callable library that lets you access AMPL models and run AMPL commands from external programs (AMPL, 2020) – for instance, commercial software such as Python, R, C++, C#, Java and MATLAB.

Thesis overview

In Chapters 2 and 3, the chemical aspects, applications, production methods, and the different stages of hydrogen production, focusing on water electrolysis, are presented. The first part of Chapter 4 describes electricity price scenarios for today, medium, and long term horizons and their characteristics. The chapter continues with a discussion of important parameter values and costs for alkaline water electrolysis. Chapter 5 presents the mathematical optimization model, while results are presented, compared, and discussed in Chapter 6. Further, in Chapter 7, we discuss method and data limitations and present suggestions for further work. In Chapter 8, conclusions are drawn based on the results and discussion in the previous chapter.

2 Hydrogen

This chapter explains the theoretical aspects of hydrogen regarding production, storage, and applications. Section 2.1 presents the theory behind hydrogen production and how it can be converted back to electricity. Section 2.2 contains a more detailed description of different electrolysis technologies and recent innovations within hydrogen production. Section 2.3 consists of the theory behind compression, liquefaction, and hydrogen storage, while Section 2.4 describes the current market and hydrogen use.

2.1 How hydrogen is produced

In 2019, the annual global hydrogen production was approximately 70 million tonnes. The most common ways of producing H_2 are from fossil fuels and biomass, water electrolysis, or a mix of the two. Out of the 70 million tonnes produced, about 75% are produced from natural gas reforming, 23% are produced from coal gasification, while the remaining 2% of the production comes from oil and water electrolysis. Hydrogen production today is highly dependent on using fossil fuels, making the hydrogen industry a large source of CO_2 emission (IEA, 2019). Figure 2.1 gives an overview of different hydrogen production methods.

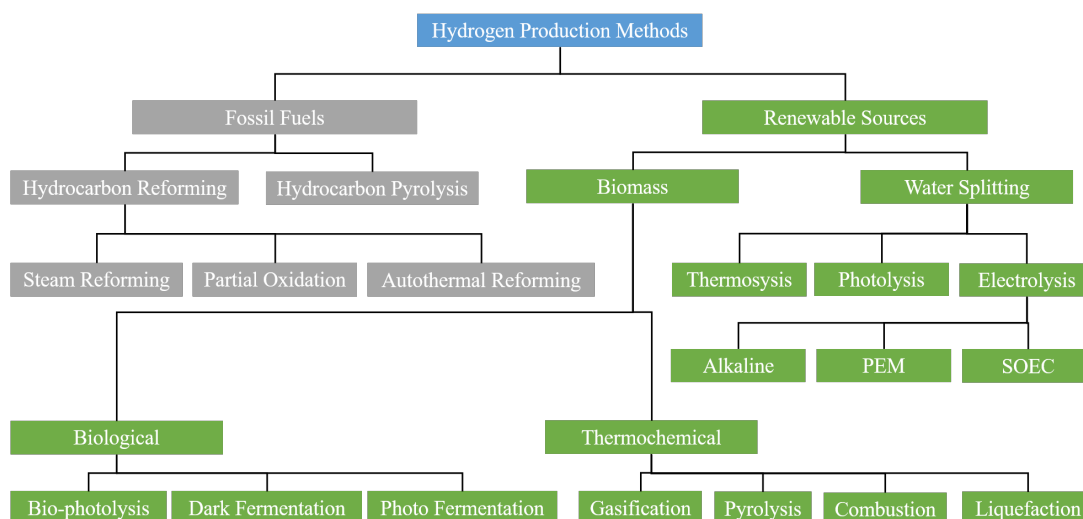


Figure 2.1: Overview of different hydrogen production methods (Shiva Kumar and Himabindu, 2019).

Our thesis focuses on hydrogen production from water, a zero-emission process if electricity

stems from renewable energy sources. The water electrolysis process, invented by William Nicholson and Anthony Carlisle in the year 1800 (Khalilpour, 2019), consists of infusing H_2O with an electric current, thus splitting it into hydrogen and oxygen (Rashid et al., 2015). Pure water electrolysis results in H_2O being split into H_2 and $1/2 \text{O}_2$. Approximately nine liters of water is required to produce one kg of hydrogen. Due to the difference in weight between the two gasses H_2 and O_2 , producing one kg of H_2 results in eight kg of O_2 . The oxygen can be applied in some local process, stored, transported and sold, or let out into the air. The hydrogen is usually compressed to 100-700 bar or liquefied. Both compression and liquefaction result in additional energy use. After compression or liquefaction, the H_2 is either used, stored on-site, or transported away.

The hydrogen can be transformed back into electricity by using a fuel cell. The fuel cell strips hydrogen atoms of their electrons, which are then forced through a circuit, thus generating electricity. After passing through the circuit, the negative electrons combine with the previously released positive protons and oxygen from the air, resulting in the generation of fuel cell by-products: water and heat. The energy content, which is the amount of energy that can be generated from one kg of H_2 , is equal to 33.3 kWh. The production of one kg H_2 requires between 41-56 kWh, resulting in an electrolyzer efficiency between 59-80%. Compression and liquefaction reduces the efficiency further. Converting the H_2 back into electricity results in additional losses due to the fuel cell's current efficiency of approximately 40-60% (U.S. Department of energy, 2015). Figure 2.2 supplies a simplified illustration of energy losses in different stages of the hydrogen process.

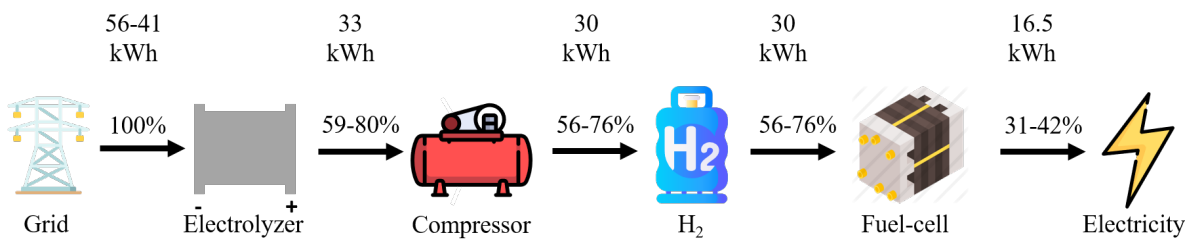


Figure 2.2: Energy losses for different steps in the hydrogen production chain and transformation back to electricity.

2.2 Water electrolysis technologies

Within water electrolysis literature, researchers frequently discuss three electrolyzer technologies. These are alkaline (AEL), polymer electrolyte membrane (PEM), and solid oxide (SOEC) electrolyzers. Each of the technologies has its pros and cons regarding the output from the production or production costs. Out of the three methods, SOEC is the least developed and is not used commercially yet (IEA, 2019; DNV GL, 2019). Thus, we will only explain the former two: AEL and PEM.

2.2.1 Alkaline electrolysis (AEL)

The most developed technology is the AEL. It works by sending an electric current through a cathode, which splits $2\text{H}_2\text{O}$ into H_2 and 2OH^- . The hydroxide anions (2OH^-) then travel through the electrolyte to the anode, where it loses its electrons and becomes $1/2 \text{O}_2$ and H_2O . The electrons return to the positive terminal of the direct current power source. The H_2 and O_2 are then separated using a diaphragm and stored separately. Figure 2.3 shows a graphical illustration of the alkaline electrolysis process.

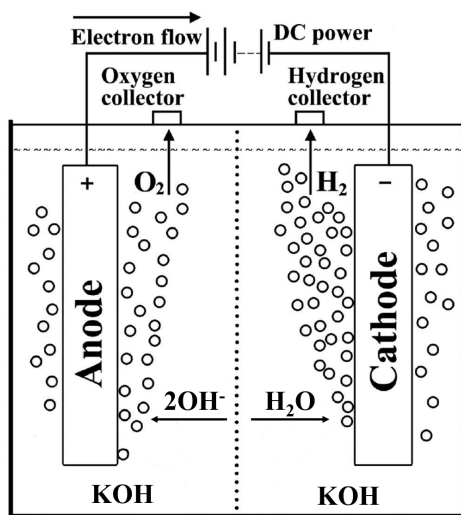


Figure 2.3: Graphical illustration of AEL (Ziazi et al., 2017).

AEL uses a strong base as the electrolyte in the electrolyzer. Using a base as an electrolyte, contrary to an acid, allows for non-precious metals in the electrodes, often nickel (Ni), which makes the electrolyzer's capital expenditure lower. The use of non-precious metals is the largest contributor to the cheaper investment costs in AEL technology today than

other electrolysis technologies. The base allows for the use of less precious metals because it avoids the corrosion that would occur when using acids as the electrolyte. If the system uses acids, precious metals also have to be used to avoid corrosion. Using base solutions also reduces the operational expenditures, as the equipment is less exposed to deterioration, allowing it to last longer. Corrosion of the diaphragm used to separate H_2 and O_2 depends upon the temperature. A higher temperature leads to more corrosion. Thus, increasing the electrolyzer's efficiency through increasing temperatures leads to more corrosion, which leads to a shorter life for the electrolyzer. Because of these issues, there has been much effort to research hydroxide conducting polymers suitable for AEL. Recent research has found that a hydrocarbon-based polymeric membrane might reduce the deterioration (Keçebaş et al., 2019). Overall, both the capital expenditure and the operational costs of AEL are low relative to the competing electrolysis technologies.

2.2.2 Polymer electrolyte membrane electrolysis (PEM)

The PEM-electrolyzer works by pumping water into the anode. The H_2O is split into O_2 , H^+ , and e^- . The protons are passed through the electrolyte to the cathode. The electrons travel through an external power circuit and are re-combined with the protons to produce H_2 at the cathode. As the membrane separates the anode and cathode, there is no need for a diaphragm in the PEM electrolyzer to separate the H_2 and O_2 gases. Figure 2.4 shows a graphical illustration of the electrolysis using PEM.

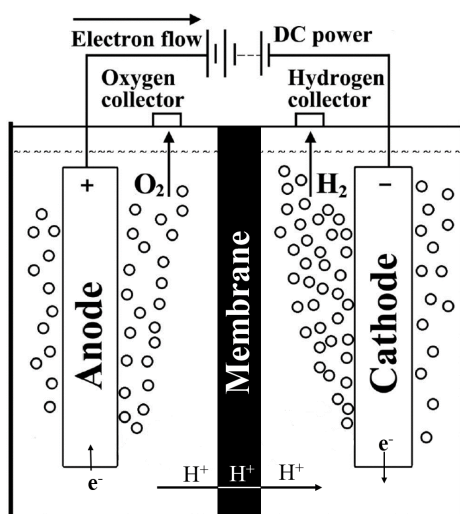


Figure 2.4: Graphical illustration of PEM electrolysis (Ziazi et al., 2017).

Shiva Kumar and Himabindu (2019) provide a thorough review of hydrogen production from PEM electrolyzers. The PEM electrolyzer uses solid polysulfonated membranes as electrolytes, compared to the liquid KOH-solution used in AEL. PEM technology holds many advantages over AEL technology. Some of these advantages are compact system designs, quicker changes when increasing or decreasing the production rate, purer hydrogen, increased pressure of the output H₂, and higher energy efficiency, meaning that more of the energy input is stored when PEM is used. The fact that the PEM-electrolyzers can react quicker to the amount of input electricity makes it more applicable to industry use and a preferred technology when hydrogen production is combined with renewable energy sources to store energy during high production periods. However, when connecting the electrolyzer to an electric grid, this is not as necessary.

Nevertheless, the success of the PEM-electrolyzers is also the root of its disadvantages. The increased efficiency, pressure, and purity of hydrogen requires precious metals in the anode and cathode, increasing the technology's capital expenditure significantly, making it more expensive to invest in PEM than AEL technology. There has, however, been much research put into the use of other less precious metals that can replace the ones used today. Doing so could reduce the capital expenditure of the technology while still keeping the advantages presented above.

2.2.3 System comparison

The PEM technology holds many advantages, and if electrolyzer manufacturers can reduce the cost of the technology, it should become the preferred option out of PEM and AEL. However, AEL technology is more used commercially as it is cheaper and more developed. Much research is being done on the solid oxide electrolyzer cell technology, which does not use precious metals, has a higher efficiency than PEM, and produces H₂ at high pressures. Nevertheless, the technology is not commercialized yet.

2.3 Compression, liquefaction, and storage

After producing hydrogen, it must either be used momentarily, or stored in some way, either for transportation purposes or on site for later use. How the hydrogen is stored is reliant upon how the producer chooses to handle it after production. While hydrogen has

the highest gravimetric density of all fuels, meaning that it holds the most energy per kg, it has the lowest volumetric density, meaning that it contains a low amount of energy per m^3 . This relationship is illustrated in Figure 2.5. Having such low volumetric density means compression or liquefaction is required to store the hydrogen in a reasonably sized compartment.

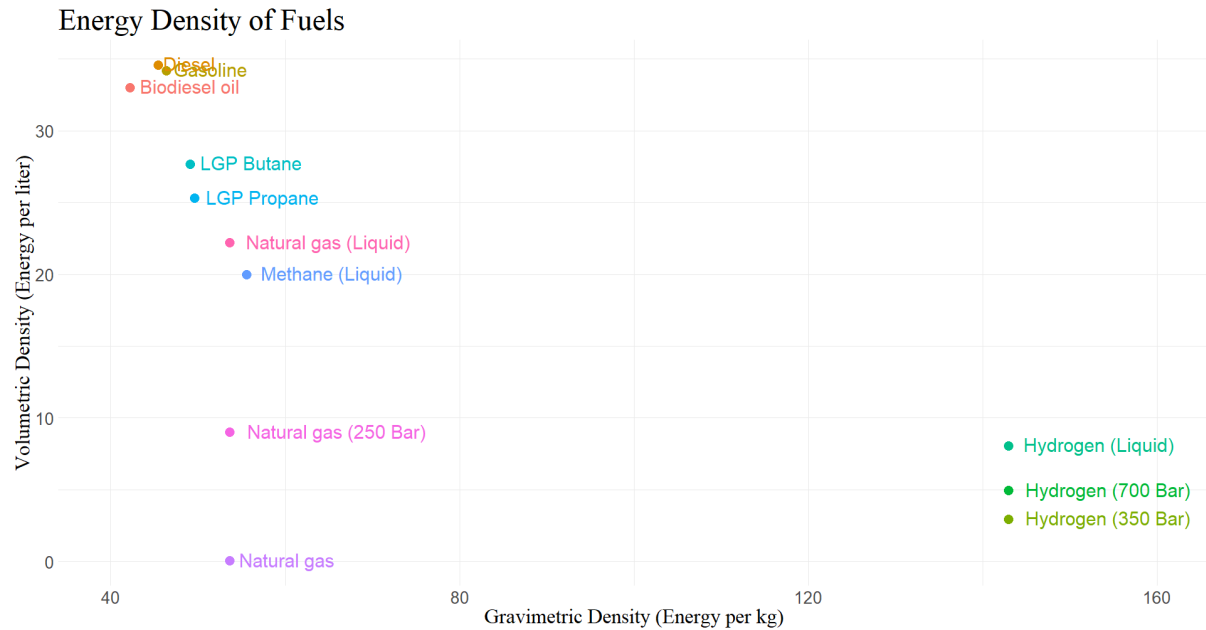


Figure 2.5: Gravimetric and volumetric density of different fuels (Mazloomi and Gomes, 2012; Dagdougui et al., 2018).

2.3.1 Compression of hydrogen

Compressing hydrogen means increasing the pressure the gas is subject to, thus increasing its density. The pressure of the hydrogen output from both PEM and AEL is between 1-30 bar, meaning 1-30 times the pressure we experience on the earth's surface. The hydrogen is then usually compressed to either 350 or 700 bar. At 350 and 700 bar, the hydrogen density is equal to 23 kg/m^3 and 38 kg/m^3 at 27°C , respectively (Sheffield et al., 2014). When the gas is compressed to 350 and 700 bar, the volumetric energy density becomes 2.95 and 4.93 MJ/L, respectively (Dagdougui et al., 2018). Comparing this to the 32 MJ/L for gasoline, we see that, even in a highly compressed state, H_2 has a low volumetric energy density compared to other fuels. More advanced fuel cells could increase the volumetric energy density by taking advantage of the latent heat of the steam produced from combustion, which is referred to as the higher heating value (HHV), as opposed to the lower heating value (LHV).

Compressing hydrogen increases its volumetric energy density, thus allowing it to take up less space. Doing so does, however, come at a cost. The compression of hydrogen requires the use of additional energy, which increases the production costs. Compressing the gas to a pressure of 700 bar will demand energy equal to 13-18% of the LHV (Møller et al., 2017).

2.3.2 Liquefaction of hydrogen

Another option to increase the volumetric energy density of H₂ gas is to use a technique called liquefaction, which is performed by reducing the gas temperature until it reaches its liquid state, at -253°C. Liquefaction of hydrogen results in even higher volumetric density than compressing the gas to 700 bar. LH₂ can achieve a density of 70.6 kg/m³. The volumetric energy density then becomes 7.63 - 8.49 MJ/L (Dagdougui et al., 2018), compared to the 2.95 and 4.93 MJ/L for compressed hydrogen at 350 and 700 bar, respectively. Thus, the liquefaction of H₂ is practical for transportation of the fuel over long distances where space is a concern. The liquefied hydrogen does, however, still have a much lower volumetric energy density compared to gasoline and other fuels. The liquefaction process is also costly as the equipment requires a high capital investment and the additional energy cost associated with the liquefaction itself is rather high (De-León Almaraz and Azzaro-Pantel, 2017).

2.3.3 Storage of hydrogen

The storage of hydrogen does, as mentioned earlier, rely upon how the manufacturer handles it after production. The three main storage methods are in compressed gaseous form, liquid form (LH₂), or in a solid-state, which we have not mentioned earlier. When storing the H₂ in gaseous form, the most common way is to store the gas in steel cylinders that can contain hydrogen with a pressure of up to 800 bar. Another storage option that researchers and manufacturers have explored is underground storage. In that case, the H₂ is led down in the ground, through pipes, into empty salt caverns, depleted gas/oil fields, or aquifers. Large amounts of hydrogen can then be stored at a relatively low cost over more extended periods of time. The hydrogen is then brought back up through pipes and either used in its original form or transformed into electricity through a fuel cell. Tarkowski (2019) explored this particular storage method concerning long-term storage of

excess electricity produced from renewable energy sources, such as wind and solar power plants. In his article, Tarkowski (2019) mentioned several advantages of underground gas storage, including increased safety, better space management, and reduced cost per kg of storage capacity. The method has been explored to store hydrogen in the US and the UK and is widely used to store natural gas. Figure 2.6 illustrates the process of underground hydrogen storage.

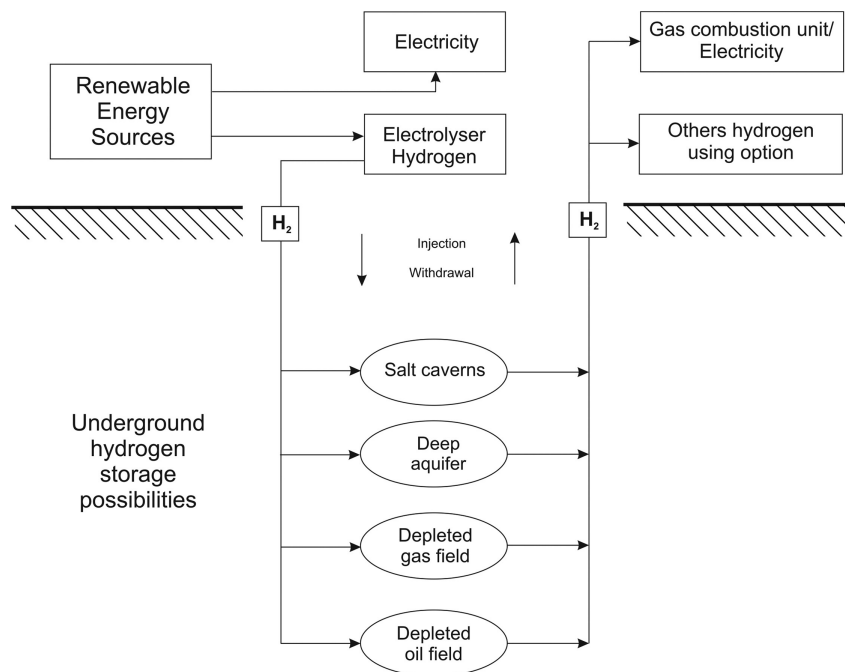


Figure 2.6: Illustration of underground hydrogen storage (Tarkowski, 2019).

LH_2 storage is performed by inserting hydrogen into cryogenic tanks holding a temperature of about $-253^\circ C$ so that the H_2 remains in liquid form. Storing LH_2 is, as with the conversion into it, costly as it must keep a very low temperature at close to atmospheric pressure. The process of liquefying and storing hydrogen in cryogenic tanks results in a 40% loss of energy content in the hydrogen (Makridis, 2016). The method does hold some crucial advantages, mainly revolving around its high volumetric density, allowing for easier transportation, as it requires less space. However, due to its high energy demand and the fact that we focus upon on-site hydrogen production, we will not focus on the use of LH_2 as a storage method further in this thesis.

The last hydrogen storage method is solid storage through absorption as chemical compounds or by absorption on carbon materials. Abe et al. (2019) published an article containing a review and recommendations regarding hydrogen economy, energy,

and storage, stating that hydrogen storage is a key enabling technology for sustainable hydrogen energy development. They conclude that solid-state metal hybrids are considered the most viable solution for hydrogen storage among several options. This storage method takes advantage of hydrogen's chemical aspects, mainly that it reacts with a wide variety of transition metals and metallic alloys at high temperatures to form metal hybrids. The advantage of these metallic hybrids is that they can store large amounts of hydrogen in a relatively small space, resulting in a low volumetric density. Lanthanum-nickel alloy (LaNi_5), an inter-metallic hybrid, can store hydrogen with a volumetric density of 115 kg/m^3 , which is even denser than LH_2 . However, this metallic hybrid does not support easy retraction/release of the hydrogen, making the use of this hybrid infeasible. Other solid storage methods have also been explored, such as complex chemical hybrids and nanostructured carbon materials, which are developed to solve the problems of storage using regular metal hybrids. However, none of the techniques are implemented commercially, and there is still much research performed on the topic (Zacharia and Rather, 2015). Because storage in solid-state is not yet commercially viable, we will not consider this option further in our thesis. In the later sections, where we define the costs present in the model, we will focus on the storage costs in compressed gaseous form. Moreover, we will consider both storage in traditional tanks and the possibility for storage in caverns.

2.4 Applications of hydrogen

Hydrogen applications in energy production and as a component in industry practices have existed for centuries, and various industries have tested the commercial use of the gas. In this section, we explore the different applications of hydrogen today and the potential applications in the coming years. We divide the usages of hydrogen into two different categories – material-based and energy-based use.

2.4.1 Material-based hydrogen applications

Material-based hydrogen usage is a typical hydrogen application method today and means that a fuel-cell does not convert hydrogen into electricity. Instead, hydrogen is used as a component in some other industry aspect. The most common uses of hydrogen today is

oil refining (33%) and ammonia production (27%) (IEA, 2019). Hydrogen is also used in metal-working, flat glass production, the electronics industry, and corrosion prevention in electricity generation (Hydrogen Europe, 2017). IEA (2019) states that virtually all of the hydrogen used for industrial purposes today stem from fossil fuels, thus indicating an essential role for green and blue hydrogen in reducing emissions in the coming years.

An emerging industrial application of hydrogen is within the field of steel production, in which the amount of CO₂ emissions today are very high. The European Union and the Paris agreement seek heavy reductions in CO₂ emissions within this industry in the next 30-40 years (Vogl et al., 2018). Using hydrogen to separate oxygen from iron ore can prove the right way to achieve the desired emission reductions, resulting in an increased demand for green and blue hydrogen in the coming years.

Furthermore, the use of hydrogen in fuel refineries is widespread. Hydrogen is used in the process of refining crude oils into fuels, such as gasoline and diesel. It is also used to remove contaminants from the fuels. The demand for hydrogen within this industry has increased in the last couple of years due to regulations requiring low sulfur content in diesel fuels, increased consumption of low-quality crude oils, and increased oil consumption in India and China. Hydrogen is also an important element in methanol production (CH₃OH) (Hydrogen Europe, 2017).

2.4.2 Energy-based hydrogen applications

The use of hydrogen for the generation of energy is performed by running H₂ gas through a fuel cell, thus producing electricity with water and heat as by-products. Transformation of hydrogen into energy can be performed within several industries, for instance, transportation and stationary electricity production facilities. Within the transportation sector, hydrogen has been widely explored. Even NASA has used it in their space expeditions since their establishment in 1958, both in liquid form as fuel for launching their rockets and on-board combination with exhaled carbon dioxide for water renewal (Bray, 2017).

2.4.2.1 Transportation applications

Due to hydrogen's high energy content and its properties, which allow it to generate zero-emission energy when produced through electrolysis using renewable energy or fossil

fuels combined with carbon capture, it has been explored widely within the transportation sector. It is experimented with for planes, both for generating electricity and fuel purposes, due to its widespread use in space programs. The same applications of hydrogen have been tested for marine transportation and use in trains and trams. Though the experimentation has been present, the applications within these fields are limited. The larger applications have been within material-handling vehicles, passenger cars, semi-trucks, and busses. For material handling at warehouses or airports, hydrogen fuel cell vehicles are applicable due to their "lack" of local pollution and low operating noises. Also, they hold an advantage over electric vehicles, as they can be refueled much faster than their electric counterparts, thus resulting in increased utilization (IEA, 2019; Castetter, 2019). In the passenger car industry, the use of fuel cells has been extensively researched, and as of 2020, three commercial options exist – Hyundai Nexo, Toyota Mirai, and Honda Clarity. According to Kane (2020), global sales of hydrogen cars in 2019 amounted to around 7,500 cars, increasing by 90% from the year before, while IEA (2019) states 11,200 cars were in operation as of 2019. The biggest concern about hydrogen cars as of today is the need for a good global/national infrastructure of hydrogen fueling stations (Rösler et al., 2014). In the semi-truck industry, hydrogen-fueled trucks are approaching commercial use, with Nikola, Toyota, and Hyundai exploring the industry applications of hydrogen to fuel long-distance transportation with zero-emission. The bus industry has also explored hydrogen as fuel and is commercially used in North America, Europe, and China. Today, around 500 hydrogen buses are operated worldwide (IEA, 2019).

The use of hydrogen in transportation has shown relatively large growth over the past years and is projected to increase over the next years. However, the industry struggles to keep up with the pure electric transportation methods that pose a tremendous competitor. Nevertheless, the growth does seem to continue in all transportation industry applications, which implies an increased demand for pure hydrogen in the coming years.

2.4.2.2 Electricity generation

The use of fuel cells allows hydrogen to be converted into electricity by combining H_2 and O_2 . Doing so can allow hydrogen to be used as an energy carrier for electricity, as an alternative to other storage technologies such as batteries, which are more energetically

expensive per unit of storage because it makes less effective use of manufacturing energy inputs. By transforming the excess electricity from renewable energy sources, such as wind turbines or solar panels, into hydrogen, it is possible to store the hydrogen and transform it back into electricity at periods with lower electricity generation (Pellow et al., 2015). Thus, hydrogen production and storage can balance the grid to stabilize prices through supply/demand management, resulting in a more predictable and stable electricity spot market. Especially in countries where renewable energy becomes an increasingly important source of energy, which leads to more weather dependant prices, storing the excess electricity for seasons with less electricity generation can prove a very viable solution. Due to the incredible increase in the number of renewable energy sources, this solution has been highly researched over the last decade. However, this approach carries a disadvantage in which the production of hydrogen, the compression and liquefaction, the storage, and the transformation back into electricity is quite an energy-intensive process, resulting in far lower energy output in the end, compared to the original generation (Steilen and Jörissen, 2015). Another disadvantage is that the storage of hydrogen is quite expensive, and it demands much space, which can prove to cost more than it yields.

Another application of electricity production using hydrogen is in the domestic sector. Hydrogen can provide electricity to a house, and the excess heat from the fuel cell can be used for heating purposes. The excess heat can also be exploited on a larger scale, with the heat from a hydrogen electrolysis plant supplying heat for other industrial processes or heating for surrounding areas. Using the heat and electricity from the fuel cells can allow the efficiency to reach 95% of the theoretical limit (Hydrogen Europe, 2017).

3 Alkaline electrolysis production process

In this chapter, we intend to explain the production process of hydrogen. We focus on alkaline water electrolysis, and in the following subsections, the attention will be directed towards this technology. In Section 3.1, the production process is summarized to achieve an overview, while each production stage is described in greater detail throughout Sections 3.2-3.7. Lastly, in Section 3.8, we present assumptions about the production process used when modeling costs later in the thesis.

3.1 Process overview

The hydrogen production process using alkaline water electrolysis is rather complex, and the details on a molecular level are described in Section 2.2. In this section, the production process steps will be described, from the input of electricity and water to the output of compressed hydrogen. A graphical overview of the process is illustrated in Figure 3.1.

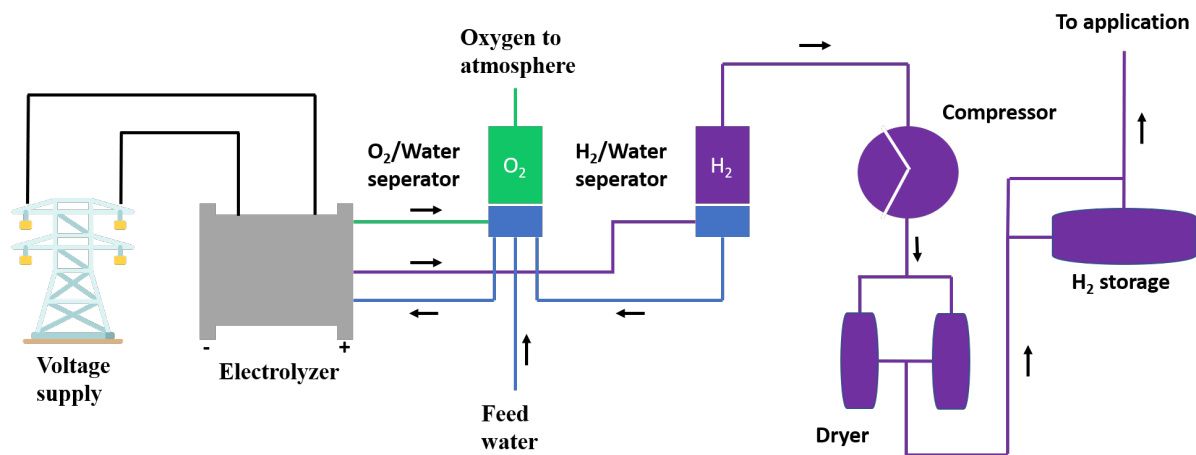


Figure 3.1: Illustration of the hydrogen production process using alkaline water electrolysis (NEL, 2019).

Hydrogen production from water electrolysis begins with the infusion of electricity into water. The electricity can come from various sources and has been tested using electricity stemming from a grid or directly connecting the electrolyzer equipment to a renewable energy source. Connecting an electrolyzer directly to renewable energy sources is thought to be more applicable with PEM electrolyzers due to the quick response time compared to alkaline electrolyzers. However, the differences between the two technologies are less

impactful when connecting the electrolyzer to a grid. Afterward, the water is split into O_2 and H_2 , which are separated into different tanks. The hydrogen is then often purified through a string of smaller processes, referred to as drying in Figure 3.1. When the hydrogen is pure enough for its purpose, it is either stored on site, transported to another location, or applied immediately.

3.2 Power supply

Water electrolysis requires a supply of electricity to perform the splitting of water. In this thesis, the electrolyzer is assumed to be grid-connected, and the prices are derived from the regional Nord Pool el-spot prices for the NO2 region. Thus, to understand the production process that creates the foundation for further modeling, it is important to understand the Nord Pool el-spot market.

The Nord Pool el-spot market is divided into several regions for which different spot prices are determined on the day ahead market. Participants in the market send their bids to Nord Pool Spot by noon the day before the energy is delivered (Houmøller, 2017). This goes for both the sellers and buyers who want to participate in the market. Each participant must deliver bids for each hour they want to sell or buy electricity, with a corresponding amount and price. After noon, the bids are aggregated into 24 supply and demand curves, one for each hour of the next day, which are then used to calculate the price for each given hour. Some inter-temporal restrictions make sure that all 24 hours are cleared together in one optimization problem. If there were no market coupling, nor market splitting, the exchange price would be set exactly at the intersection between the supply and demand curves. However, each region's submitted orders are matched with the Pan-European market coupling process, the Single Day-Ahead Coupling (SDAC), through an algorithm called Euphemia. The hourly prices are then calculated based on different constraints to form the hourly prices for each region. The prices are then usually announced at 12:42 CET or later to the market participants (Nord Pool, 2020).

In addition to the hourly electricity spot prices, participants in the regional electricity market must pay fees to use the available grid network. For businesses, these fees consist of a fixed monthly cost, a variable monthly cost, and a variable cost based on the total power consumption. The variable monthly cost is computed regarding the hour of the

largest power consumption during a month. This is heavily influenced by the size of the electrolyzer, which often requires several MWs. Grid companies are also imposed to collect fees and taxes on behalf of the Norwegian Tax Administration. However, electricity used for electrolysis is exempted (Forskrift om særavgifter, 2001).

3.3 Water electrolysis

In short, water electrolysis is a method of splitting water into hydrogen and oxygen gases. The water is pumped into the electrolyzer and mixed with a KOH-solution. This is done to increase the conductivity of the water, which speeds up the process of electrolysis. In theory, the KOH-solution is not affected by the chemical reactions; however, it has to be periodically replenished based on the losses in the system (Keçebaş et al., 2019). How much hydrogen a production plant can generate per hour depends on its production capacity and system efficiency. The system's capacity is usually denoted in the plant's maximum hourly power demand (kW, MW, GW) or the amount of hydrogen produced per day/hour (kg, tonnes). The system efficiency is the amount of electricity a system requires to produce one kg of hydrogen. The electrolyzer is subject to some operation and maintenance, which mainly include routine maintenance and cleaning. In addition, the cell-stacks in the electrolyzer lose some of their efficiency as time passes, resulting in a decrease in the production capacity over time. The stacks have a lifetime between 7-10 years today. The costs for operation and maintenance (O&M) and cell-stack replacements are directly affected by the plant's size.

An electrolyzer can, in theory, operate in three different states. These states are explained in detail by Matute et al. (2020). The first state is a production state, in which the electrolyzer is turned on and can produce hydrogen. When this state is active, the electrolyzer needs to maintain a minimum production utilization of 10-15% of the maximum production capacity to preserve the electrolyzer's required pressure and temperature. The second state is a hot-standby state, in which the electrolyzer does not produce hydrogen, but the pressure and temperature are preserved. Additional energy is required to keep the system in this state. Lastly, the third state is an idle state, in which the electrolyzer is depressurized and cold. Maintaining the system in this state requires minimal energy for power supply to control units and anti-freezing systems in regions where necessary. After

it has been in the idle state, turning the system back on is referred to as performing a cold start. Quite a lot of energy is needed to heat the electrolyzer and recapture the lost pressure required to efficiently run the electrolyzer.

3.4 Oxygen and hydrogen separation

After the electrolysis process, the hydrogen and oxygen are separated. Both gasses contain a reasonable amount of steam from the electrolytic process and need initial filtering. The water is led back to the electrolyzer. The hydrogen is separated from the steam before it is transferred further in the system. The oxygen is often let out into the air, as it is difficult to profit from the oxygen sale if it has to be stored, compressed, and/or transported. However, concerning the COVID-19 pandemic, the shortage of oxygen deliveries to hospitals has posed as a problem (Pedroso and Picheta, 2021), thus indicating that it can be economical or even ethical uses for the excess gas.

3.5 Compression

The compression of hydrogen is when the gas is pressurized, usually to a value between 100-800 bar. This process is performed to fit the hydrogen into a reasonably sized compartment and requires additional power. The additional power consumption is dependent on the amount of gas to be compressed and to what pressure. If the gas is to be stored in a storage tank, it needs to be compressed to between 350 and 700 bar. If the gas is stored in underground caverns, the required pressure is much lower and has to be in the range of 80-160 bar. Thus, substantially less energy is demanded to compress the hydrogen in cases of underground storage.

3.6 Purification

The purification process is, in reality, a four-step process that is performed on the hydrogen gas to increase its purity for applications that require very pure hydrogen. It includes scrubbing, which removes any traces of KOH-solution present in the hydrogen; deoxygenation, which removes any traces of O₂ that remains in the H₂; cooling, which reduces the temperature of the gas and removes some water; and a designated dryer, that

removes any water remaining in the gas.

3.7 Storage and application

After the hydrogen is purified to the required level for its application purpose, it can either be stored on-site for later use or applied immediately. For industrial applications with storage on a larger scale, the hydrogen can be stored in storage tanks or large-scale underground storage facilities. The costs of the two storage methods differ substantially.

There are several different tanks and methods applied for hydrogen storage. However, storage in steel tanks with 30 kg H₂ at 380 bar capacity is considered the go-to option for tank storage in this thesis. For underground storage, rather large facilities are required to achieve the extremely low storage cost, which can only be filled and exploited fully by large hydrogen production plants. In an overview from 2013, in relation to the HyUnder framework program (Kruck et al., 2013) initiated by the European Union, salt caverns are presented as the most suitable method for long-term underground storage of hydrogen. Thus, we consider salt caverns when underground storage is applied.

3.8 Production process assumptions

This subsection intends to provide a brief overview of production process assumptions related to the data and model presented in Chapter 4 and 5, respectively. Nonetheless, each of these is explained further throughout the thesis.

- (1) Electricity prices are derived from hourly el-spot prices for the NO2 price region in Norway and also consider grid fees for the specific region.
- (2) The electrolyzer can operate in three different states: production, standby, or idle. When the electrolyzer is in a production state, the utilization (production rate) can not drop below 10-15%. When the electrolyzer is in a standby state, the utilization drops to 0%, but still requires some energy to maintain pressure and temperature. When the electrolyzer is in an idle state, the utilization is 0% and consumes little to no power. However, turning the system on from an idle state requires a significant amount of power to achieve the required pressure and temperature.
- (3) Cell-stack replacements are performed once in year 10, and all cell-stacks are replaced

completely.

(4) Costs of KOH-solution and water are assumed to be included in the overall operational costs of the electrolyzer equipment and are not modeled separately.

(5) We assume that the oxygen is released into the atmosphere, as it is difficult to make the gas profitable in cases where it needs to be transported, compressed, or handled in some other way.

(6) All H₂ is compressed, regardless of whether it is stored or applied immediately. However, due to the lower required pressure when stored in underground caverns compared to storage tanks, we neglect compression costs when considering underground storage.

(7) The purification (drying) of the hydrogen is not considered a separate step in the model. Rather, it is assumed to be included in the electrolyzer's overall system efficiency. A recent study by Ligen et al. (2020) found this process to consume power of 0.5 kWh/kg H₂.

(8) The two storage methods – tanks and underground are considered separately, meaning that we do not consider a scenario that combines tank and underground cavern-storage.

4 Data

This section presents and describes our data sources, the initial data processing, and assumptions regarding the data used as input in our model. The data can mainly be split into two parts: electricity prices and plant costs. Electricity price data is retrieved from Nordpool's FTP server and adjusted based on future estimates from Norwegian energy agencies. Costs associated with investing and running an alkaline water electrolysis plant, such as CAPEX, production costs, and other operational costs, are drawn from literature, energy agencies, and qualitative interviews with Greensight AS. Each key cost parameter is described and evaluated to provide a transparent economic analysis of alkaline water electrolysis and hydrogen storage. Familiarity with cost parameters is of importance to understand the economic modeling of the system.

4.1 Electricity price data

In Section 4.1.1, we present the initial cleaning and structuring of the raw data. Following in Section 4.1.2, we present the benefits of aggregated electricity price data and how it can reduce the computational time in a multi-period optimization model. In Section 4.1.3 we explain the adjustments and structuring of the final electricity price scenarios based on future expectations. We create three different aggregated sets of electricity data that are further used as input for our model.

4.1.1 Raw electricity prices

Kuckshinrichs et al. (2017) find that the electricity cost has a major impact on the overall costs of alkaline water electrolysis. Consequently, it is important to specify realistic electricity price scenarios that successfully capture the expected development and uncertainty of future electricity prices. Identifying future electricity price scenarios is subject to a range of assumptions. Several factors such as generation mix, market-driven components, and political provisions affect the level and fluctuations of electricity prices.

Our electricity price data contains hourly prices for NO2 and is denominated in €/MWh. NO2 is one of the five electricity price regions in Norway, covering the south-western part of the country. Many factors influence electricity prices in Norway. For instance, changes

in temperature and rainfall lead to changes in supply and demand for electricity. After Norway joined EU ETS³ in 2008 (European Commission, 2016), Norwegian electricity prices have been more influenced by European policies. Wolff and Feuerriegel (2019) found European electricity prices to be more affected by the European Emission Allowances during the EU ETS phase III than during phase II. Consequently, we base the electricity price data on recent years, specifically the years after initiating the EU ETS's third phase, 2013-2019.

In the raw data from Nord Pool, each row contains 24 hourly electricity price observations from one day and one variable to determine the date. However, our data is transformed into a different format, more similar to a time series, better suited for plots, analysis, and modeling. The transformation results in an increased number of observations and a decreased number of variables. Each observation now represents the electricity price at a given hour for a specific day, month, and year. Table 4.1 illustrates the structure of our electricity price data for 2019.

Table 4.1: Data structure for electricity prices in 2019.

Day	Month	Year	Hour	Price
1	1	2019	1	48.77
1	1	2019	2	49.25
1	1	2019	3	49.17
...
2	1	2019	1	49.16
2	1	2019	2	48.14
2	1	2019	3	48.14
...
3	1	2019	1	50.03
3	1	2019	2	48.89
3	1	2019	3	48.31
...
31	12	2019	24	32.56

Dialogues with Statistics Norway⁴ suggested adjusting our historical price data for inflation using the consumer price index⁵. Hereafter, the electricity prices are denominated in real prices for 2019 and cleaned for missing values⁶.

³European Union Emission Trading System

⁴Statistisk Sentralbyrå. Norway's national statistical institute and main producer of official statistics. www.ssb.no

⁵Consumer Price Index (CPI, 2019 = 100) for Norway is used to adjust electricity prices.

⁶An initial analysis maps out one missing value for each year. Through dialogues with Nord Pool, we

Summary statistics of the data, presented in Table 4.2, illustrates the variability of the electricity prices. The variation in the prices could enable an attractive opportunity for optimizing the production schedule of hydrogen through water electrolysis.

Table 4.2: Summary statistics of electricity prices (€/MWh) for Nord Pool NO2 region in real 2019-values (2013-2019).

Year	Minimum	25% quantile	Mean (μ)	75% quantile	Maximum	St. dev. (σ)
2013	1.59	38.58	43.14	46.15	126.57	7.97
2014	0.67	26.97	30.82	35.50	79.99	6.87
2015	1.14	14.68	21.96	28.27	77.21	8.48
2016	6.43	22.75	26.90	29.94	101.67	7.03
2017	3.12	28.07	30.28	32.35	120.46	4.86
2018	1.96	38.76	44.21	50.87	107.35	9.59
2019	5.86	34.18	39.27	42.88	109.45	8.23

4.1.2 Time series aggregation of electricity price data

Kotzur et al. (2018) discuss the need for aggregation of time series data intended for use in energy system modeling and mention that the size of the input data directly affects the size of the optimization problem. They continue the article by discussing the need to aggregate time series into representative operational periods that capture the data's important seasonal variations. To achieve robustness, we intend to model a long time horizon that contains a large variety of price levels and fluctuations. Using hourly electricity price data to model the production schedule across the system lifetime of a water electrolysis plant would result in approximately 177,200 observations. Consequently, using the entire data set would be computationally infeasible. Therefore, aggregation is needed to compress the data. As we depend upon the fluctuations in the electricity price data to develop a realistic model, the most suitable way to aggregate the data must be determined while keeping the daily, weekly, and yearly seasonal variations. Seasonality refers to the known electricity price patterns within a time period.

have been informed that these values occur as European countries adjust for summertime during March every year, meaning that March contains one less hour than other months. Following, this introduces an additional hour in October each year when the clock is readjusted. These values account for 0,01% of a year's sample size and are removed before further handling the data.

First, we consider the daily seasonality, which occurs from hourly variations in electricity prices. The electricity prices vary throughout the day, depending on the hourly supply and demand. Generally, the demand is greater during hours in which households are actively using electricity for heating/cooling, cooking, charging electric cars, etc. This results in typical patterns of higher prices during the morning and when people return home from work and school, and slightly lower prices in the middle of the day. Also, prices are usually substantially lower during the night. The pattern is illustrated using historical data in Figure 4.1.

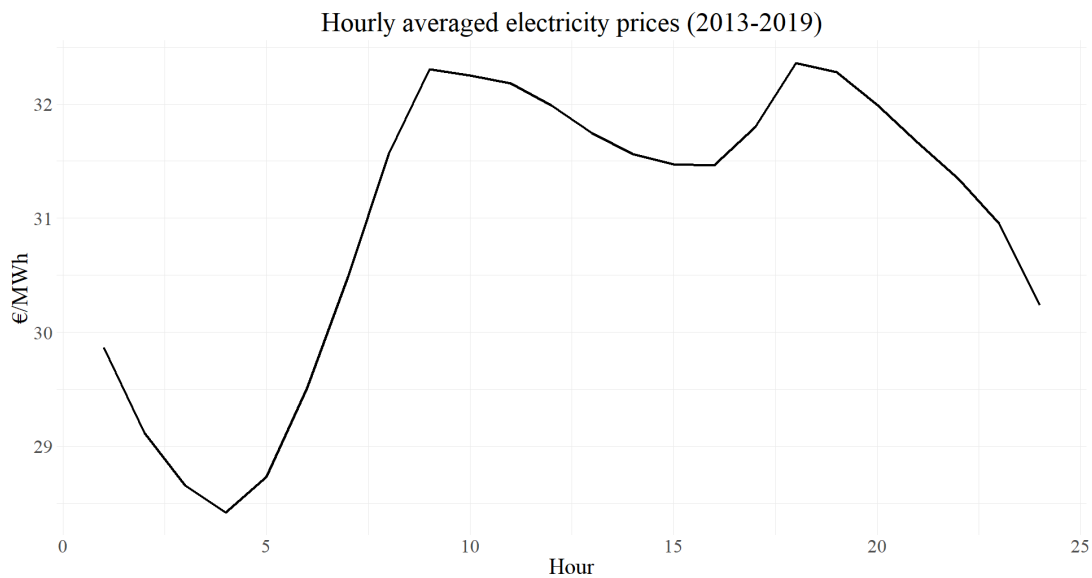


Figure 4.1: Hourly average of electricity prices for Nord Pool NO2 region (2013-2019).

Second, we consider the weekly seasonality from Monday through Sunday. This includes the variations between each day of the week. The difference between weekdays and weekends are especially prominent, while the difference between each weekday is less noticeable⁷. Spikes are often less prominent during the weekends, and the average price is often lower compared to weekdays. Figure 4.2 illustrates the difference between weekdays and weekends, in which the average price level for Saturday and Sunday are considerably lower than for the rest of the week. We also spot a trend where prices during afternoon on Friday's is generally lower than the other days.

⁷Weekdays are considered Monday through Friday while the weekend is considered Saturday and Sunday.

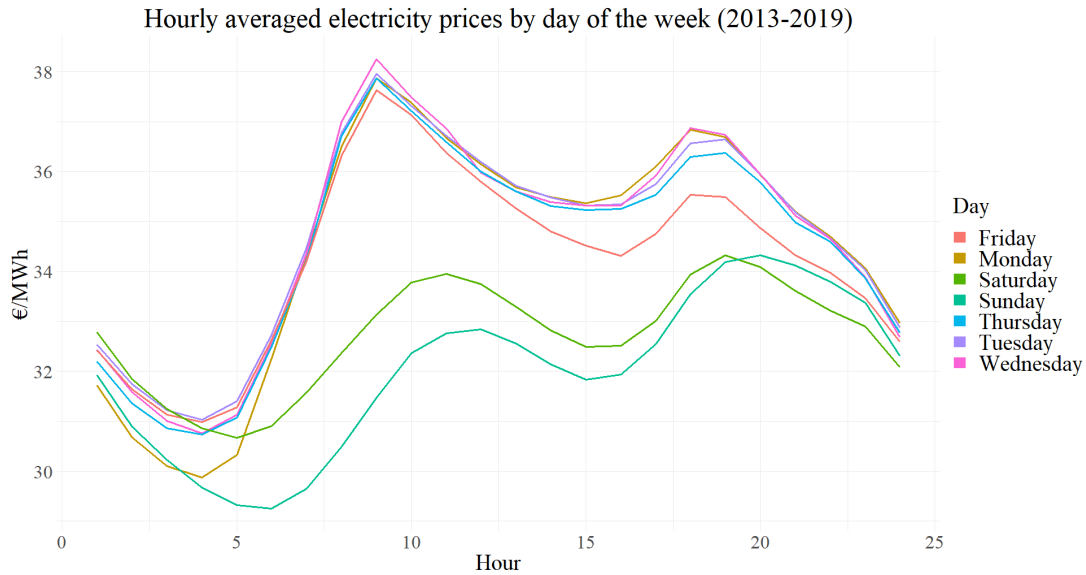


Figure 4.2: Hourly average, filtered by day of the week, of electricity prices for Nord Pool NO2 region (2013-2019).

Lastly, we consider the seasonal variations that occur throughout a year. In Norway and other Nord Pool countries, the temperatures decrease during the winter months. Hence, the power consumption for heating purposes increases, which leads to an increase in electricity prices. In Norway, less power is needed for heating during the summer months, decreasing the demand compared to the supply. Seasonal factors such as weather conditions also affect the supply of electricity. To capture these variations in the aggregated data, two methods can be considered. Either to use a monthly mean, or a seasonal mean with periods divided into winter, spring, summer, and fall⁸. Although the use of a monthly mean provides a more detailed picture of the seasonality in the prices throughout a year, we find the use of a seasonal mean captures most of the information that is needed to distinguish electricity prices between seasons. The seasonal, hourly mean for 2013-2019 can be seen in Figure 4.3, illustrating higher prices during the winter and lower prices during the summer. There also appear to be less variation throughout an average day in the summer and fall compared to the winter and spring.

⁸December, January, and February are considered winter; March, April, and May are considered spring; June, July, and August are considered summer; and September, October, and November are considered fall.

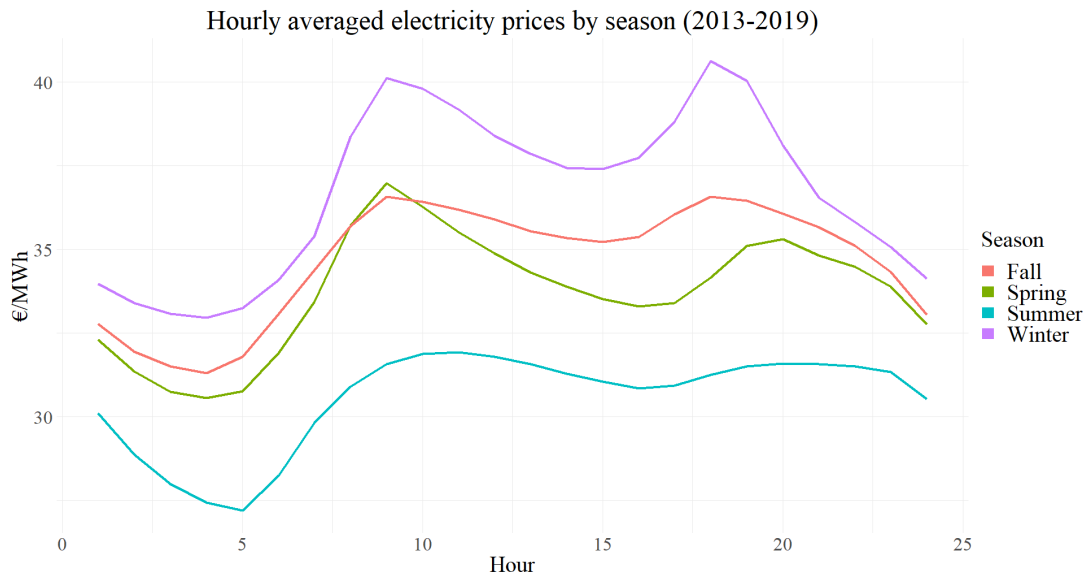


Figure 4.3: Hourly average, filtered by season, of electricity prices for Nord Pool NO2 region (2013-2019).

Having determined important seasonal variations to include in the aggregated data, the next step is to reduce the number of observations while still maintaining said seasonality. We achieve this by creating an hourly average, representative weeks for each season and year. Consequently, leaving us with $24 \cdot 7 \cdot 4 = 672$ observations each year, meaning 4,704 observations for 2013-2019, compared to 61,344 observations in the raw data. A graphical illustration of the aggregation for 2019 is shown in Figure 4.4, in which the first 24 hours are an average Monday, and so on.

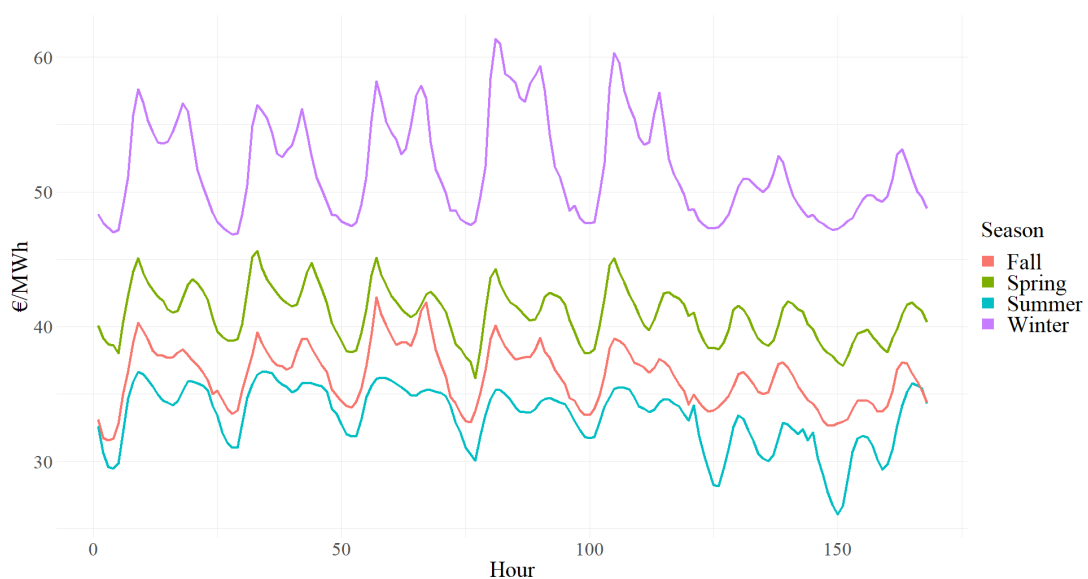


Figure 4.4: Representative weeks for winter, spring, summer and fall 2019 for Nord Pool NO2 region.

4.1.3 Data sampling

After aggregating the data, 28 representative weeks remain across the period from 2013 to 2019. Next, to allow for realistic and robust results, the aggregated data is used to create a sample representing electricity prices 20 years ahead. A 20-year sample is created, which allows for year-to-year variations, such that the model does not become too dependent on one single year of observations but instead allows the model to optimize based on a sequence of several different years.

The price level and variance of the sample are adjusted to follow future estimates from Norwegian energy agencies. Projections suggest that the difference between high and low energy prices are expected to become more evident as we move towards 2050. This increases the incentives to avoid hydrogen production during hours of expensive electricity prices (Statnett, 2020). Therefore, it becomes important to capture this development in the electricity price data used in the model. We consider future electricity price estimates from Statnett and the Norwegian Water Resources and Energy Directorate (NVE) when creating future electricity price scenarios. Estimates for Nord Pool NO2 region are presented in Table 4.3, while an overview for all regions can be found in Appendix A2.1 and A2.2.

Table 4.3: Future electricity prices estimates for Southwestern Norway (NO2) from Statnett and NVE (Statnett, 2020; NVE, 2020a).

Year	Statnett (€/MWh)	NVE (€/MWh)
2020	28.00	-
2022	-	36.99
2025	34.00	40.93
2030	36.00	39.04
2040	39.00	39.53

Note: NVE's estimates are originally denoted in øre/kWh. These are converted to €/MWh with an exchange rate of 0.093 €/NOK.

Modeling one year of production, using an annuity to scale and derive 20 years of cost, in similarity to the model from Kaut et al. (2019), will result in the same electricity price pattern throughout the system lifetime. As mentioned, we intend to achieve certain

robustness by introducing years with different price levels, patterns, and fluctuations. We start by drawing 20 years, at random, from the sample of aggregated years (2013-2019). This is done to create a degree of uncertainty and stochastic sense in the data, creating an unknown/unpredictable pattern of variation between years, seasons, days, and hours. After creating a sample data-frame with 20 years' worth of observations, the data is adjusted based on future projections regarding price level and fluctuations. When adjusting the level of our price scenarios, we use the predictions by NVE to maintain robustness and avoid overly optimistic scenarios, as these prices are higher than the estimates provided by Statnett. We begin the price adjustments by centering the data around zero by subtracting the mean for each given year, illustrated in Figure 4.5.

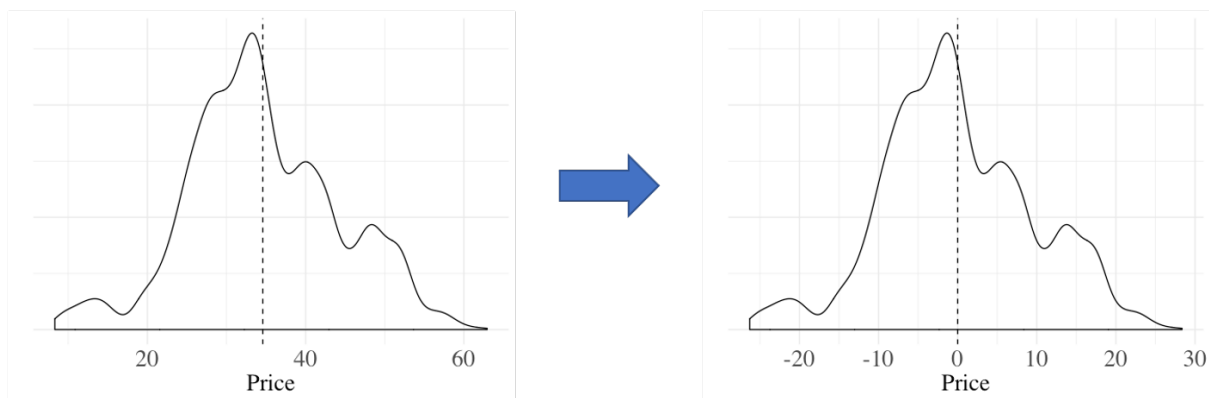


Figure 4.5: Transformation of the data from original mean to zero mean.

Further, we re-level the data by adding the estimated price for the given year, thus retaining the same historical fluctuations but changing the mean. The mean electricity price for 2019 is used to level the first two years, the estimate for 2022 is used to level years 3-5, the 2025 estimate is used to level years 6-10, the 2030 estimate is used to level years 10-19, and the 2040 estimate is used to level year 20. This adjustment of electricity prices is performed for our base scenario, noted as *today* in Table 4.4. The mean of the medium and long-term scenarios corresponds to future estimates, in which the price level in the *medium term* consists of 50/50-weighted estimates for 2030 and 2040 while the price level for the *long term* consists only of 2040-estimates. Furthermore, Statnett states that future electricity prices will be subject to increased volatility and larger gaps between winters and summers due to the introduction of more renewable energy sources such as wind and solar (Statnett, 2020). This is assumed to apply when we compute future electricity prices. To adjust the data for the projected increase in volatility in future scenarios, the

zero-mean data is multiplied with a factor to amplify the spikes both in positive and negative directions before the estimated mean is added. The increased volatility in the long-term scenario introduces 9 periods with negative spot prices, a phenomenon that has been observed in 2020 in some parts of Norway (NVE, 2020a). Consequently, we assume this to be more likely to occur in the future as well. However, it is conceivable that water electrolysis during off-peak hours and batteries could counteract this (Statnett, 2020).

Table 4.4: Summary statistics of electricity price scenarios (€/MWh).

Case	Minimum	25% quantile	Mean (μ)	75% quantile	Maximum	St. dev. (σ)
Today	18.82	35.24	39.39	43.31	61.69	6.11
Medium term	2.71	31.34	39.29	46.88	81.05	11.94
Long term	-5.89	29.67	39.53	48.99	91.43	14.93

A graphical illustration of the different electricity price scenarios is shown in Figure 4.6. There are fluctuations and patterns throughout the period, with spikes in either direction. The increase in fluctuations is evident when comparing today's and future prices. As mentioned previously, the bottom scenario (long-term) also introduces occurrences of negative prices.

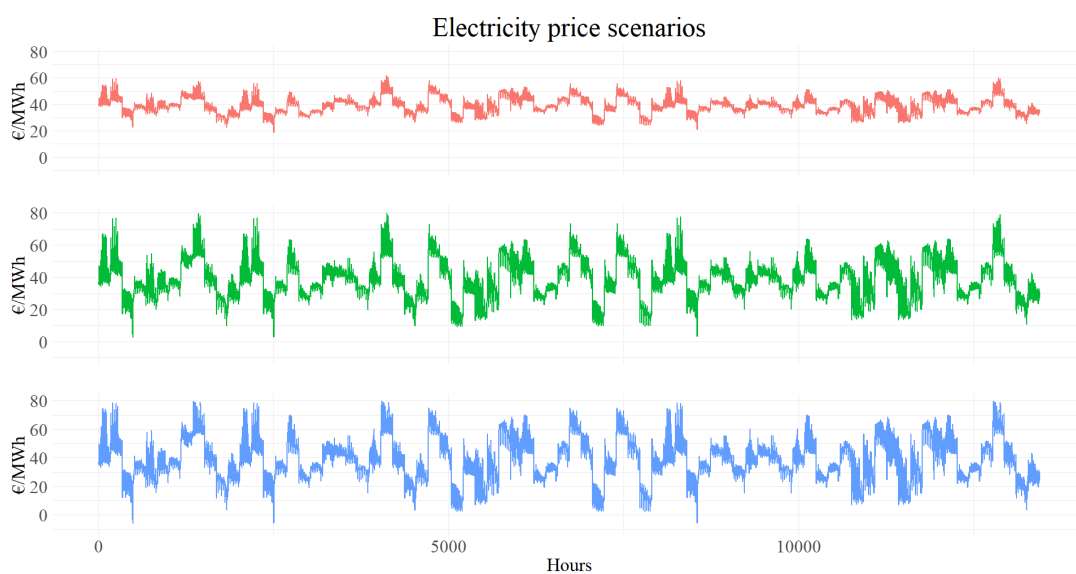


Figure 4.6: 20 year aggregated electricity price scenarios for different time horizons. Top: today. Middle: medium-term (2030). Bottom: long-term (2040).

4.2 Plant costs

In 2019, The International Energy Agency (IEA, 2019) published a report based on the latest available information and data from publications, governments, and industry contacts, regarding the production and usage of hydrogen. The report states that various technical and economic factors influence the production costs of water electrolysis. Due to computational limitations, our focus will remain on the most important plant costs, which according to IEA are – electrolyzer CAPEX, electrolyzer OPEX, electrolyzer cell-stack replacements, storage CAPEX, electricity costs, and other operational costs. In other words, the cost of a hydrogen plant mostly depends on the capital and operational expenditures of the production and storage equipment and the production cost of the hydrogen, which depends on the cost of electricity and the equipment efficiency.

Several studies confirm IEA’s cost assumptions. Recently, Yates et al. (2020) developed a framework for computing the cost of hydrogen from water electrolysis powered with renewable energy. A Monte Carlo analysis indicated that system size, capital costs, and electrolyzer efficiency are the three most important factors affecting the levelized cost of hydrogen. Even though their study considered off-grid, stand-alone PV, we assume that their conclusions about important cost parameters are transferable to our case regarding grid-connected, on-site electrolysis. There is, however, a range of variability for all cost parameters. Buttler and Spliethoff (2018) published a review regarding the current status of water electrolysis. The results were gathered through market surveys, discussions with manufacturers, project reports, and literature and compared to provide a basis for required parameters. These findings are also partially used by IEA (2019). However, IEA’s report has been supplemented with research from several other studies as well. Brynolf et al. (2018) published an article that reviews the production costs of electro-fuels for the transport sector. The production costs were assessed through (1) a literature review to determine important parameters, (2) a more comprehensive review of costs at different production steps, and (3) calculations to compare production costs and perform a sensitivity analysis of important cost parameters. Adam Christensen (2020) published an assessment of hydrogen production costs with a focus on transparency regarding cost assumptions with the purpose of comparable H₂ prices without the need to examine all the details. We will address the details of the mentioned cost parameters related to our

mathematical model in the following subsections. A complete overview and comparison between studies can be found in Appendix A3.

4.2.1 Electrolyzer CAPEX

The International Renewable Energy Agency (IRENA) and IEA both state that electrolyzer capital expenditure is one of the critical cost parameters that need to be reduced to reach a viable hydrogen economy (IRENA, 2019; IEA, 2019). There is a common consensus within the hydrogen literature that innovative solutions within electrolysis technology will influence future electrolyzer CAPEX in terms of cheaper materials, improvements in manufacturing (automation), supply chain development, and economies of scale (IEA, 2019). Future projections often estimate electrolyzer CAPEX to be less than half of today's value. Electrolyzer costs are often denoted in €/kW in literature and reflect the unit cost for different system sizes. IEA (2019) states that there is a wide agreement in the literature that today's electrolyzer CAPEX range between 423-1183 €/kW, including power electronics, gas-conditioning, and plant components. The large span in unit costs represent different system sizes; however, they note that the average unit size from 2015-2019 was 1 MW. Proost (2019) specifically states that realistic CAPEX today is 750 €/kW for a single stack 2 MW system, meaning total capital costs of $2,000 \text{ kW} \cdot 750 \text{ €/kW} = \text{€}1,500,000$ for a 2 MW stack. With an average specific energy consumption of 50 kWh to produce 1 kg of H₂, a plant of such size can produce $\frac{2,000 \text{ kW}}{50 \text{ kWh/kg}} = 40 \text{ kg/h}$, resulting in $40 \text{ kg/h} \cdot 24 \text{ h} = 960 \text{ kg/day}$. Further, a production plant can be expanded by combining multiple single stack systems (IEA, 2019). In this thesis, we assume expansions of 2 MW \approx 1 tonne daily production capacity.

Kuckshinrichs et al. (2017) present an engineering top-down approach for cost scaling. This is similar to the cost function from Hanan Luss (1982) regarding capacity expansions, in which economies of scale often is present. It enables to estimate the cost of an investment, given different capacities.

$$Inv_x = Inv_{base} \cdot \left(\frac{Cap_x}{Cap_{base}} \right)^\alpha \quad (4.1)$$

where

Cap = capacity (MW or tonne)

Inv = investment

x = new (investment/capacity)

$base$ = old (investment/capacity)

α = scaling exponent.

Equation 4.1 leads to cost advantages when $Cap_x > Cap_{base}$ and $\alpha < 1.0$. If the scaling exponent is unknown, a value of 0.60-0.70 is often used as default, which is referred to as the six-tenths or seven-tenths rule (Ereev and Patel, 2012). However, Kuckshinrichs et al. (2017) used a higher scaling exponent ($\alpha = 0.85$) for AEL electrolyzer equipment because of its mature technology. Recall that Proost (2019) estimated 750 €/kW for a 2 MW stack, meaning total capital costs of €1,500,000. When up-scaling to a 100 MW plant, which is considered a relatively large plant today, investment costs are expected to be $€1,500,000 \cdot \left(\frac{100 \text{ MW}}{2 \text{ MW}}\right)^{0.85} = €41,707,654$. This is equal to $\frac{€41,707,654}{100,000 \text{ kW}} = 417 \text{ €/kW}$, which correspond to the low-range estimates from IEA today. These calculations are within a similar range as the findings of Proost (2019), who concludes that capital costs for a 100 MW AEL system is expected to be 400 €/kW.

The same calculations can be performed to find the investment costs for different system sizes when the production capacity is denoted in CAPEX/tonne as well, for a given specific energy consumption. We illustrated that a 2 MW plant has an hourly production capacity of 40 kg, equivalent to a daily production capacity of 960 kg when assuming a specific energy consumption of 50 kWh/kg H₂. For the mentioned 100 MW plant, this equals a production capacity of $\frac{100,000 \text{ kW}}{50 \text{ kWh/kg}} = 2,000 \text{ kg/h}$, equivalent to a daily production capacity of $2,000 \text{ kg/h} \cdot 24 \text{ h} = 48,000 \text{ kg/day}$. Using economies of scale from Equation 4.1, we find investment costs to be $€1,500,000 \cdot \left(\frac{48,000 \text{ kg/day}}{960 \text{ kg/day}}\right)^{0.85} = €41,707,654$ for a plant with daily production capacity of 48 tonnes. This is exactly equivalent to the previous example for a 100 MW plant, thus showing that the relationship between MW and tonnes also work for cost scaling. Hence, CAPEX can be denoted as $\frac{€41,707,654}{48 \text{ tonne}} = 868,909 \text{ €/tonne}$. Figure 4.7 illustrates the effect of economies of scale when adjusting the investment between 1-60

tonnes (2-125 MW). The graph illustrates that a 100 MW plant costs 417 €/kW. Given a specific energy consumption of 50 kWh/kg hydrogen, this equals 868,909 €/tonne. Larger system sizes, MW, are related to larger daily production capacity, tonnes, which both lead to lower capital costs per unit.

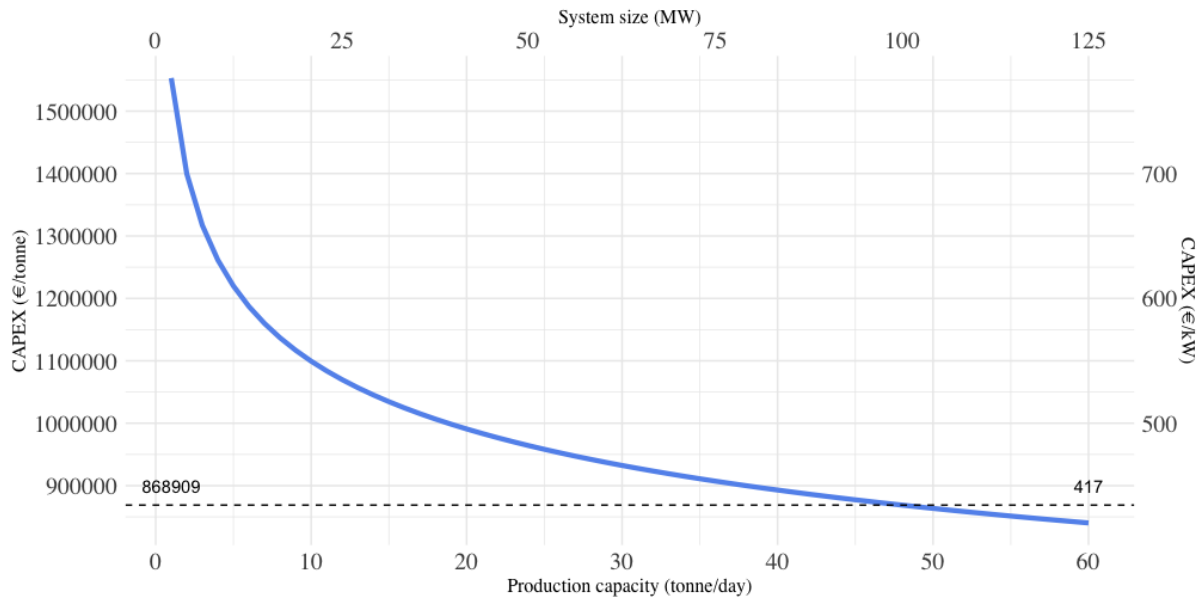


Figure 4.7: Economies of scale for an AEL system using Equation 4.1. Based on CAPEX of 750 €/kW for a 2 MW stack, specific energy consumption of 50 kWh/kg, and scaling exponent of 0.85.

It is expected that scaling up the supply chain of electrolyzer equipment will provide further cost reductions within the industry (IEA, 2019). For future reference, IEA expects CAPEX for AEL systems to be 340-723 €/kW and 170-595 €/kW, depending on system size, for 2030 and in the long term, respectively. The amount of daily production capacity can then be determined given a specific power consumption (efficiency) to produce 1 kg H₂, which is expected to improve in the future.

4.2.2 Storage CAPEX

For storage CAPEX, we use the same cost curves as Mayyas et al. (2020) for stationary tanks. These costs range between 595-422 €/kg for approximately 3 and 30 tonnes storage capacity, respectively. The cost curves display an exponential decrease in unit costs and based on these we use Equation 4.1 to compute a scaling exponent of approximately 0.85 ($\alpha = 0.85$). Total costs are 595 €/kg \cdot 3,000 kg = €1,785,000 for 3 tonnes of storage

capacity and €12,660,000 for 30 tonnes storage capacity. This represents an up-scaling of 10x, from 3,000 to 30,000 kg, meaning that

$$1,785,000 \cdot 10^\alpha = 12,660,000 \Rightarrow \alpha \approx 0.85, \quad (4.2)$$

for storage capacities greater than 3,000 kg and less than 30,000 kg.

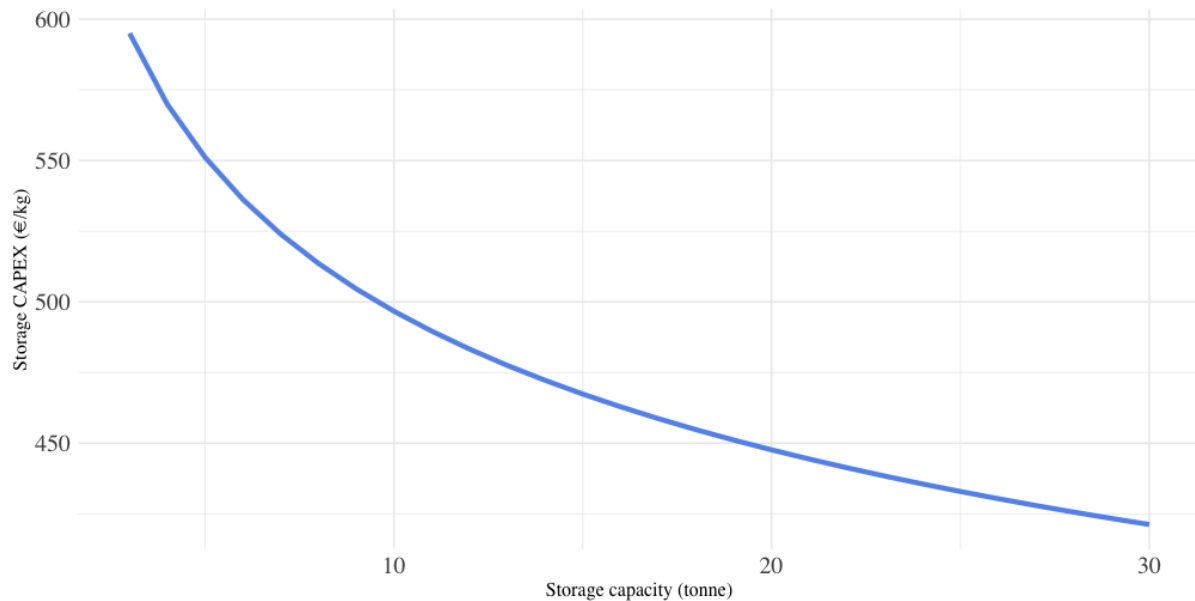


Figure 4.8: Storage CAPEX for different capacities.

For underground storage, other costs apply. The HyUnder overview (Kruck et al., 2013) estimated an investment cost of €28.1 million to initialize a storage cavern with a geometric volume of 500,000 m³. They anticipate that the investment cost can vary immensely between €20-50 million based on infrastructure and prior knowledge about the site. Associated with such an investment, one can store a maximum of 4,000,000 kg of H₂ at 60-180 bar, resulting in a CAPEX of 7.02 €/kg H₂. Crotagino (2016) estimates a specific investment cost of €30-50 per geometric m³, which is lower than the €56 estimated in the HyUnder overview (Kruck et al., 2013). However, 30 €/m³ is an estimation for very large storage facilities of up to 1 000 000 m³. Other research suggests the cost of storage per kg H₂ to be in the range between €0.1 and €35 (Le Duigou et al., 2017; Lord et al., 2014; Ahluwalia et al., 2019). The same research suggests that the storage facilities' size can range between 100,000 m³ and 1,000,000 m³.

For our purpose, we use Ahluwalia et al. (2019) estimates for underground storage as they

provide the latest and most detailed analysis of large-scale underground storage costs. These costs are assumed to be 29.75 €/kg for a total storage capacity of 500,000 kg H₂, equivalent to a total investment cost of €14,875,000.

4.2.3 Electrolyzer OPEX

Electrolyzer OPEX is considered as operating and maintenance expenses relating to electrolyzer equipment. These costs are most commonly computed as a fraction of CAPEX costs, and many studies agree upon a range of values. Brynolf et al. (2018) mention that OPEX range between 2-5% per year of CAPEX, while Buttler and Spliethoff (2018) present a more narrow interval between 2-3%. Most of the costs are fixed costs for routine maintenance and cleaning. Variable costs, such as the cost of water and KOH-solution, which depends on the production quantity, are so small that they are often considered negligible. Yates et al. (2020) state that water costs are only to be considered in cases of uncertainties regarding the water supply. However, we assume this not to be the case for the location selected in this thesis.

4.2.4 Storage OPEX

Storage facilities' operational costs are limited and rarely focused upon when modeling hydrogen production with storage. Kharel and Shabani (2018) do not include any operation and maintenance costs in their study of hydrogen storage. Some have, however, included it as a fixed parameter cost based on the storage CAPEX. Gorre et al. (2019) suggest that the variable OPEX is priced into the fixed OPEX, which sums to equal 1.5% yearly of storage CAPEX.

4.2.5 Cell-stack replacement

AEL carries several advantages compared to other electrolyzer technologies, one of them being the long lifetime of cell-stacks. IEA (2019) estimates cell-stack lifetime of 60,000–90,000 operating hours today. Assuming a plant constantly running at 100% utilization, these estimates equal to a lifetime of 7-10 years⁹. Brynolf et al. (2018) estimated cell stack replacement costs to be approximately 50% of the initial investment. However,

⁹60,000 operating hours: $60,000 \text{ h} \div 8760 \text{ h/yr} = 6,84 \text{ yrs}$. 90,000 operating hours: $90,000 \text{ h} \div 8760 \text{ h/yr} = 10,27 \text{ yrs}$.

Matute et al. (2019) found 45% to be reasonable, while the recent study from Yates et al. (2020) used a nominal replacement cost of 40% with 35% as a lower bound and 45% as a higher bound. Also, the production capacity is often modeled to decrease over time. Yearly degradation is considered to be in the range of 0.3-1.5% (Buttler and Spliethoff, 2018; Yates et al., 2020).

4.2.6 Grid fees

Water electrolysis plants are often regulated by local grid fees. For Norwegian electricity customers, there is no exception. Grid fees in Norway are paid to local companies that own the grid and can be both fixed and variable (NVE, 2019). AEN (2020)¹⁰, a local grid company in the NO2 region, states on their website that they operate with a grid fee of 4.20 €/kW/month¹¹ during winter and 0.69 €/kW/month¹² during summer. Additionally, a variable fee of 0.00156 €/kWh¹³ occur. A dialogue with AEN tells us that, as of 2020, these fees assume energy-demanding customers with a facility greater than 15MW, more than 5,000 yearly operating hours, and high voltage connection to the regional grid. A 15MW electrolysis plant has a daily production capacity of approximately 7 tonnes of hydrogen, well within the limit of large-scale hydrogen production plants. The fixed cost of 4.61 €/month¹⁴ is neglected in our case.

Additionally, Norwegian grid companies are also required by law to charge taxes on behalf of the government¹⁵. However, Forskrift om særavgifter (2001) § 3-12-13 state that electric power used for electrolysis is exempted from this, and therefore, it is not considered in our case.

4.2.7 Electricity consumption

The consumption of electricity is an important variable cost and relates the efficiency and the hydrogen production quantity. Buttler and Spliethoff (2018) found that the efficiency of available electrolysis stacks is in the range of 63-71% (LHV), meaning a

¹⁰Agder Energi Nett (Agder Energy Grid).

¹¹45.48 NOK/kW/month.

¹²7.49 NOK/kW/month.

¹³16.8 NOK/MWh.

¹⁴50 NOK/month.

¹⁵Referred to as *forbruksavgift*.

specific energy consumption of 46-52 kWh/kg. Adam Christensen (2020) uses IEA's estimates for efficiency (LHV) of 63-70% and 70-80% for 2020 and long term, respectively. This converts to a specific energy consumption of 47-52 kWh/kg today and 41-47 kWh/kg in the future. However, these rates are assumed to apply for electrolyzer stacks rather than the system efficiency, meaning that they involve the electrolytic process but excludes energy lost to the balance of system components. Buttler and Spliethoff (2018) differentiates between the stack and system efficiency, in which the latter is found to be 51-60% (LHV), or 55-65 kWh/kg. This is slightly worse than Brynolf et al. (2018), which determined a system efficiency of 65% (LHV), or 51 kWh/kg. Recent research from Yates et al. (2020) who also consider system efficiency, rather than stack efficiency, operate with a nominal specific energy consumption of 54 kWh/kg with values ranging between 50-58 kWh/kg for their Monte Carlo simulation. Additionally, hydrogen from alkaline water electrolysis is usually produced at around 20 bar. Therefore, it requires energy to compress hydrogen to an appropriate storage or transmission pressure of 380 bar. The additional energy for compression is approximately 3 kWh/kg on top of the original electricity consumption.

4.2.8 Utilization

The energy consumption is also related to the utilization of the electrolyzer. An AEL system must satisfy a minimum load at 10% to 20% of the nominal load when it is turned on, according to IEA (2019) and Buttler and Spliethoff (2018), respectively. However, NEL, a Norwegian electrolyzer manufacturer, informs that their AEL systems have a 15-100% load range (NEL, 2020). Operating the equipment at a lower utilization has some advantages. The main advantage is that it requires less power to produce the same amount of hydrogen (Brynolf et al., 2018). However, changing between high and low utilization requires additional power, which is assumed to counteract the benefits of running the system at a lower utilization. For scheduling optimization in chemical problems, variable dependant efficiencies often lead to very complex models, so that these types of characteristics usually are simplified to be constant values (Schulte Beerbühl et al., 2015).

4.2.9 Cold starts and standby

If an electrolyzer system is turned off, it is depressurized and becomes cold. It needs additional power to build up the required pressure and temperature to produce hydrogen whenever it is turned back on. Even though several researchers discuss cold-starts, the focus is more on the time it takes to perform a cold start, often < 15 min, rather than its cost. However, Greensight states that cold starts could range between 100-500 kWh/tonne of daily production capacity.

Another possibility is to run the electrolyzer in standby mode, meaning it is on but does not produce any hydrogen. This is desirable to maintain pressure and temperature and can be beneficial for shorter periods of time. Over longer periods, cold starts may be beneficial instead. To maintain pressure and temperature, Matute et al. (2019) state that power consumption is 2% of full load.

4.2.10 Discount rate

For discounting, we choose to calculate the weighted average cost of capital (WACC). NVE (2016) provides a detailed explanation of how this parameter can be calculated, and we find it suitable for our purpose since much of their work revolves around energy-related projects. Investments in water electrolysis are also based on available capital, either equity or bank loans. Kuckshinrichs et al. (2017) state that a reasonable equity-debt-ratio is 25:75 for Western European countries, while NVE (2016) considers 40:60. Debt financing provides the benefit to leverage a small amount of capital, enabling growth that may not otherwise be possible. The downside of debt is the interest payments; however, these are generally tax-deductible (Berk and DeMarzo, 2017). For our case, we consider equity of 100%, in similarity to Yates et al. (2020). Despite the fact that this might be unrealistic, we do not expect the debt leverage to change the decisions regarding the production schedule in terms of how much, and when, to produce on an hourly basis. Kuckshinrichs et al. (2017) also mention that the inflation rate is one of the macroeconomic parameters that are the most difficult to predict over long-term horizons. Nevertheless, we choose to operate with the central bank of Norway's long-term inflation target of 2% (Norges Bank, 2020). The tax rate is considered to be 22% according to the Norwegian Ministry of Finance (2019). For equity beta, Damodaran (2020) provides a detailed overview of beta

values for renewable companies in Western Europe. We base our calculations on these numbers, which provides us with an equity beta of 1.01. This is used to replace NVE's equity beta value of 0.875 for a grid company. Hence, our calculation for the WACC is

$$WACC_{pre-tax}^{real} = (1 - G) \cdot \left[\frac{R_f + infl + \beta_e \cdot MP}{1 - t} \right] + G \cdot (Swap + P_d),$$

where

G = Gearing (Debt share of total capital): *Irrelevant*,

R_f = Real risk free rate for equity: 1.50%,

$infl$ = Inflation rate: 2.00%,

β_e = Equity beta: 1.01,

MP = Market premium: 5.00%,

$Swap$ = Nominal rate for debt: *Irrelevant*,

P_d = Debt premium: *Irrelevant*,

t = Tax rate: 22.00%.

A few of the variables differ from NVE (2016), mainly the equity beta and the gearing parameter. Due to the assumption of using 100% equity financing, the cost of debt is not considered. The real, pre-tax WACC is computed to be $\frac{1.5\%+2\%+1.01 \cdot 5\%}{1-22\%} = 10.96\%$. This is just above the findings from Kuckshinrichs et al. (2017), which finds $WACC^{real}$ for energy technologies in Western European countries to be within 4-10%. However, the equity-debt-ratio affects the weighted average cost of capital so that an increase in equity leads to a higher WACC, which is present in our case.

5 Model

This chapter explains the mathematical formulation of the model used to minimize the production cost of hydrogen. Section 5.1 presents an introduction and the general idea of the model, while the associated sets, parameters, and decision variables follow in Section 5.2 and 5.3. Section 5.4 and 5.5 explain the objective function and constraints, respectively.

5.1 Model introduction

Schulte Beerbühl et al. (2015) mention that short-term models often feature a profit maximization objective, whereas long-term analysis, with horizons of 15 to 45 years, are usually formulated as cost minimization problems. Our model aims to solve a production and capacity planning problem by scheduling optimal hydrogen production over a system lifetime to minimize total costs. We explore investments in different production and storage capacities while being subject to a minimum demand each period. By combining excess production capacity with storage possibilities, we seek to minimize the total production costs for an alkaline water electrolysis plant. The demand is assumed to be equal for all decision periods. Yet, our problem lies in the many possible combinations of satisfying hourly demand, either through production, storage withdrawals, or a combination of the two. We use multi-period, mixed-integer linear programming (MILP) to minimize costs for investing, running, and maintaining a hydrogen production plant over its lifetime. The purpose is to explore the possibility of reducing the cost of hydrogen by investing in additional production and storage capacity to satisfy the demand during expensive electricity price periods, through production during inexpensive electricity price periods. The model is subject to some assumptions due to computational limitations. However, the most vital cost components in hydrogen production, according to the International Energy Agency (IEA, 2019), are incorporated.

MILP is a mathematical optimization method in which the objective function, and the constraints, are linear functions of some variables. Also, problems of this kind consist of both integer and continuous variables. The introduction of integer constraints cause a stricter, more complex, and thus more computationally expensive approach compared to

simple linear programming (Larrosa et al., 2020). However, two important advantages of MILP compared to mixed-integer non-linear programming (MINLP) are outlined by Urbanucci (2018). The first advantage is that MILP guarantees the program to converge towards an optimal solution at the global maximum or minimum. However, when the program is unbound – or there are no feasible solutions due to the contradiction between constraints – the solution will not converge towards the optimal solution. The second advantage is that linear programs are less computationally expensive, and well-written algorithms assure efficient solving by commercially available solvers, such as CPLEX, Gurobi, and Xpress. This is beneficial when the planning horizon reaches thousands of time steps, such as in our case. An efficient program allows for quick adjustments and the possibility to run multiple scenarios without time being a major concern.

Our model consists of a multi-period optimization problem, meaning that the decision variables are determined for several periods. Several aspects need to be considered to solve problems of this kind. First and foremost, the balance between periods needs to be considered, as the initial balances for each period must be aligned with the outgoing balances from previous periods. If this is not done properly, the model will not yield realistic results, and the output from the model can be misleading. Also, multi-period modeling allows constraints and values to change between periods, which can result in different solutions for each period. However, a limitation of multi-period models is that they become more computationally expensive for each additional period included in the model.

Another aspect of the optimization in this thesis is that it consists of two layers. The decision model itself is a production planning model that decides when and how much hydrogen to produce and store to minimize the total cost of a hydrogen production plant over its lifetime, subject to electricity prices and different parameter values, and a set of equality and inequality constraints. Outside the decision model itself, we investigate several different production and storage capacities to see which ones yield the overall lowest total costs while keeping the other parameter values constant. Thus, production and storage capacity are treated as exogenous variables set prior to solving the decision model. Given a production and storage capacity, the decision model finds the optimal values for a set of endogenous variables concerning the most cost-efficient production

schedule. An endogenous change is a response to an exogenous change that is imposed upon the model. Meaning that each combination of production and storage capacity yields different results in terms of the production schedule. Consequently, the model aims to find the lowest overall cost based on production and storage capacity (exogenous) and the associated production schedule (endogenous). Therefore, in contrast to standard optimization procedures, we choose to include several fixed costs in the objective function as it makes it possible to compare results when changing production and storage capacities. Lastly, the periods in the model are calculated as representative periods to reduce the computational expensiveness of the multi-period model. These periods are structured following the aggregation of the electricity data presented in Section 4.1.2. Each year consists of four representative weeks, one for each season, and each representative week is constructed of seven days, each consisting of 24 hours. Thus, all hourly decision variables in the model represent one hour in a representative week. In reality, all representative weeks are repeated approximately 13 times within a season, depending on the number of days in the season.

5.2 Sets and parameters

Because we want to be able to distinguish between different periods in the model, based on the hour of the day, in a season and year, we have opted to stray away from the traditional approach of having one set, $t \in T$, for defining periods. Instead, we operate with four different sets, representing all years, seasons, days, and hours over the modeled period. However, this increases the number of constraints when handling the flow from the end of the previous period to the beginning of the current period. In a traditional scheduling problem, the flow from $t - 1$ to t must be satisfied, often to ensure correct inventory balance. For the following model in this thesis, the flow must be satisfied from the last hour in year $y - 1$ to the first hour in year y ; the last hour in season $s - 1$ to the first hour in season s ; the last hour in day $d - 1$ to the first hour in day d ; and from hour $h - 1$ to hour h . Although requiring some additional attention regarding constraints, we find that it enhances the structure of the outputs and maintains an easy to follow flow between representative periods. A description of all sets is presented in Table 5.1.

Table 5.1: Model sets.

Set	Description	Value
Y	Set of all years.	$\{1, 2, \dots, 20\}$
S	Set of all seasons.	$\{1, 2, 3, 4\}$
D	Set of all weekdays.	$\{1, 2, \dots, 7\}$
H	Set of all hours.	$\{1, 2, \dots, 24\}$
$Y_{restack}$	Set of years to perform cell-stack re-stack.	$Y_{restack} \subset Y$

The set containing the years represent the system lifetime and the overall operational period (1-20); the set of seasons is divided into winter (1), spring (2), summer (3), and fall (4); the set of weekdays is divided into Monday (1), Tuesday (2), Wednesday (3), Thursday (4), Friday (5), Saturday (6) and Sunday (7); while the set of hours represent all hours in a day (1-24).

Most parameter values are described throughout Chapter 4. A more tidy presentation of each parameter's exact value is specified later for different scenarios. While most parameter values remain unchanged, the most important parameters to explore are the production capacity, Cap_{prod}^{tonne} , which represents the amount of daily production capacity in tonnes; and storage capacity, Cap_{stor} , which represents the maximum amount of storage. These parameters set a limit for the available daily production quantity and storage quantity and are subject to changes to investigate the financial benefit of investing in excess production capacity and storage. These are considered fixed parameters because exponential cost functions for economies of scale, such as Equation 4.1 in Section 4.2.1, would introduce non-linearity if capacities are treated as decision variables. Hence, we compute total CAPEX for a fixed capacity and run the model multiple times with different capacities to maintain linearity. We explore a broad range of capacities to derive an optimal decision regarding daily production and storage capacity.

Table 5.2: Model parameters.

Parameter	Description	Unit
$Offtake$	Minimum off-take of hydrogen in each period.	kg
$Cap^{prod,tonne}$	Maximum daily production capacity.	Tonne

Table 5.3: Continuation of Table 5.2

Parameter	Description	Unit
$Cap^{prod,kg}$	Same as $Cap^{prod,tonne}$. Denoted in kg for readability purposes.	kg
Cap^{stor}	Maximum storage capacity in any period.	kg
C^{Elec}	Electrolyzer capital expenditure.	Euro/kW
$C^{Storage}$	Storage capital expenditure.	Euro/kg
O^{Elec}	Yearly OPEX for electrolyzer.	%
$O^{Storage}$	Yearly OPEX for storage.	%
α^{prod}	Scaling exponent for electrolyzer capital costs.	$0 < \alpha^{prod} < 1$
α^{stor}	Scaling exponent for storage capital costs.	$0 < \alpha^{stor} < 1$
$Restack$	Stack replacement cost.	%
$Periods_{y,s}$	Amount of weeks in a season s , in a given year y . Found by dividing the number of days in a season by seven.	Weeks
$Price_{y,s,d,h}$	Price of electricity in year y , season s , day d and hour h .	Euro/kWh
$Efficiency$	Specific energy consumption to produce 1 kg H_2 (system efficiency).	kWh/kg
$Compression$	Specific energy consumption to compress 1 kg H_2 from 20 bar to 380 bar for storage.	kWh/kg
$Standby_prc$	Specific energy consumption to maintain pressure, temperature, etc., when the system is on standby. Percentage of system efficiency.	%
$Cold_start$	Specific energy consumption due to cold starts. Related to the system size.	kWh/tonne
$Grid_cost_s$	Grid costs in season s dependant on electrolyzer size.	Euro/kW

Table 5.4: Continuation of Table 5.2 and Table 5.3.

Parameter	Description	Unit
$Grid_cost^{var}$	Variable grid fee dependant on power consumption.	Euro/kWh
Cap_red	Yearly degradation of electrolyzer cell stack capacity.	%
Min_util	Minimum utilization of electrolyzer capacity when it is in a production state.	%
$Rate$	Yearly discount rate (WACC).	%
T^{stor}	Indicating whether tank or underground storage is assumed.	$\begin{cases} 0: \text{Underground} \\ 1: \text{Tank} \end{cases}$
M	Big M parameter to linearize the product of two variables.	Large number

5.3 Decision variables

Model decision variables are presented below in Table 5.5 and can be both continuous or binary. Current capacity is computed subject to maximum production capacity, yearly degradation of electrolyzer equipment, and when re-stacks are set to occur (Kaut et al., 2019). Production quantity and storage quantity represent the amount of hydrogen produced or stored in a given period. A combination of production and storage withdrawals must satisfy the minimum required off-take of hydrogen. The model aims to find the most cost-efficient combination of the two, in regards to electricity prices and other costs, as well as operational constraints. Two other operational variables are used to track the electrolyzer equipment's state, determining whether the system is on, off, or in standby mode. The system must operate within a given range of utilization when it is on. However, it can be set in an idle or standby state, thus stopping production when this is financially beneficial. Running the system in a standby state still requires some power to maintain a certain pressure and temperature. If the system is in an idle state, turning the system back on requires a significant amount of additional power to reach the desired pressure and temperature.

Table 5.5: Model decision variables.

Variable	Description	Type
cap_y	Daily production capacity each year y subject to degradation.	Continuous
$\mathbf{x}_{y,s,d,h}$	Amount of hydrogen in kilos produced in year y , season s , day d and hour h .	Continuous
$\mathbf{s}_{y,s,d,h}$	Amount of stored hydrogen in kilos in year y , season s , day d and hour h .	Continuous
$\text{idle}_{y,s,d,h}$	Whether electrolyzer is on or off in year y , season s , day d and hour h .	$\begin{cases} 0: \text{On} \\ 1: \text{Off} \end{cases}$
$\text{standby}_{y,s,d,h}$	Whether electrolyzer is in standby-mode in year y , season s , day d and hour h .	$\begin{cases} 0: \text{Not standby} \\ 1: \text{Standby} \end{cases}$
$\text{cold_start}_{y,s,d,h}$	Determines whether a cold start occurred in year y , season s , day d and hour h .	$\begin{cases} 0: \text{No cold start} \\ 1: \text{Cold start} \end{cases}$

5.4 Objective function

The objective function consists of capital costs and operational costs. Capital costs depend on system size, e.g., the amount of daily production capacity and storage capacity. Some other costs are also related to the system size and storage capacity, such as cell-stack replacements, electrolyzer and storage OPEX, and monthly grid costs. Variable operational costs are considered to be affected by the cost of electricity and variable grid costs. These costs depend on production quantity, which leads the model to find how much to produce and when, how much to store and when, and what state to operate the electrolyzer in at any given time. The mentioned costs are considered to be the most influential when determining hydrogen costs from water electrolysis (IEA, 2019).

A detailed explanation of the different costs included in the objective function is presented in the following paragraphs. The objective function is explained in the following order: (1) capital cost of electrolyzer, (2) capital cost of storage, (3) electrolyzer OPEX, (4) storage OPEX, (5) cell-stack replacement costs, (6) grid fees, (7) production costs, (8) standby

costs, and (9) cold start costs. (1)-(6) are dependant on the pre-determined production and storage capacities, while (7)-(9) are dependant on scheduling optimization. Hence, we intend to explore how total costs are affected by investment in different production and storage capacity combinations. Although (1)-(6) are not affected by the decision variables and unrelated to changes in the production scheduling itself, we choose to include them in the objective function as a part of total costs for the system lifetime. The combination of capital and operational costs (1)-(9) is of interest when establishing the relationship between daily production capacity and storage capacity to derive the overall hydrogen cost.

5.4.1 Electrolyzer CAPEX

We provide a general approach to derive electrolyzer CAPEX for different system sizes because we intend to explore various daily production capacities. The electrolyzer CAPEX is originally denoted in cost per kW, which is assumed to be €/kW for a 2 MW stack (Proost, 2019). Daily production capacity, however, is measured in production output and denoted in tonnes or kg. For a given daily production quantity, kg, and system efficiency, kWh/kg, we can compute the plant size in power. The plant size, kW, can be computed by multiplying the hourly production capacity, kg/h, with the specific energy consumption required to produce 1 kg of hydrogen, kWh/kg.

$$Cap^{prod,kW} = \frac{Cap^{prod,kg}}{|H|} \cdot Efficiency. \quad (5.1)$$

Equation 5.1 derives the hourly energy consumption, kWh, required to produce a given amount of hydrogen each day. This is equivalent to the plant size in power, kW.

Further, Equation 4.1 (economies of scale) is used to adjust CAPEX for different system sizes. Recall that 2 MW (2,000 kW) is assumed as *base* when up-scaling. We insert Equation 5.1 into Equation 5.2, where

$$CapeX^{Tot_elec} = (C^{Elec} \cdot 2,000) \cdot \left(\frac{Cap^{prod,kW}}{2,000} \right)^{\alpha^{prod}} \quad (5.2)$$

is computed to derive total capital expenditure for electrolyzer equipment. $C^{Elec} \cdot 2,000$ is the total investment for a 2 MW plant, $\frac{Cap^{prod,kW}}{2,000}$ represents the up-scaling from a 2

MW plant, and α^{prod} is the scaling exponent.

5.4.2 Storage CAPEX

Storage capital expenditure in Equation 5.3 is computed similarly to the electrolyzer CAPEX. However, the calculation of the storage equipment CAPEX depends on whether storage tanks or underground salt caverns are assumed. When considering tank storage, $T^{stor} = 1$, the first part of Equation 5.3 is initiated. A base capacity of 3,000 kg is assumed, and the costs are scaled in accordance with the discussion in Section 4.2.2. If underground storage is assumed, $T^{stor} = 0$, the second part of the equation is initiated. The base investment is then calculated based on a storage capacity of 500,000 kg, which is multiplied by the associated storage CAPEX per kg.

$$\begin{aligned} Capex^{Tot-stor} = & C^{Storage} \cdot 3,000 \cdot \left(\frac{Cap^{stor}}{3,000} \right)^{\alpha^{stor}} \cdot T^{stor} \\ & + C^{Storage} \cdot 500,000 \cdot (1 - T^{stor}). \end{aligned} \quad (5.3)$$

5.4.3 Electrolyzer OPEX

Equation 5.4 computes the yearly operational and maintenance (OPEX) costs for the electrolyzer equipment. Yearly OPEX is computed as a fraction of capital expenditure for electrolyzer production equipment and discounted yearly. We refer to the discussion in Section 4.2.3, in which variable OPEX is considered so small that they are computed as part of the fixed OPEX.

$$Opex_y^{Elec} = \frac{Capex^{Tot-elec} \cdot O^{Elec}}{(1 + Rate)^y}, \forall y \in Y. \quad (5.4)$$

5.4.4 Storage OPEX

Equation 5.5 computes the yearly operational and maintenance (OPEX) costs for storage. Yearly OPEX is computed as a fraction of capital expenditure for storage equipment and discounted yearly. In similarity to electrolyzer OPEX, variable operational costs linked to hydrogen storage are considered insignificant when modeling total plant costs. As we refer to the discussion in Section 4.2.4, the variable OPEX is considered a part of the fixed

OPEX.

$$Ope x_y^{Storage} = \frac{Capex^{Tot_stor} \cdot O^{Storage}}{(1 + Rate)^y}, \forall y \in Y. \quad (5.5)$$

5.4.5 Cell-stack replacement

Equation 5.6 computes costs related to the cell-stack replacement. Cell-stack replacement costs are computed as a fraction of the electrolyzer capital costs, independent of *lost* capacity, and discounted yearly.

$$Restack_costs_y = \frac{Capex^{Tot_elec} \cdot Restack}{(1 + Rate)^y}, \forall y \in Y_{restack}. \quad (5.6)$$

5.4.6 Grid fees

When operating in Norway, a water electrolysis plant is subject to grid fees, resulting in several calculations. The grid fees are divided into three joints, discussed in Section 4.2.6. In this paragraph, we calculate the monthly variable grid fee, which is computed based on the maximum hourly energy consumption in a given month and depends on whether the current month occurs during the summer or winter. The maximum amount of energy used in a period depends on the plant size. This can be computed in the following way when assuming a plant runs at 100% utilization at least once within a month. First, we calculate the sum of efficiency, kWh/kg, and compression, kWh/kg, which is the specific energy consumption needed to produce and compress 1 kg H₂.

$$Power_cons = Efficiency + Compression. \quad (5.7)$$

The specific energy consumption per kg hydrogen, kWh/kg, can then be multiplied with the hourly production capacity to compute to maximum hourly energy consumption, kWh. We insert Equation 5.7 into Equation 5.8, where

$$Max_cons = \frac{Cap^{prod,kg}}{|H|} \cdot Power_cons. \quad (5.8)$$

The maximum hourly energy consumption, kWh, is equivalent to the plant size, kW, which is multiplied with the monthly grid fee, €/kW, to derive the monthly grid costs. This is multiplied by 3 because each season consists of three months. Hence, we insert Equation 5.8 into Equation 5.9, where

$$Grid_costs_y = \frac{\sum_{s \in S} (Max_cons \cdot Grid_cost_s \cdot 3)}{(1 + Rate)^y}, \forall y \in Y. \quad (5.9)$$

5.4.7 Production cost

The production cost depends on how much and when the hydrogen is produced. *When* is important due to the difference in electricity prices between periods. The calculation involves the specific energy consumption to produce and compress hydrogen, the cost of energy, and the amount produced. The amount of hydrogen produced in one model period is multiplied by the number of weeks in the corresponding season to compute the total production costs for a representative period.

First, the energy cost can be computed as the sum of the variable grid fee, €/kWh, and electricity price, €/kWh, for the representative period.

$$Power_cost_{y,s,d,h} = (Grid_cost^{var} + Price_{y,s,d,h}), \forall y \in Y, s \in S, d \in D, h \in H. \quad (5.10)$$

Second, the specific energy consumption to produce and compress 1 kg H₂ is the sum of efficiency, kWh/kg, and compression, kWh/kg, which is equal for all periods. This is calculated in Equation 5.7. Third, because we operate with representative periods in the model, the production in a given hour is multiplied by the number of weeks in the corresponding season to find the real produced quantity in that hour.

$$\mathbf{q}_{y,s,d,h} = (\mathbf{x}_{y,s,d,h} \cdot Periods_{y,s}), \forall y \in Y, s \in S, d \in D, h \in H. \quad (5.11)$$

Yearly production cost can then be computed as the sum of hydrogen produced, kg, multiplied by the specific energy consumption, kWh/kg, and the cost of energy, €/kWh.

$$\mathbf{prod_costs}_y = \frac{\sum_{s \in S} \sum_{d \in D} \sum_{h \in H} (\mathbf{q}_{y,s,d,h} \cdot Power_cons \cdot Power_cost_{y,s,d,h})}{(1 + Rate)^y}, \quad (5.12)$$

$\forall y \in Y.$

In reality, the specific energy consumption in water electrolysis, *Efficiency*, is dependant on the production rate. The required energy to produce 1 kg H₂ is lower at lower production rates and vice versa. However, we assume a simplification of the relationship between specific energy consumption and production rate, in which the specific energy consumption is kept constant. This is because the specific energy consumption increases when the production ramps up and down, meaning that it is more efficient to run at a constant rate. These two counteracting effects are assumed to balance each other out somewhat.

5.4.8 Standby costs

When combining hydrogen production through electrolysis, with excess production capacity and storage, switching the system to a standby state to stop production in some expensive electricity periods might be beneficial. However, some costs still occur when the system is in a standby state. First, the cost of running the system in a standby state for one hour, denoted in €/h, is given by

$$Standby_cost_{y,s,d,h} = \frac{Cap^{prod,kg}}{|H|} \cdot Efficiency \cdot Standby_prc \cdot Power_cost_{y,s,d,h},$$

$\forall y \in Y, s \in S, d \in D, h \in H$

(5.13)

The cost is determined as a percentage of running the system on full-load for one hour, denoted in kWh/kg per hour. Therefore, it is necessary to multiply it with the electricity price, €/kWh. To find the yearly standby costs, we need to multiply the sum of hours in which the system has been in standby mode with the number of weeks/repeated periods in the given season. This again has to be multiplied with the cost of having the system in

standby mode for one hour, denoted in €/h. We have that

$$\mathbf{tot_standby_costs}_y = \frac{\sum_{s \in S} \sum_{d \in D} \sum_{h \in H} (\mathbf{standby}_{y,s,d,h} \cdot \mathit{Periods}_{y,s} \cdot \mathit{Standby_cost}_{y,s,d,h})}{(1 + \mathit{Rate})^y} \quad (5.14)$$

$, \forall y \in Y.$

5.4.9 Cold starts

After it has been turned completely off, starting up the electrolyzer is referred to as a cold start. Doing so requires additional power to recover pressure and temperature that was lost when the equipment was turned off. The amount of required power is dependant on the system size. This is computed by multiplying daily production capacity, tonnes, with the required specific energy consumption, kWh/tonne. This is again multiplied with the electricity cost, €/kWh, from Equation 5.10.

$$\mathit{Startup_cost}_{y,s,d,h} = \mathit{Cap}^{prod,tonne} \cdot \mathit{Cold_start} \cdot \mathit{Power_cost}_{y,s,d,h}, \quad (5.15)$$

$\forall y \in Y, s \in S, d \in D, h \in H.$

The yearly cold start costs are summed and discounted.

$$\mathbf{cold_start_costs}_y = \frac{\left(\sum_{s \in S} \sum_{d \in D} \sum_{h \in H} \mathbf{cold_start}_{y,s,d,h} \cdot \mathit{Periods}_{y,s} \cdot \mathit{Startup_cost}_{y,s,d,h} \right)}{(1 + \mathit{Rate})^y}, \quad (5.16)$$

$\forall y \in Y.$

5.4.10 Total costs

A combination of the Equation 5.2-5.6, 5.9, 5.12, 5.14 and 5.16 make up the overall objective function **total_costs** in Equation 5.17. CAPEX, OPEX, re-stack costs, and partly grid fees are dependent on system size and are not affected by the decision variables. They do, however, play a role in determining total costs. Production, standby, and cold start costs are affected by the decision variables when determining how much and when

to produce. The objective is to minimize

$$\begin{aligned}
\mathbf{total_costs} &= Capex^{Tot_elec} + Capex^{Tot_stor} \\
&+ \sum_{y \in Y_{restack}} Restack_costs_y \\
&+ \sum_{y \in Y} (Ope_x_y^{Elec} + Ope_x_y^{Storage} + Grid_costs_y \\
&+ \mathbf{prod_costs}_y \\
&+ \mathbf{tot_standby_costs}_y \\
&+ \mathbf{cold_start_costs}_y).
\end{aligned} \tag{5.17}$$

5.5 Constraints

The constraints are developed to create a realistic model that follows the *rules* for hydrogen production through water electrolysis and take inventory balance in dynamic production scheduling into account. The constraints ensure a smooth flow between production, storage, and off-take for each period and ensure that neither storage nor production exceeds their given limits.

5.5.1 Capacity

The initial investment in production equipment decides the daily production capacity. In the first year, the daily production capacity is equal to the initial investment in production capacity:

$$\mathbf{cap}_{y=1} = Cap^{prod,kg}. \tag{5.18}$$

However, the amount of available production capacity in year y varies throughout the system lifetime. The daily production capacity \mathbf{cap}_y decreases by a yearly degradation parameter Cap_red , which computes

$$\mathbf{cap}_y = \mathbf{cap}_{y-1} \cdot (1 - Cap_red), \forall y \in Y : y > y_1 \text{ and } y \notin Y_{restack}. \tag{5.19}$$

The electrolyzer equipment's degradation is modeled to occur yearly, the first time at the end of year 1 (start of year 2). After cell-stack replacement in year y , the degradation is

assumed to take place at the end of year y (start of year $y + 1$).

Due to the limited lifetime of cell-stacks, it is necessary to perform replacements when these are replenished. This operation resets the production capacity back to its initial value at the designated years. We have that

$$\mathbf{cap}_y = Cap^{prod,kg}, \forall y \in Y_{restack}. \quad (5.20)$$

5.5.2 Storage and inventory balance

First, storage in the initial period is equal to the production in the first hour, minus the hourly off-take, because it does not exist any storage at the beginning of the first period in the model. Hence, the initial storage is given by

$$\mathbf{s}_{y_1, s_1, d_1, h_1} = \mathbf{x}_{y_1, s_1, d_1, h_1} - Offtake. \quad (5.21)$$

Next, to ensure a correct storage-balance between periods in the model, we distinguish between two types of constraints. The first type consists of two constraints that handle the flow between hours within the same day, $h-1$ to h , and the flow between the last hour of one day, $d-1$, and the first hour the next day, d . The second type contains two constraints that handle the flow between seasons within the same year, $s-1$ to s , and the flow between the last and first season across two years, $y-1$ to y . The latter type of constraints is needed because the model is based on representative, aggregated periods where a net difference in storage within a week is repeated multiple times in reality. This will be explained in further detail later.

We start with the balance between hours within and across days. Two constraints ensure that storage in one hour is equal to the difference between production and off-take in that hour, plus the amount of stored hydrogen from the previous hour. For the balance between two hours within the same day, we have that

$$\mathbf{s}_{y,s,d,h} = \mathbf{s}_{y,s,d,h-1} + \mathbf{x}_{y,s,d,h} - Offtake, \forall y \in Y, s \in S, d \in D, h \in H : h > h_1. \quad (5.22)$$

For the balance between the first hour one day and the last hour the previous day, we

have that

$$\mathbf{s}_{y,s,d,h_1} = \mathbf{s}_{y,s,d-1,|H|} + \mathbf{x}_{y,s,d,h_1} - \text{Offtake}, \forall y \in Y, s \in S, d \in D : d > d_1. \quad (5.23)$$

Next, as the model in this thesis uses representative periods for each season in a year, the modeling of the storage between seasons is a bit more complex than in a model that uses the complete data, where the periods follow a strict chronological pattern. Each season in the model is represented by a representative week, meaning that the winter quarter is represented by one winter week in the model. In contrast, in reality, a winter season consists of approximately 13 weeks. If a representative week has a positive net difference between production and off-take, meaning an increase in storage quantity from the start to the end of the week, the model needs to take into account that this net difference, in reality, occurs 13 times, which will result in the storage filling up over the course of the representative week. If there is a negative net difference between production and off-take, the storage needs to be gradually emptied in a similar manner. We base the methodology for modeling the storage on the work of Poncelet (2018). He highlights the need for constraints that allow for net changes in storage within the representative periods in the model, such that the storage can be filled or emptied during the representative periods. Similar to Poncelet (2018), we have that a representative period, characterized by year y and season s , is repeated $Periods_{y,s}$ number of times in reality, before the following representative period, $s + 1$, occurs¹⁶. Having established that a representative week is repeated, we have to calculate the filling or emptying of the storage over the representative periods. The amount of filling or emptying depends on the net difference between production and off-take in a given representative period and how many times the period repeats itself. We have that

$$\Delta s_{y,s} = \sum_{d \in D} \sum_{h \in H} (\mathbf{x}_{y,s,d,h} - \text{Offtake}) \cdot (Periods_{y,s} - 1), \forall y \in Y, s \in S. \quad (5.24)$$

Equation 5.24 illustrates that the net difference between production and off-take over a representative week is multiplied with the number of times the representative week is repeated in reality, minus one. One period is subtracted because that one period is

¹⁶It is also possible that the following period is given by $y + 1, s_1$

already accounted for through the modeling of the representative week. Having calculated the change in storage over the representative period, the relationship between the initial storage in one period and the exiting storage from the previous period can be expressed as

$$\mathbf{s}_{y,s1,d1,h1} = \mathbf{s}_{y-1,|S|,|D|,|H|} + \mathbf{x}_{y,s1,d1,h1} - \text{Offtake} + \Delta s_{y-1,|S|}, \forall y \in Y, \quad (5.25)$$

when the previous representative period occurred the previous year. Hence, Equation 5.25 ensures correct flow of storage quantity between the fall in year $y-1$ to the winter in year y . To ensure a correct flow of storage quantity from season $s-1$ to s within the same year, we have that

$$\mathbf{s}_{y,s,d1,h1} = \mathbf{s}_{y,s-1,|D|,|H|} + \mathbf{x}_{y,s,d1,h1} - \text{Offtake} + \Delta s_{y,s-1}, \forall y \in Y, \quad (5.26)$$

Hence, Equation 5.26 ensures correct a flow between winter and spring, spring and summer, and summer and fall within the same year y .

The theory is displayed graphically in Figure 5.1. The first blue section of the graph illustrates the representative period, which is modeled as $\mathbf{s}_{y,s,d,h}$. The blue section at the very end is the last repetition of the representative period and is defined as $\mathbf{s}_{y,s,d,h} + \Delta s_{y,s}$.

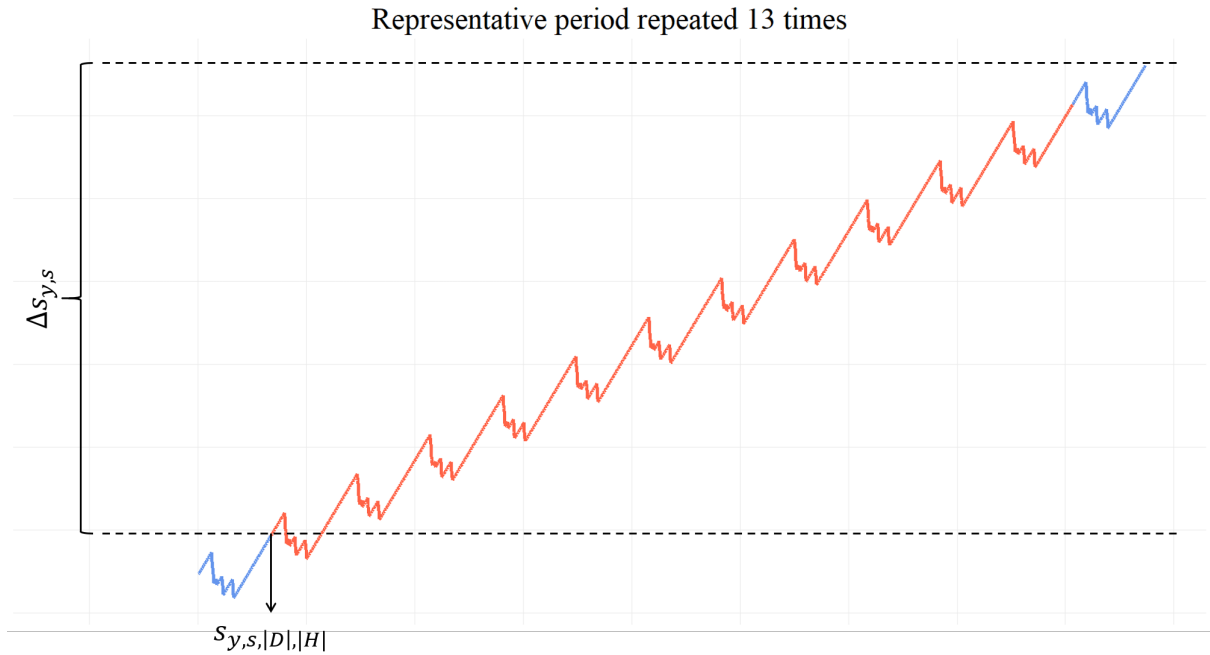


Figure 5.1: Graphical illustration of a case when the storage fills up during a representative period.

The major advantage of modeling the representative periods in the way suggested by Poncelet (2018) is that it easily tracks that the storage in any representative periods does not exceed the maximum storage capacity. As can be seen from the graph above, where storage fills up during the repetitions of the representative period, the maximum storage occurs in the last repetition of the representative period. If the opposite occurs, where the storage empties, the maximum storage for that period is during the representative period's first repetition. Thus, the maximum storage within a season will always occur during the first or last repetition of a representative period. Therefore, to ensure that the storage never exceeds the maximum storage capacity, we have that

$$\mathbf{s}_{y,s,d,h} \leq Cap^{stor}, \forall y \in Y, s \in S, d \in D, h \in H, \quad (5.27)$$

which checks that the storage does not exceed the maximum storage capacity during the first repetition of the representative period, and

$$\mathbf{s}_{y,s,d,h} + \Delta s_{y,s} \leq Cap^{stor}, \forall y \in Y, s \in S, d \in D, h \in H. \quad (5.28)$$

ensuring that the storage capacity is not exceeded during the last repetition of the representative period. Lastly, a constraint is needed to ensure that in a case of emptying the storage during the repetitions of the representative period, the storage does not fall below zero. We have that

$$\mathbf{s}_{y,s,d,h} + \Delta s_{y,s} \geq 0, \forall y \in Y, s \in S, d \in D, h \in H. \quad (5.29)$$

5.5.3 Production

Production is subject to several constraints in our model. The hourly production can not exceed the maximum hourly production capacity of the plant. We have that

$$\mathbf{x}_{y,s,d,h} \leq \frac{\mathbf{cap}_y}{|H|}, \forall y \in Y, s \in S, d \in D, h \in H. \quad (5.30)$$

There can be no production when the plant is in a standby or idle state, which Equation

5.31 ensures. We have that

$$\mathbf{x}_{y,s,d,h} \leq (1 - \mathbf{standby}_{y,s,d,h} - \mathbf{idle}_{y,s,d,h}) \cdot M, \forall y \in Y, s \in S, d \in D, h \in H, \quad (5.31)$$

where M is a finite, vast number used to relax the constraint so that the production has to be less than some vast number when the plant is running and zero when it is in a standby or idle state. Hence, the maximum production is constrained by Equation 5.30 if the system is on and has to be zero when the plant is not running.

When the system runs, there is a minimum utilization (production rate) that the electrolyzer must exceed to retain the required pressure and temperature to produce hydrogen efficiently. To operate the equipment on a level less than the minimum utilization, the system must either be put in a hot standby state, retaining the required temperature and pressure while not producing, or turned completely off. We have that

$$\mathbf{x}_{y,s,d,h} \geq \frac{\mathbf{cap}_y}{|H|} \cdot \mathit{Min_util} - (\mathbf{standby}_{y,s,d,h} + \mathbf{idle}_{y,s,d,h}) \cdot M, \quad (5.32)$$

$$\forall y \in Y, s \in S, d \in D, h \in H.$$

If the system is on, lower bound for hourly production is determined by $\frac{\mathbf{cap}_y}{|H|} \cdot \mathit{Min_util}$. Otherwise, the lower bound for production is constrained by non-negativity.

We also need to make sure that the system is not in multiple states simultaneously. Therefore, we have that

$$\mathbf{standby}_{y,s,d,h} + \mathbf{idle}_{y,s,d,h} \leq 1, \forall y \in Y, s \in S, d \in D, h \in H. \quad (5.33)$$

When the system is neither in standby or idle, it runs normal within the nominal load given by Equation 5.30 and Equation 5.32.

5.5.4 Cold start

A cold start occurs when electrolyzer equipment is turned back on after being completely shut off. This is determined based on a change in $\mathbf{idle}_{y,s,d,h}$ from one period to another. As we consider 4 sets of periods; years, seasons, days, and hours; the state in the last period previous year, $y - 1$, is linked to the first period in the current year, y . This logic

also applies between seasons, days, and hours. A change in state between two subsequent periods determines whether the system is turned on or off. Cold starts occur if the electrolyzer was off in one period and on in the following period. We have that

$$\begin{aligned} \mathbf{cold_start}_{y,s_1,d_1,h_1} &\geq \mathbf{idle}_{y-1,|S|,|D|,|H|} - \mathbf{idle}_{y,s_1,d_1,h_1}, \\ &\forall y \in Y : y > y_1. \end{aligned} \quad (5.34)$$

$$\begin{aligned} \mathbf{cold_start}_{y,s,d_1,h_1} &\geq \mathbf{idle}_{y,s-1,|D|,|H|} - \mathbf{idle}_{y,s,d_1,h_1}, \\ &\forall y \in Y, s \in S : s > s_1. \end{aligned} \quad (5.35)$$

$$\begin{aligned} \mathbf{cold_start}_{y,s,d,h_1} &\geq \mathbf{idle}_{y,s,d-1,|H|} - \mathbf{idle}_{y,s,d,h_1}, \\ &\forall y \in Y, s \in S, d \in D : d > d_1. \end{aligned} \quad (5.36)$$

$$\begin{aligned} \mathbf{cold_start}_{y,s,d,h} &\geq \mathbf{idle}_{y,s,d,h-1} - \mathbf{idle}_{y,s,d,h}, \\ &\forall y \in Y, s \in S, d \in D, h \in H : h > h_1. \end{aligned} \quad (5.37)$$

Also, cold starts are constrained only to occur if the system was off in the previous period. If not constrained this way, the model could perform a cold start to reduce costs when electricity prices are negative, despite the equipment not being off in the previous period. We have that

$$\begin{aligned} \mathbf{cold_start}_{y,s_1,d_1,h_1} - \mathbf{idle}_{y-1,|S|,|D|,|H|} &\leq 0, \\ &\forall y \in Y : y > y_1. \end{aligned} \quad (5.38)$$

$$\begin{aligned} \mathbf{cold_start}_{y,s,d_1,h_1} - \mathbf{idle}_{y,s-1,|D|,|H|} &\leq 0, \\ &\forall y \in Y, s \in S : s > s_1. \end{aligned} \quad (5.39)$$

$$\begin{aligned} \mathbf{cold_start}_{y,s,d,h_1} - \mathbf{idle}_{y,s,d-1,|H|} &\leq 0, \\ \forall y \in Y, s \in S, d \in D : d > d_1. \end{aligned} \tag{5.40}$$

$$\begin{aligned} \mathbf{cold_start}_{y,s,d,h} - \mathbf{idle}_{y,s,d,h-1} &\leq 0, \\ \forall y \in Y, s \in S, d \in D, h \in H : h > h_1. \end{aligned} \tag{5.41}$$

5.5.5 Non-negativity

Also, none of the decision variables can hold a negative value. This means that

$$\mathbf{cap}_y \geq 0, \forall y \in Y, \tag{5.42}$$

$$\mathbf{x}_{y,s,d,h} \geq 0, \forall y \in Y, s \in S, d \in D, h \in H, \tag{5.43}$$

$$\mathbf{s}_{y,s,d,h} \geq 0, \forall y \in Y, s \in S, d \in D, h \in H, \tag{5.44}$$

$$\mathbf{idle}_{y,s,d,h} = \{0, 1\}, \forall y \in Y, s \in S, d \in D, h \in H, \tag{5.45}$$

$$\mathbf{cold_start}_{y,s,d,h} = \{0, 1\}, \forall y \in Y, s \in S, d \in D, h \in H, \tag{5.46}$$

and

$$\mathbf{standby}_{y,s,d,h} = \{0, 1\}, \forall y \in Y, s \in S, d \in D, h \in H. \tag{5.47}$$

6 Results

In this chapter, we run several scenarios using different values for daily production capacity, storage capacity, cost parameters, and electricity prices. In Section 6.1, we explain metrics used to investigate and compare model results. In Section 6.2, we present an overview of scenario-specific characteristics. In Section 6.3, we present, illustrate, comment, compare and discuss the results obtained from the different scenarios. Section 6.4 includes an alternative cost structure, in which the impact of grid fees are neglected, to illustrate results from discounted, off-grid, or subsidized alkaline water electrolysis.

6.1 Metrics

To evaluate the results, metrics are needed to effectively shed light on the impact of different model parameters.

A common approach to quantify the results from a full-scale hydrogen production model is to use the levelized cost of hydrogen (LCOH) (Kuckshinrichs et al., 2017; Nguyen et al., 2019; IEA, 2019; IRENA, 2019; Adam Christensen, 2020; Yates et al., 2020). This metric is used to compare overall costs from different model results throughout Chapter 6. The LCOH formula uses discounted cash flows to derive the minimum sales price for hydrogen required to achieve a net present value equal to zero. First, we begin by computing the total cost of hydrogen production as the sum of capital costs, discounted operational costs, and discounted production costs. Second, the LCOH is then computed by dividing total discounted costs related to hydrogen production by the sum of discounted production quantities (Yates et al., 2020; Nguyen et al., 2019; Kuckshinrichs et al., 2017). We have that

$$LCOH = \frac{\mathbf{total_costs}}{\sum_{y \in Y} \left(\frac{\sum_{s \in S} \sum_{d \in D} \sum_{h \in H} \mathbf{q}_{y,s,d,h}}{(1+Rate)^y} \right)}$$

where **total_costs** is the objective function from Equation 5.17 and $\mathbf{q}_{y,s,d,h}$ is the total produced quantity in year y , season s , day d and hour h . Hence, total costs are divided by the sum of all production volumes discounted yearly. In similarity to Yates et al. (2020), our model does not include transmission/transport of hydrogen, nor does it include region-

specific taxation. However, we extend our calculations further by including compression costs from 20 to 380 bar, standby costs, cold start costs, and storage in tanks or caverns. The inclusion of grid fees makes the LCOH more case-specific.

We use the production cost from Equation 5.12, which is a part of **total_costs**, throughout the lifetime of a hydrogen production plant to illustrate how the production cost changes for different production and storage capacities. We derive the production cost per kg H₂ in a similar approach as the LCOH by dividing the total production costs by the sum of discounted production quantities.

6.2 Scenario overview

In this section, we present characteristics for each scenario. Common for scenarios 1, 2, and 3 is that storage tanks are considered instead of underground storage. Different time horizons also characterize each scenario; scenario 1 resembles a scenario set to today; scenario 2 simulates a medium-term horizon; scenario 3 mirrors parameter values in the long term. The scenarios are also based on electricity prices adjusted to follow projected features for el-spot prices today, in the medium and long-term. The different electricity prices are described previously in Section 4.1. A main characteristic for the electricity price scenarios is that the fluctuations increase for scenarios that project prices longer into the future, as fair assumptions assume more volatile electricity prices (Statnett, 2020). Other plant costs and parameter values are determined based on today's and future estimates, presented in Section 4.2. Parameter values decrease gradually for future scenarios as larger impacts of economies of scale and improving manufacturing processes are expected to reduce plant costs (IEA, 2019).

Scenarios 4 and 5 project the same time horizons as scenarios 2 and 3, respectively, but consider the possibility of cavern storage, characterized by large storage capacity and cheap storage costs per unit compared to storage tanks. Norway has the potential of such underground storage in offshore caverns located subsurface in the North Sea Basin (Caglayan et al., 2020).

Nguyen et al. (2019) stated that a large-scale hydrogen production plant ranges between 4,000 - 40,000 kg H₂/day. Hence, we consider a daily off-take of 40,000 kg H₂/day, meaning 1,667 kg H₂/hour. The minimum hourly off-take is equal for all periods. Table 6.1 sums

up important parameter values for each scenario.

Table 6.1: Summary of scenario parameters.

Scenarios	Tank storage			Underground storage	
	1	2	3	4	5
Horizon	Today	Medium	Long	Medium	Long
System lifetime (years)	20	20	20	20	20
Daily production capacity (tonne)	44-60	44-60	44-60	44-60	44-60
Storage capacity (tonne)	0-30	0-30	0-30	500	500
Electrolyzer CAPEX (€/kW) @ 2 MW	750	532	383	532	383
Storage CAPEX (€/kg) @ 3 tonne	595	446	298	29.75	29.75
Electrolyzer OPEX (% of electrolyzer CAPEX)	2.5	2.5	2.5	2.5	2.5
Storage OPEX (% of storage CAPEX)	1.5	1.5	1.5	1.5	1.5
Efficiency (kWh/kg)	54	50	46	50	46
Compression (kWh/kg)	3	3	3	0	0
Standby (% of efficiency)	2	2	2	2	2
Cold start (kWh/tonne production capacity)	250	250	250	250	250
Yearly degradation (%)	0.8	0.8	0.8	0.8	0.8
Restack (year)	10	10	10	10	10
Restack cost (% of electrolyzer CAPEX)	45	40	35	40	35
Nominal load range (%)	15-100	10-100	10-100	10-100	10-100
WACC (%)	10.96	10.96	10.96	10.96	10.96

Note: Total capital expenditure for electrolyzer and storage varies, depending on production and storage capacities. Equation 4.1 (economies of scale) is used to compute total capital expenditure for a given production and storage capacity. Storage CAPEX @ 3,000 kg is only applicable in scenario 1, 2 and 3. Scenarios 4 and 5 consider a storage capacity of 500,000 kg.

For each scenario, we run the model several times with different values for the production and storage capacities to evaluate how excess production capacity and storage affect the LCOH and the production cost. The limits for production capacity are set in the range between the minimum capacity needed to maintain the required off-take and some chosen upper limit. The lower limit is set such that the plant can satisfy the required off-take, given flat production, even in the later periods when the production equipment's deterioration is at its greatest. To find this lower limit, we have that

$$\begin{aligned}
Cap^{prod,kg} \cdot (1 - Cap_red)^{Restack} &\geq Offtake \\
\Rightarrow Cap^{prod,kg} \cdot (1 - 0.8\%)^{10} &\geq 40,000 \\
\Rightarrow Cap^{prod,kg} &\geq \frac{40,000}{(1 - 0.8\%)^{10}} \\
\Rightarrow Cap^{prod,kg} &\geq 43,345.43
\end{aligned}$$

As we consider whole tonnes, the lower limit is set at 44 tonnes to have enough daily production capacity to satisfy the off-take in any year when subject to yearly degradation of the equipment. Moreover, the upper limit is set to 60 tonnes, which is 50% higher than the daily off-take and gives a good interval to investigate the effects of excess production capacity. The lower and upper limits for storage are based on the discussion in Section 4.2.2 and ranges from 0-30 tonnes when considering storage tanks. When underground storage is considered, the storage capacity is set to 500 tonnes. Scenario-specific cost curves for different production and storage capacities can be found in Appendix A4.

6.3 Scenario results

In the following subsections, we present and discuss the results from model scenarios.

6.3.1 Scenario 1

The first scenario investigates a case in which parameter values are based on well-considered estimates for an alkaline water electrolysis plant today. Thus, the equipment costs are higher, and electricity prices are less volatile than the other scenarios. A scenario concerning today's parameter values allows us to investigate the current possibilities for production scheduling through the use of excess production capacity and storage, as well as to enable us to compare and validate the LCOH from our model to other studies and literature regarding current costs of hydrogen produced from alkaline water electrolysis. The results in scenario 1 are presented in Table 6.2 for various production and storage capacities, ranging between their minimum and maximum limits.

Table 6.2: LCOH (€/kg) in scenario 1. Each column represent production capacity (tonne) while each row represent storage capacity (kg).

	44	46	48	50	52	54	56	58	60
0	3.031	3.059	3.087	3.115	3.142	3.170	3.197	3.225	3.252
3000	3.016	3.031	3.048	3.069	3.091	3.115	3.140	3.166	3.192
6000	3.025	3.037	3.052	3.069	3.086	3.105	3.125	3.146	3.168
9000	3.035	3.045	3.060	3.076	3.093	3.111	3.130	3.149	3.169
12000	3.045	3.054	3.068	3.083	3.100	3.118	3.136	3.156	3.175
15000	3.056	3.064	3.077	3.092	3.108	3.126	3.144	3.163	3.182
18000	3.067	3.075	3.086	3.100	3.116	3.134	3.152	3.170	3.189
21000	3.077	3.085	3.096	3.109	3.125	3.142	3.159	3.178	3.196
24000	3.088	3.095	3.106	3.119	3.133	3.150	3.167	3.185	3.204
27000	3.098	3.105	3.116	3.128	3.142	3.158	3.175	3.193	3.212
30000	3.108	3.115	3.125	3.138	3.152	3.167	3.184	3.202	3.220

Table 6.2 shows that the lowest LCOH is achieved at a production capacity equal to 44 tonnes combined with 3,000 kg of storage capacity. These production and storage capacities result in an LCOH of 3.016 €/kg H₂, well within the limits of other research. Calculations from DNV GL (2019) suggest that the cost of H₂ from alkaline water electrolysis in Norway today ranges between 2.08-4.06 €/kg H₂. In similarity to our case, these calculations are also subject to Norwegian electricity prices and grid fees. Other relevant research suggests similar results when estimating LCOH using parameter values that reflect costs and efficiencies today. Yates et al. (2020) find that LCOH ranges between 2.46-4.05 €/kg (2.89-4.76 \$/kg), while Nguyen et al. (2019) find that LCOH ranges between 2.49-2.74 €/kg (2.93-3.22 \$/kg). However, the latter assumes underground storage available today, which is expected to reduce hydrogen production costs from electrolysis for large production plants. IRENA (2019) calculates an LCOH of 3.00 €/kg (3.53 \$/kg) with electricity stemming from off-grid renewable sources.

Considering the results above, it appears to be economically beneficial to invest in storage capacity to avoid electricity price peaks. LCOH decreases by 0.49% compared to when no storage is available. This implies that the savings through reduced electricity costs exceed the additional required investment in storage equipment. However, a production capacity of 44 tonnes seems to give a satisfactory amount of production flexibility. The initial production capacity of 44 tonnes provides some excess production capacity in the first years before the equipment loses capacity due to degradation. This combination of excess production and storage capacity leads to a decrease in production costs by decreasing the

average cost of electricity, leading to a decrease in LCOH. However, there does not appear to be any financial incentive to increase the production capacity above the minimum capacity of 44 tonnes.

The optimal production capacity is always at 44 tonnes for any given storage capacity. This suggests that today's costs related to increased production capacity are too large compared to the savings. The LCOH increases for higher production capacities because the production cost reductions do not exceed the additional costs concerning increased production capacity. On the other hand, the results suggest that large production plants can achieve cost reductions by increasing the storage capacity. Consequently, if there are other incentives to increase a plant's production capacity, it can often be beneficial to increase the storage capacity to attain more flexibility, thus lowering total costs. For instance, given a daily off-take of 40 tonnes, a 60-tonne production plant can decrease LCOH by 0.75% by doubling the storage capacity from 3 to 6 tonnes. This points to the fact that for larger production plants, there are possibilities of savings through reduced production costs that exceed the additional storage equipment costs. Figure 6.1 illustrates how the production cost decreases when the production capacity increases because a greater share of production can be concentrated to low-cost electricity hours. However, since the electricity savings do not exceed the additional required investments, the LCOH increases as the production capacity increases.

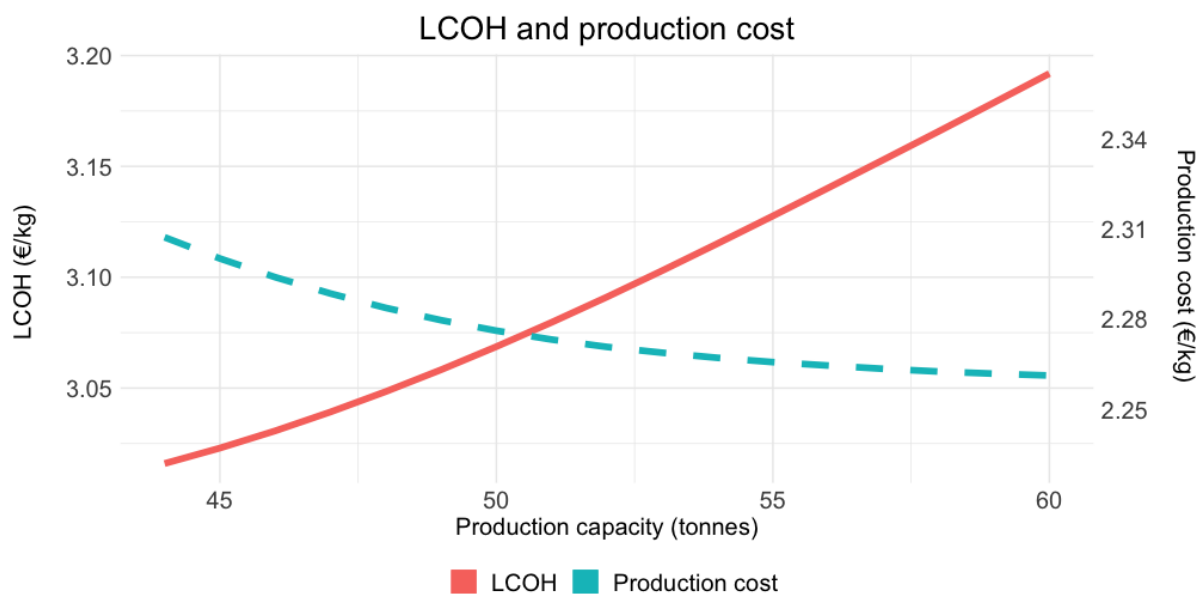


Figure 6.1: LCOH and production cost for different production capacities in scenario 1, given a storage capacity of 3,000 kg.

An increase in production capacity leads to an increase in the LCOH, given a storage capacity of 3,000 kg. Without increasing the storage capacity, the production cost begins to flatten for larger production capacities. More storage capacity is needed to fully exploit the larger production capacities to extend the decrease in production costs. However, the results in Table 6.2 indicate that today's plant costs are too high and/or electricity prices not volatile enough to allow plants to take advantage of substantial over-production. Despite reductions in production costs from water electrolysis by avoiding peak electricity prices, it can be challenging to exceed the increased costs, thus confirming the claims of Nguyen et al. (2019) who stated that it is necessary to optimize the trade-off between reduced production costs versus the increase in CAPEX. Nonetheless, several sources point towards a substantial decrease in plant costs and more volatile electricity prices in the future (IEA, 2019; IRENA, 2019; DNV GL, 2019; Statnett, 2020; NVE, 2020a), which are explored in the subsequent sections.

6.3.2 Scenario 2

Scenario 2 represents a medium-term horizon that mainly consists of lower capital costs, improved efficiency, and more volatile electricity prices compared to scenario 1. More volatile electricity prices suggest a larger potential for savings through production scheduling by exploiting the difference between high and low electricity prices. Table 6.3 illustrates the LCOH for different production and storage capacities in scenario 2.

Table 6.3: LCOH (€/kg) in scenario 2. Each column represent production capacity (tonne) while each row represent storage capacity (kg).

	44	46	48	50	52	54	56	58	60
0	2.668	2.689	2.710	2.731	2.752	2.773	2.793	2.814	2.834
3000	2.657	2.667	2.680	2.695	2.712	2.730	2.749	2.768	2.787
6000	2.663	2.672	2.683	2.695	2.708	2.722	2.737	2.752	2.769
9000	2.670	2.678	2.689	2.700	2.713	2.726	2.740	2.755	2.769
12000	2.678	2.685	2.695	2.706	2.719	2.732	2.745	2.760	2.774
15000	2.686	2.692	2.701	2.712	2.725	2.738	2.751	2.765	2.779
18000	2.694	2.700	2.708	2.719	2.731	2.744	2.757	2.771	2.785
21000	2.702	2.707	2.715	2.725	2.737	2.750	2.763	2.777	2.791
24000	2.710	2.715	2.723	2.733	2.744	2.756	2.769	2.783	2.796
27000	2.718	2.723	2.730	2.740	2.750	2.762	2.775	2.789	2.802
30000	2.725	2.730	2.738	2.747	2.758	2.769	2.781	2.795	2.808

The optimal LCOH is equal to 2.657 €/kg and is found at 44 tonnes daily production

capacity and 3,000 kg storage capacity. More volatile electricity prices, combined with reduced plant costs and improved efficiency, leads to a decrease in the LCOH of 11.9%, compared to scenario 1. The LCOH reduction between the two scenarios shows potential for rather large cost reductions if expenses and efficiency reach the projected values. Furthermore, to illustrate the effect of excess production capacity, we look at the LCOH and production cost achieved at different production capacities, given different amounts of storage capacities. Figure 6.2 illustrates how different production and storage capacities affect the LCOH and the production cost.

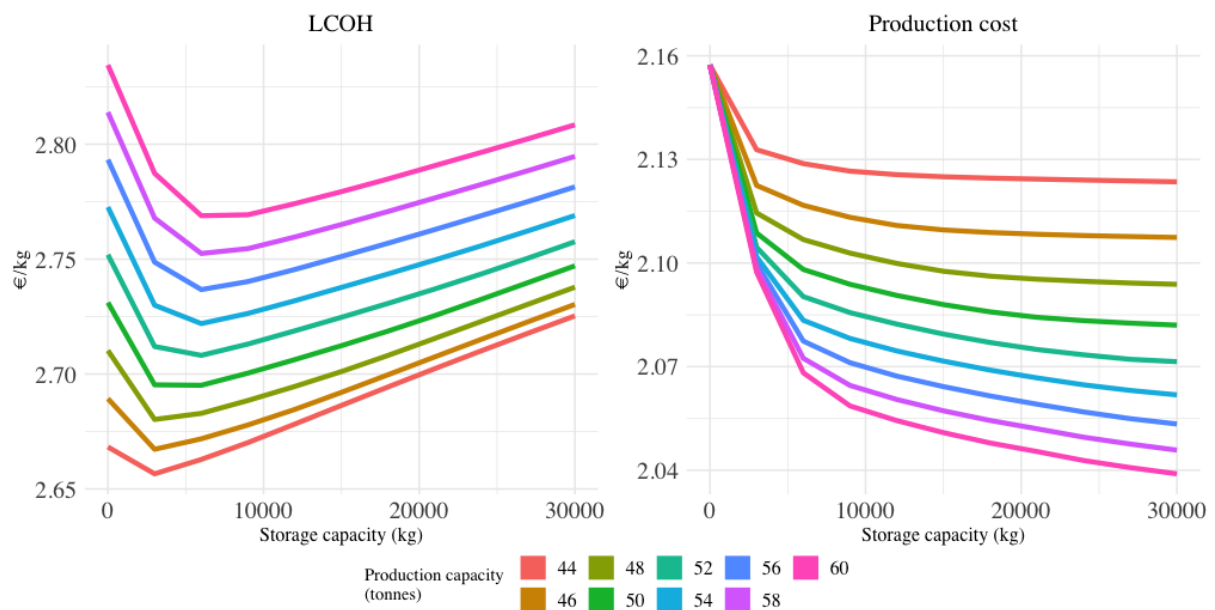


Figure 6.2: LCOH and production cost for different production and storage capacities in scenario 2.

Two observations are noted – (1) some storage is included in the optimal decision in all cases, and (2) the optimal amount of storage increases for larger production capacities. First, investments in storage are economically beneficial as it results in LCOH reductions for all production capacities. This fact is supported by the decrease in production cost displayed in the right panel of Figure 6.2. The decrease in production cost is largest for the first, initial storage investment, from 0 to 3,000 kg for all production capacities. The reduction in production costs becomes rather flat after the initial descent for smaller production capacities, indicating that additional storage capacity investments provide insufficient savings. Second, similarly to scenario 1, the optimal storage capacity increases as the production capacity increases. Thus, if an existing plant already has excess production

capacity available, investing in more storage capacity should be considered. This is also supported by the graph showing the production cost. For larger production capacities, the decrease in production cost continues as the amount of storage capacity increases. However, with medium-term plant costs and electricity price estimates, substantial excess production capacity increases LCOH. Therefore, the financial benefit from electricity price savings does not seem to exceed the associated costs of investing in excess production capacity over the minimum limit of 44 tonnes or storage over 3,000 kg.

6.3.3 Scenario 3

Scenario 3 represents a long-term, futuristic scenario and consists of even lower capital costs and improved efficiency compared to the previous scenarios. Electricity prices are more volatile than scenario 2 and even contain some instances of negative prices. The results are presented in Table 6.4.

Table 6.4: LCOH (€/kg) in scenario 3. Each column represent production capacity (tonne) while each row represent storage capacity (kg).

	44	46	48	50	52	54	56	58	60
0	2.401	2.418	2.434	2.450	2.466	2.482	2.498	2.514	2.530
3000	2.382	2.386	2.393	2.402	2.414	2.426	2.440	2.455	2.469
6000	2.384	2.386	2.391	2.397	2.404	2.412	2.421	2.432	2.443
9000	2.388	2.388	2.393	2.399	2.405	2.413	2.421	2.429	2.439
12000	2.393	2.392	2.395	2.401	2.407	2.415	2.422	2.431	2.440
15000	2.398	2.396	2.399	2.404	2.410	2.417	2.425	2.433	2.442
18000	2.403	2.401	2.403	2.407	2.413	2.420	2.427	2.435	2.444
21000	2.408	2.406	2.407	2.411	2.416	2.423	2.430	2.438	2.447
24000	2.413	2.411	2.412	2.415	2.420	2.426	2.433	2.441	2.449
27000	2.418	2.416	2.417	2.419	2.424	2.430	2.436	2.444	2.452
30000	2.423	2.421	2.421	2.424	2.428	2.433	2.440	2.447	2.455

The LCOH reaches a minimum value of 2.382 €/kg. In similarity to previous scenarios, this is found at a daily production capacity of 44 tonnes and a storage capacity of 3,000 kg. The decrease in the LCOH is equal to 21.02% and 10.35% compared to the optimal cases in scenarios 1 and 2, respectively. Despite substantially more volatile electricity prices than scenario 1 and heavily reduced investment costs, the optimal decision regarding production and storage capacity remains unchanged. Nevertheless, changes are starting to appear in the results. Recall that 44 tonnes were the optimal production capacity

for all storage capacities in scenarios 1 and 2. In this scenario, larger storage capacities favor larger production capacities, indicating that production and storage capacity is a combinatorial decision, in which the optimal amount of production capacity depends on the amount of storage capacity and vice versa. Figure 6.3 shows a graphical illustration of the effect of different production and storage capacities on LCOH and the production cost in scenario 3.

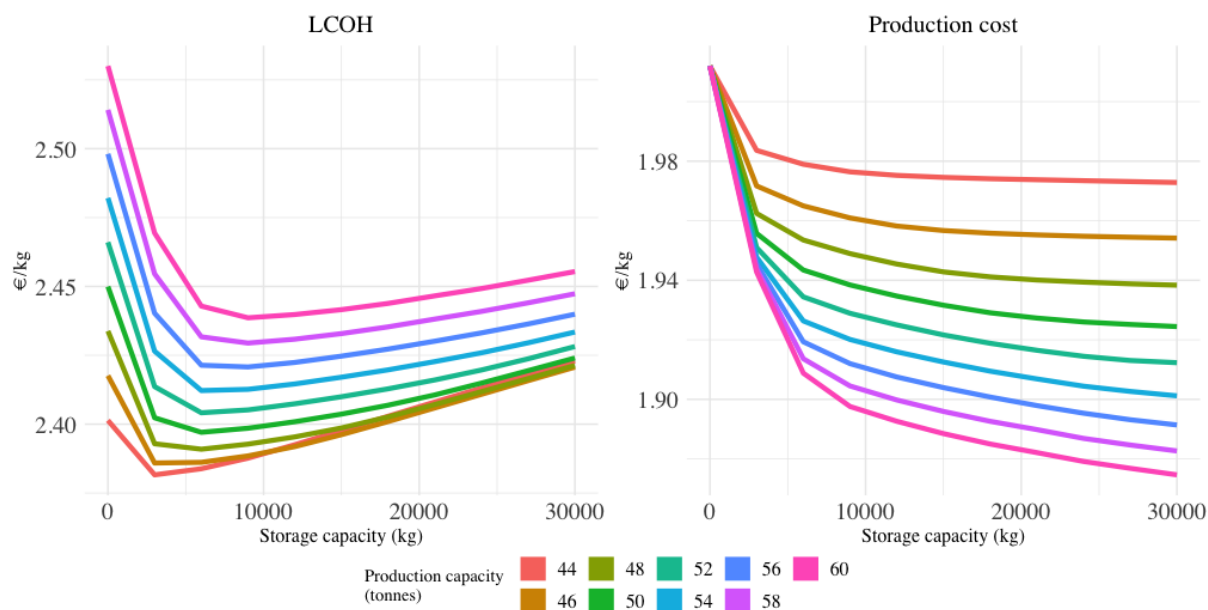


Figure 6.3: LCOH and production cost for different production and storage capacities in scenario 3.

The graphs representing the LCOH, shown in the figure's left panel, are more clustered than in scenario 2, indicating a shift towards a case where substantial over-production and storage can eventually become economically viable. A plausible reason for how the LCOH reacts to the changes in production and storage capacities, compared to previous scenarios, is the increased volatility in the electricity prices and lower plant costs. As shown in the right panel of Figure 6.3, the production cost drops approximately 6.83% for 60 tonnes of production capacity, comparing zero and 30,000 kg of storage capacity. For comparison, the equivalent decrease in scenario 2 was 5.49%. Thus, the positive effect of increased electricity price fluctuations becomes more evident for production plants with larger production and storage capacities. However, the increased savings in production costs do not exceed the additional costs required to achieve it as we still find the minimum LCOH at 44 tonnes production capacity and 3,000 kg storage capacity. One possibility for why excess capacity does not contribute to a lower LCOH is that the profitability of excess

production capacity depends on the distribution of low and high electricity prices. For instance, if prices are low for the 20 subsequent hours and *extremely* high for the following 4 hours, small amounts of excess production capacity could be very profitable. However, suppose high and low prices are evenly distributed throughout a day. For instance, half of the prices lie below the daily average and the remaining half above. In that case, more excess production and storage capacity is needed to increase production during the twelve cheap hours to satisfy the demand in the twelve expensive hours. In this case, a higher degree of production must be concentrated to a lesser number of cheap electricity price hours. If prices are extremely low for several subsequent weeks or months, followed by a whole month of overly high prices, very substantial amounts of production and storage capacities are required to take advantage of the low-cost periods. In such cases, there might be a need for large-quantity, low-cost storage to exploit such fluctuations, which we will explore further in scenarios 4 and 5.

Another point that can be drawn from the results is the possibility of achieving flexibility through additional production and storage equipment without significantly increasing the LCOH. A 46-tonne production plant with 6,000 kg of storage capacity has an increased LCOH of only 0.17%. Through the increased flexibility a hydrogen production plant can provide grid balancing, which could be a possibility for flexible, energy-demanding industries to gain additional revenues, as suggested by Statnett (2020) and NVE (2020a). Nguyen et al. (2019) also stated that increased flexibility should be considered when a hydrogen production plant can gain additional revenues from providing ancillary services, such as providing balance to the grid. In scenario 1, the increase in LCOH associated with achieving the maximum flexibility, meaning 60 tonnes of production capacity and 30 tonnes of storage capacity, is equal to 6.76%. The equivalent increase is 5.68% and 3.06% in scenarios 2 and 3, respectively. This shows that increasing the flexibility of a plant today to provide flexibility is rather expensive. Thus, large compensations would have to be provided to make it profitable for a hydrogen production plant. However, as equipment costs decrease and electricity price fluctuations increase, the overall costs to achieve flexibility decrease. Thus, it could prove to be financially viable for energy generators and grid companies to provide flexible hydrogen producers with compensations to incentivize them to invest in excess production capacity and storage facilities.

6.3.4 Scenario 4

Unlike the previous scenarios, we now consider underground storage in a medium-term scenario. This option allows for the storage of large quantities of hydrogen over long periods of time, resulting in a very low unit cost per kg of stored H₂, compared to storage tanks. Table 6.5 presents the LCOH and the production cost in scenario 4.

Table 6.5: LCOH (€/kg) and production cost (€/kg) in scenario 4 for different production capacities and storage capacity of 500,000 kg.

Production capacity (tonne)	44	46	48	50	52	54	56	58	60
LCOH (€/kg)	2.620	2.622	2.628	2.637	2.647	2.658	2.670	2.682	2.694
Production cost (€/kg)	1.978	1.960	1.946	1.934	1.923	1.914	1.905	1.896	1.888

By combining underground storage in caverns while still maintaining production capacity at 44 tonnes, the model achieves an LCOH of 2.620 €/kg H₂. It seems that medium-term values for CAPEX, efficiency, and electricity prices do not lead to a purely financial incentive to increase the production capacity above 44 tonnes, even when combined with large-scale underground storage. However, the large amounts of available storage make way for increased flexibility, allowing to take advantage of inter-seasonal storage options, granting the possibility to use hydrogen produced during the summer to cover the demand of more expensive seasons, such as winter and fall. Figure 6.4 shows the average net change in storage for each season, specifically how the storage fills and empties during different seasons.

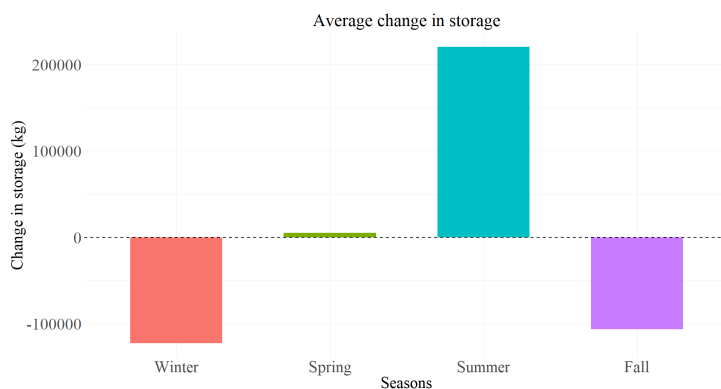


Figure 6.4: Illustrating the average change in storage during different seasons.

The figure shows how hydrogen stored from excess production during the summer is emptied during the fall and winter seasons to cover demand when prices increase. By doing so, a hydrogen producer can avoid the absolute worst production hours throughout a year. An interesting aspect of scenario 4 is that it shares similar parameter values with scenario 2, except that scenario 4 considers underground storage, whereas scenario 2 considers storage tanks. Thus, it is interesting to see how underground storage affects LCOH and the production cost. Figure 6.5 shows a comparison of the results from the two scenarios when increasing the production capacity. Storage capacity in scenario 2 is 3,000 kg, while scenario 4 is 500,000 kg.

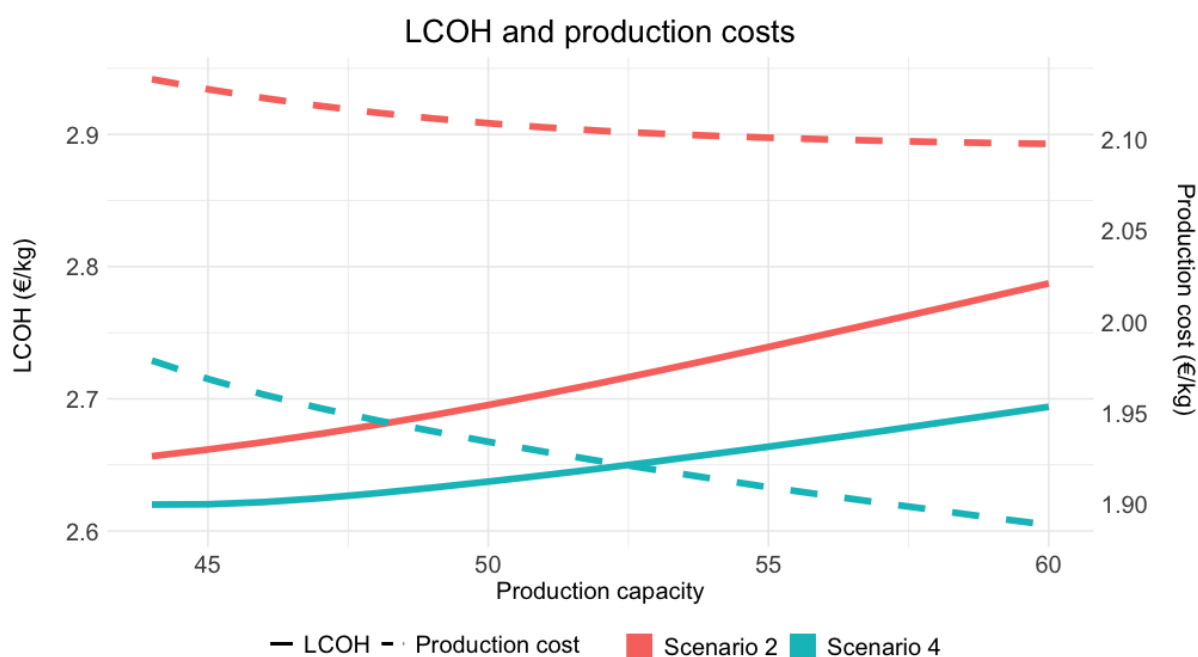


Figure 6.5: A comparison of LCOH and production costs between scenario 2 and 4.

First, we note that the LCOH is lower in scenario 4 than scenario 2, despite considerably larger investments in storage facilities.

Storage CAPEX comparison:

$$\text{Scenario 2: } 446 \text{ €/kg} \cdot 3,000 \text{ kg} = \text{€}1,338,000$$

$$\text{Scenario 4: } 29.75 \text{ €/kg} \cdot 500,000 \text{ kg} = \text{€}14,875,000$$

The difference in total capital expenditure for storage between scenario 2 and scenario 4 is equal to €13,137,000. The fact that the LCOH is lower in scenario 4 suggests

that underground storage leads to greater electricity price savings than the additional investment costs required for the underground storage facility. In scenario 2, the LCOH was 2.668 €/kg in a flat production schedule with no storage and 44-tonne production capacity. In scenario 4, we achieve an LCOH of 2.620 €/kg by including a storage capacity of 500,000 kg. This represents a decrease in the LCOH by 1.80% when including underground storage.

Second, we note that the LCOH increases in both scenarios for larger production capacities, while production costs decrease. This means that even though the increase in production capacity yields lower production costs, it is not substantial enough to the point where the benefits exceed the associated costs of investing in additional electrolyzer equipment.

6.3.5 Scenario 5

Scenario 5 also considers underground caverns for long-term, large quantity hydrogen storage. However, electricity prices are more volatile than scenario 4, and parameter values represent a long-term projection of equipment costs and efficiency. Associated values for the LCOH and production costs in scenario 5 are presented in Table 6.6.

Table 6.6: LCOH (€/kg) and production cost (€/kg) in scenario 5 for different production capacities and storage capacity of 500,000 kg.

Production capacity (tonne)	44	46	47	48	50	52	54	56	58	60
LCOH (€/kg)	2.344	2.338	2.337	2.338	2.340	2.344	2.348	2.354	2.360	2.366
Production cost (€/kg)	1.823	1.802	1.793	1.786	1.772	1.760	1.749	1.738	1.728	1.719

The results in Table 6.6 show a minimum LCOH of 2.337 €/kg when the daily production capacity is 47 tonnes, given a storage capacity of 500 tonnes. This is the lowest LCOH, as well as the largest production capacity out of all five scenarios. It proves that cheaper capital expenditure, improved efficiency, more volatile electricity prices, and low-cost storage with a large capacity can eventually lead to a situation in which excess production capacity is desirable. These findings support the claims of Statnett (2020) who found production cost reductions to be greater than the associated investment costs in a similar scenario. Comparing the results from this scenario with the ones from scenario 3, in

which the only difference is the storage method, we find that the availability of cheap, large volume storage is necessary to exploit the electricity price fluctuations. As a result, electricity price savings exceed the cost of investing in three additional tonnes of electrolyzer equipment, which include not only an increase in total CAPEX but also an increase in OPEX, grid costs, and cell stack replacements related to the plant size. Figure 6.6 shows how the LCOH and the production cost change as the daily production capacity increases.

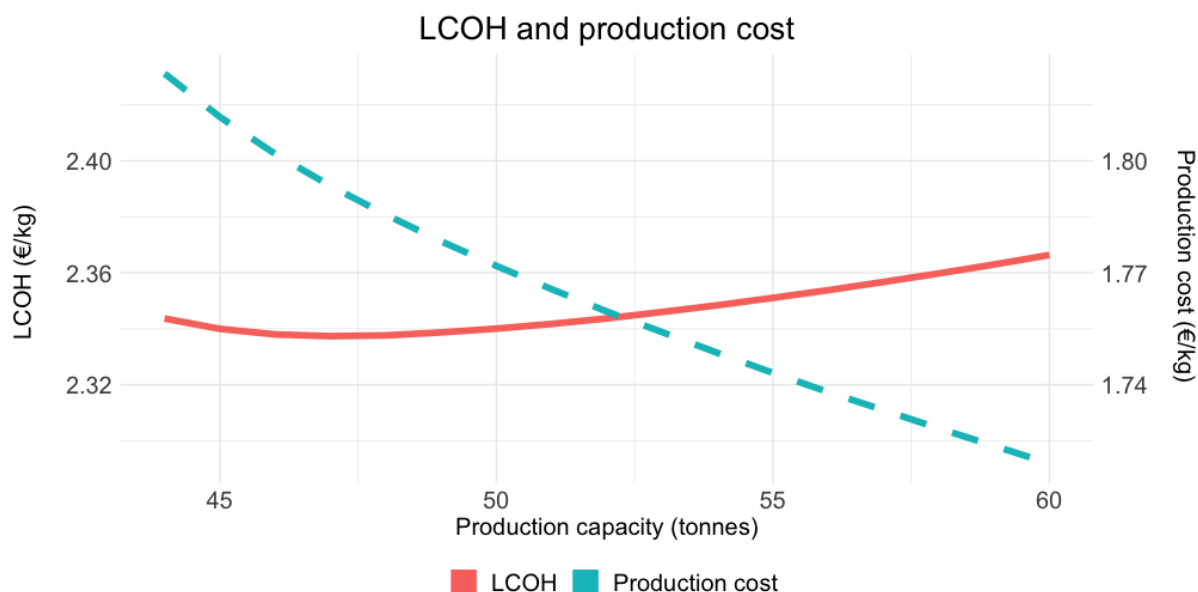


Figure 6.6: LCOH and production cost for different production capacities in scenario 5, given a storage capacity of 500,000 kg.

The red graph in Figure 6.6 illustrates a minimum LCOH at 47 tonnes production capacity. The production cost decrease from 1.823 €/kg at 44 tonnes production capacity to 1.793 €/kg at 47 tonnes production capacity, while at 60 tonnes production capacity, the production cost is 1.719 €/kg. The reductions in production costs are a result of electricity price savings due to flexible production scheduling. Knowing that electricity is a major cost in water electrolysis, a decrease in electricity costs could lead to substantial decreases in production costs (Kuckshinrichs et al., 2017). This effect is assumed to continue for larger production capacities, although it will flatten out if the storage capacity is kept constant.

Figure 6.7 illustrates how it is possible to combine excess production capacity and storage to exploit low-cost electricity prices to produce H₂ at a lower cost. The hourly production schedule represents an average week across the system lifetime, in which hours 1-24 are

an average Monday, hours 25-48 are an average Tuesday, etc.

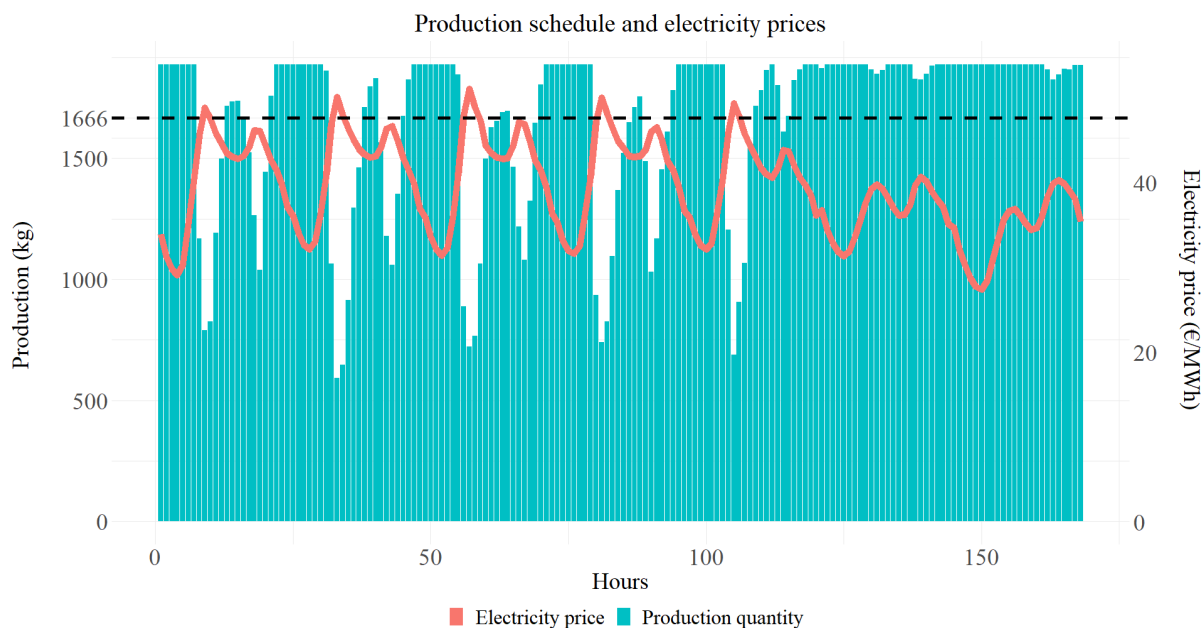


Figure 6.7: Hourly, weekly average, production schedule and electricity prices in scenario 5.

The figure illustrates the production schedule and electricity price in the optimal scenario in which a 47-tonne production plant is combined with 500,000 kg of storage capacity. The plant satisfies a daily demand of 40 tonnes by scheduling production to minimize costs. The dashed, horizontal line represents the hourly demand for hydrogen. The figure shows that the plant exploits low-cost hours and avoids electricity price peaks, illustrated by the clear dips in production at hours of expensive electricity prices. Lower production cost occurs when the most expensive hours are avoided. By avoiding electricity price peaks, a water electrolysis plant can decrease its most expensive production price. However, the potential for electricity price savings decreases as more peak hours is avoided because the gap between the lowest and highest production price becomes more narrow. This effect explains the optimal decision in excess production capacity. When the saving potential decreases, eventually, the additional investments will exceed the savings, and further capacity expansions will no longer be profitable.

However, even as electricity price peaks are avoided, changes in LCOH resulting from excess production capacity are minor. Thus, it becomes imaginable that some costly effects counteract the reductions in production costs. Consequently, exploiting low-cost electricity to cover hydrogen demand during peak hours requires large, additional investments

and other costs. We quantify the additional electrolyzer CAPEX when increasing the production capacity from 44 to 47 tonnes.

$$2,000 \text{ kW} \cdot 383 \text{ €/kW} \cdot \left(\frac{\frac{44,000 \text{ kg} \cdot 46 \text{ kWh/kg}}{24 \text{ h}}}{2,000 \text{ kW}} \right)^{0.85} = \text{€}18,426,916$$

$$2,000 \text{ kW} \cdot 383 \text{ €/kW} \cdot \left(\frac{\frac{47,000 \text{ kg} \cdot 46 \text{ kWh/kg}}{24 \text{ h}}}{2,000 \text{ kW}} \right)^{0.85} = \text{€}19,489,516.$$

Hence, the increased CAPEX from 44 to 47 tonnes is $\text{€}19,489,516 - \text{€}18,426,916 = \text{€}1,062,600$. Also, increasing the production capacity leads to an increase in grid costs. The formula for an annuity is used to compute the total increase. An increase of three tonnes daily production capacity sums to

$$\frac{3,000 \text{ kg}}{24 \text{ h}} \cdot 46 \text{ kWh/kg} = 5,750 \text{ kW}$$

$$\implies 5,750 \text{ kW} \cdot 4.2 \text{ €/kW/month} \cdot 6 \text{ months} = 144,900 \text{ €/year}$$

$$\implies 144,900 \text{ €/year} \cdot \frac{1 - \frac{1}{1.1096^{20}}}{0.1096} = \text{€}1,156,911,$$

additional grid costs in the winter months alone, assuming that the grid fee does not increase. The summer months' grid costs come on top of that; however, the summer fees are not as significant as the winter fees. Also, there is an additional yearly OPEX of approximately 2.5% of the total increase in CAPEX. Thus, there is quite a large amount of money to be saved by reducing the average purchase price of electricity, as all these costs are neglected by the decrease in production costs, in addition to the LCOH being reduced on top of that.

Similar to the discussion at the end of scenario 3, in scenarios 4 and 5, the increase in LCOH related to achieving the maximum flexibility is 2.82% and 1.24%, respectively. Illustrating that with the option of underground storage, the cost of increased flexibility is even lower. Consequently, hydrogen production plants can use the additional flexibility to balance an increasingly unstable grid resulting from a decreasing share of energy stemming from dispatchable sources. If the compensation is greater or equal to the costs of the increased LCOH, it should be considered. Additionally, excess production capacity can also be a solution to exploit excess electricity directly from renewable energy sources,

which is currently being developed (Siemens Gamesa, 2020).

6.4 The effect of grid fees on water electrolysis

Calculations in the previous subsection suggest that grid fees greatly impact the cost chain in a hydrogen production process when considering grid-connected water electrolysis. It has become apparent that grid fees heavily affect larger production plants, making it unfavorable to implement excess production capacity to exploit electricity price fluctuations. Therefore, in this section, we intend to explore the previously discussed scenarios when neglecting the impact of grid fees.

When neglecting grid fees in the model, we assume either that the water electrolysis plant is directly connected to a renewable energy source, such as a wind farm, thus making it possible to produce H_2 without being subject to grid fees. Doing so could be beneficial for both the hydrogen producer and the renewable energy producer. The hydrogen producer can avoid grid fees, increasing the economic incentive to invest in excess production capacity. Hydrogen production can then be even more concentrated on hours of low-cost electricity. A water electrolysis plant purchasing electricity directly from a renewable energy producer during hours of low-cost electricity will likely counteract occurrences of extremely low electricity prices. Consequently leading to more profitable renewable energy sources. This approach also makes hydrogen a way to store excess energy that otherwise would be lost. Moreover, flexible operation schedules and high power consumption make water electrolysis an option for grid balancing. In Norway, grid companies can offer a *disconnectable option* in which water electrolysis plants can get discounted fees by committing to reducing consumption during specific periods (NVE, 2020b). Compared to other industries, water electrolysis has advantages such as one product (hydrogen), simple process (mostly automated), and quick response time to follow intermittent schedules within short notice (Nguyen et al., 2019). Another reason to explore a case without grid fees is the possibility of subsidies. Norwegian Ministry of Climate and Environment (2020) states that Norway will participate in a broader European focus on hydrogen development by joining IPCEI¹⁷. The participation makes subsidies more available for transboundary investments that exceed existing limits.

¹⁷Important Project of Common European Interest.

In Norway, grid fees are computed based on three different joints. These are (1) fixed costs, (2) variable production costs related to electricity consumption, and (3) variable power costs. The fixed costs occur independently of any parameter or decision variable of a plant. The variable production costs are directly dependent on the total electricity consumption. The variable power cost is dependant on the hour with the highest energy consumption within a month, which often can be assumed equivalent to the plant size. Based on today's parameter values, a production plant with a daily production capacity of 44 tonnes have power costs equal to

$$\begin{aligned} & \frac{44,000 \text{ kg}}{24 \text{ h}} \cdot 54 \text{ kWh/kg} = 99,000 \text{ kW} \\ \implies & 99,000 \text{ kW} \cdot (4.2 \text{ €/kW/month} + 0.69 \text{ €/kW/month}) \cdot 6 \text{ months} = 2,904,660 \text{ €/year} \\ \implies & 2,904,660 \text{ €/year} \cdot \frac{1 - \frac{1}{1.1096^{20}}}{0.1096} = \mathbf{\text{€}23,191,398}, \end{aligned}$$

assuming that the plant is run at 100% utilization at least once a month. If the daily production capacity increases to 60 tonnes, the variable power joint of the grid costs are equal to

$$\begin{aligned} & \frac{60,000 \text{ kg}}{24 \text{ h}} \cdot 54 \text{ kWh/kg} = 135,000 \text{ kW} \\ \implies & 135,000 \text{ kW} \cdot (4.2 \text{ €/kW/month} + 0.69 \text{ €/kW/month}) \cdot 6 \text{ months} = 3,960,900 \text{ €/year} \\ \implies & 3,960,900 \text{ €/year} \cdot \frac{1 - \frac{1}{1.1096^{20}}}{0.1096} = \mathbf{\text{€}31,624,634}. \end{aligned}$$

Hence, the following statement applies to grid-connected water electrolysis today. Larger water electrolysis plants, intending to exploit electricity price fluctuations, need to save the amount equal to the investment costs of excess production capacity and the increase in grid fees related to the plant size. The example above illustrates that it is necessary to save more than €8.43 million, only to cover the additional grid fees when up-scaling from a 44-tonne to 60-tonne production plant, given today's parameter values. To understand the magnitude of that sum, the increase in electrolyzer CAPEX from 44 to 60 tonnes today equals €12.47 million, indicating that the increase in grid fees is approximately 68% as large as the increase in CAPEX. Thus, to reduce the LCOH through excess production capacity and storage, the savings in production costs need to cover the increase in grid

fees, the cost of additional production and storage equipment, and the increased OPEX of the additional storage and production equipment. On top of that, the savings have to provide a positive net profit to make it the more attractive option. Based on the reasoning in the previous paragraph, we find it interesting to look at the consequences of neglecting the effect of grid fees from the previous scenarios.

Table 6.7 presents the production capacity, storage capacity, and production cost related to the minimum LCOH of the five scenarios when grid fees are present and not. A complete overview of LCOH for all production and storage capacities in each scenario when neglecting grid fees is presented in Appendix A5.

Table 6.7: Optimal production capacity (tonnes), storage capacity (kg), LCOH (€/kg) and production cost (€/kg) in scenarios 1-5 with and without grid fees.

	With grid fees				Without grid fees			
	Production capacity	Storage capacity	LCOH	Production cost	Production capacity	Storage capacity	LCOH	Production cost
1	44	3,000	3.016	2.307	44	3,000	2.717	2.218
2	44	3,000	2.657	2.133	44	3,000	2.379	2.050
3	44	3,000	2.382	1.984	53	6,000	2.114	1.854
4	44	500,000	2.620	1.978	48	500,000	2.350	1.868
5	47	500,000	2.337	1.793	60	500,000	2.064	1.647

In scenarios 1 and 2, the optimal production and storage capacities are the same as when grid fees are included. However, LCOH is significantly lower, approximating a 10% decrease in both scenarios. In the later scenarios, changes can be observed regarding the optimal production and storage capacities. The optimal production capacity increases by 20.5% in scenario 3, from 44 to 53 tonnes; 9.1% in scenario 4, from 44 to 48 tonnes; and 27.66% in scenario 5, from 47 to 60 tonnes. Thus, grid fees significantly impact a production plant's optimal size when the equipment prices are lower, and electricity prices fluctuate more. Optimal storage capacity in scenario 3 increases from 3,000 kg to 6,000 kg. For scenario 3, 4, and 5, the LCOH decrease is 11.25%, 10.31%, and 11.68%, respectively. Figure 6.8 shows a comparison of the LCOH in scenarios 1-5 with and without grid fees. Neglecting the effect of grid fees affect the LCOH in several ways. Two direct effects reduce the overall cost. The first is a result of removing the monthly grid cost related to the maximum hourly power consumption within a month, referred to as *grid cost* in the

figure below¹⁸. The second direct effect is a result of removing grid fees related to the total energy consumption¹⁹, which is included in the production cost. The removal of grid fees also indirectly affects the LCOH as investments in larger production plants and more storage becomes a more viable strategy, leading to lower production costs due to flexible production scheduling.

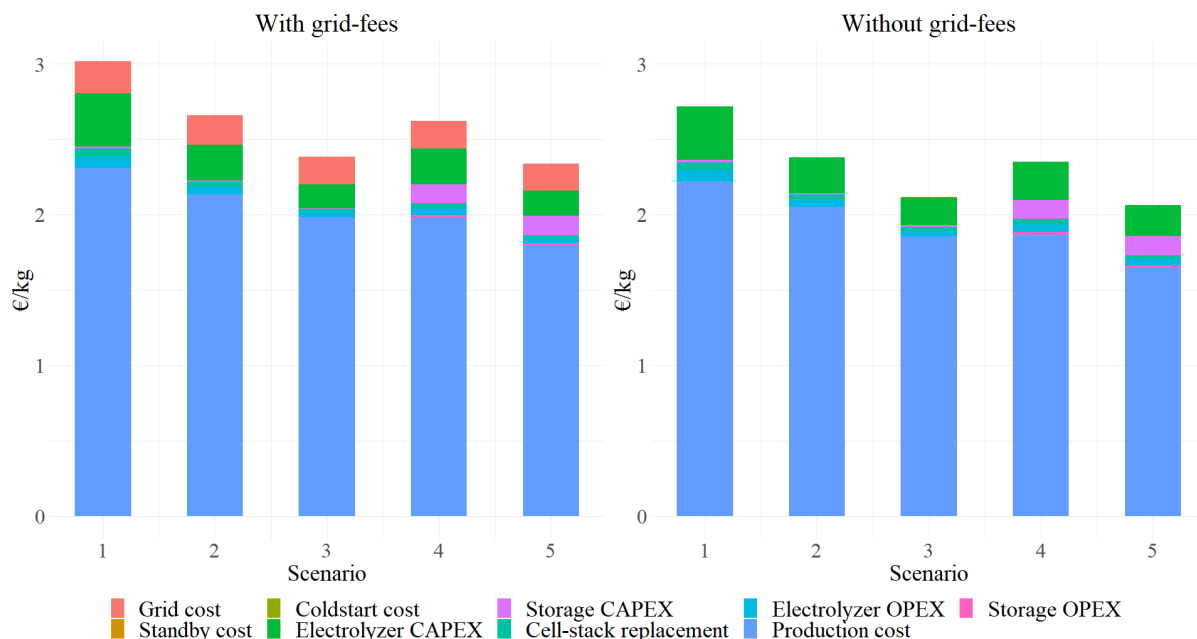


Figure 6.8: Stacked LCOH for optimal cases in scenarios 1-5 with and without grid fees.

Disregarding grid fees allow for larger plants that can exploit electricity price fluctuations. Thus, resulting in substantial decreases in the production costs. In scenarios 1 and 2, there are no differences in terms of production and storage capacity. The decrease in production costs of 3.86% and 3.89% is single-handedly a consequence of the exemption of grid fees related to the total electricity consumption. However, other effects are revealed as these aspects change. The production cost reductions are equal to 6.55%, 5.56%, and 8.86% in scenarios 3, 4, and 5, respectively. The reductions in production costs in the last three scenarios are not only a result of the omission of grid fees but also increased flexibility from excess production capacity and storage. The increase in flexibility can be illustrated through the number of hours the system is operated in standby mode and the number of cold starts across the system lifetime. When grid fees are considered and production capacities of 44 and 47 tonnes is applied, the number of cold starts and hours in standby

¹⁸Norwegian: effektledd

¹⁹Norwegian: energiledd

mode are 64 and 628 in scenarios 4 and 5, respectively. When grid fees are exempt and production capacities increase to 48 and 60 tonnes in the same scenarios, these numbers increase to 884 and 1,007; thus, showing how a plant can exploit low price periods and switch the electrolyzers to standby or idle mode in periods of expensive electricity. Figure 6.9 shows the number of hours the modeled plant operates in standby mode and the number of cold starts over a system lifetime for all scenarios, both with and without grid fees.

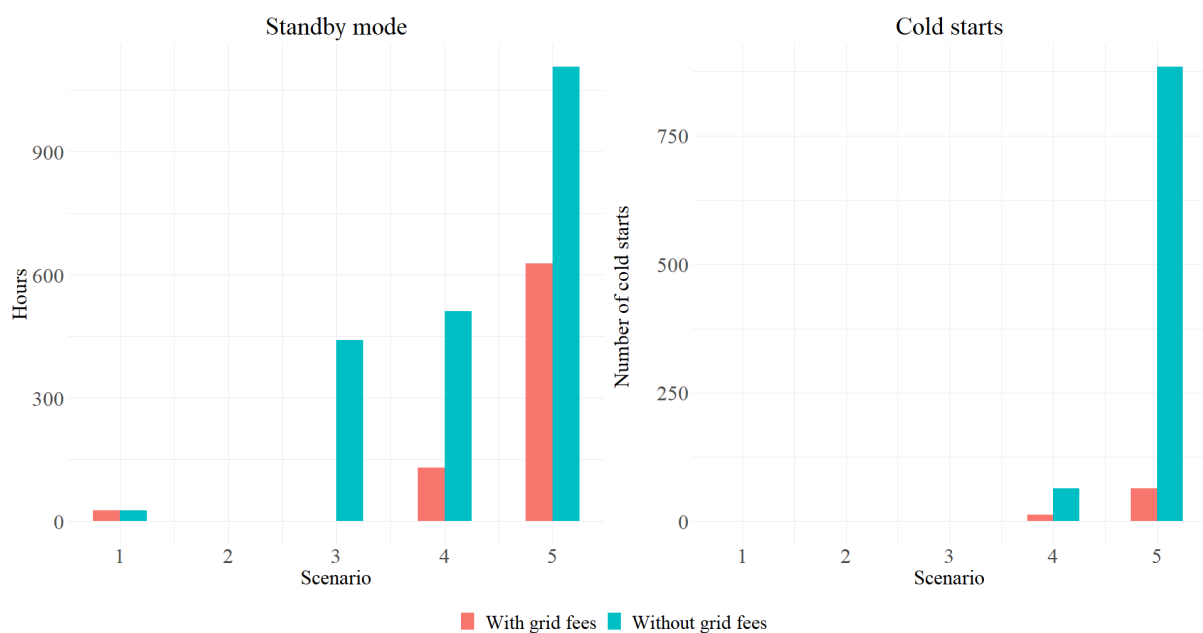


Figure 6.9: Left: Number of hours the modeled plant has operated in standby-mode. Right: Number of cold starts performed over the modeled plants lifetime.

Thus, providing reduced grid fees related to water electrolysis can not only provide a pure economic relief in the form of reduced costs but can also provide hydrogen production plants with more incentive to invest in excess production capacity and storage facilities to obtain production flexibility and reduce the overall cost of hydrogen even further.

7 Discussion

In Chapter 6, we have discussed and compared our model results therebetween and their significance for future developments. In this chapter, we discuss the limitations of the data and model and the external validity of the methods used throughout the thesis. Furthermore, we propose and discuss future topics that relate to the research performed in this thesis.

7.1 Limitations and external validity

Both the model and data in this thesis are subject to assumptions that might affect or limit the results. The assumptions are further discussed below.

Implications of electricity price forecasts

Because electricity prices are an important parameter value when modeling hydrogen production from water electrolysis, it is important to be aware of the uncertainty in the projections regarding future fluctuations and price levels. Although there exist estimates about future electricity prices from reliable energy agencies, the projections are subject to a range of presumptions. Changes in seasonality or trends may distinguish or strengthen the differences between scenarios. The development of smart technologies/charging, working from home, more extreme weather, or changes to the generation mix structure are only a few examples that complicate long-term electricity price forecasts.

Implications of electricity price aggregation

The consequences of aggregating data and using representative periods in a model that seeks to exploit electricity prices' seasonality are not well documented in other literature. An advantage of using aggregated data is to model the production over the entire lifetime of the plant and allowing for robust results that take seasonal patterns and variations between years into account. A disadvantage of modeling with aggregated data is the loss of detail in terms of variation, randomness, and extreme values, as all data-points are averaged values.

Implications of flat hydrogen demand

In this thesis, the hydrogen demand is assumed to follow a flat delivery commitment with equal off-take every hour over the hydrogen production plant's lifetime. However, future hydrogen demand curves depend on which industries adopt hydrogen and to what degree. If hydrogen becomes a mere method of storing electricity over longer periods to stabilize the energy sector, the hydrogen demand pattern will follow electricity price curves as hydrogen can produce power when electricity prices are high due to shortcomings in electricity generation from non-dispatchable sources. On the other hand, if hydrogen becomes important in diverse industrial fields, the demand pattern might become more constant. Hence, the future establishment of hydrogen strategies could benefit from mapping the hydrogen demand, specifically green hydrogen.

Implications of full lifetime modeling

This thesis focuses on production across the entire system lifetime with large amount of electricity price data instead of modeling a short period and repeat the schedule. Doing so has led to limitations regarding computational expensiveness. (1) The lifetime of the cell-stacks is originally determined on an hourly basis. Modeling the lifetime of cell-stacks on an hourly level could allow for a more realistic view of when cell re-stacks are required. It could also allow for production scheduling to increase the stacks' lifetime by operating more hours in an idle or standby state, potentially increasing the benefits of excess production capacity. (2) In a more detailed production schedule, electrolyzer stacks could also be modeled as separate nodes, allowing the model to determine each electrolyzer stack's utilization and state separately.

Implications of financial estimates

In this thesis, the weighted average cost of capital (WACC) was in the higher range compared to other models considering renewable energy technologies. A lower WACC would lead to future savings being of higher importance today but also lead to a higher LCOH in a cost minimization problem of this kind. A high WACC could disfavor the implementation of excess production capacity and storage, as total costs are more heavily weighted by initial investments in electrolyzer and storage equipment. In contrast, less weight is distributed to production costs over the system lifetime. However, a higher

WACC would also make other costs, such as cell-stack replacements and grid-fees, more impactful on the total costs; thus, counteracting some of the effects. The possibility to exploit debt leverage, as opposed to 100% equity, could also spread parts of the initial investment across the system lifetime, providing cheaper financing. Other research could benefit from different financial estimates, especially as hydrogen technology's private and public economics differentiates.

Implications of uncertain parameter values

Throughout the thesis, we have developed a model that is dependent on several different parameters that reflect the process of hydrogen production through water electrolysis. We have sought to provide the reader with a transparent view of how we have gathered the information and have mostly operated within the boundaries of parameter values proposed by other researchers and institutions. However, we have not performed a sensitivity analysis to investigate the effect of changing specific parameters. Thus, it is possible that using different parameter values and changing specific parameters separately can lead to other findings than the ones presented in this thesis.

External validity

We have developed a general framework based on electricity prices and grid fees for the NO2 region of the Nord Pool market. There are, however, some aspects regarding the external validity that has to be considered. First and foremost, electricity prices vary heavily between different nations, regions, seasons – and the amount of savings that can be achieved through production flexibility is highly dependent on the patterns of electricity prices. Second, the results are also based on grid fees for the Nord Pool NO2 region in specific and may vary between different regions and other countries or areas. Also, the price level of grid fees today may not be representative of future grid costs.

7.2 Further work

We propose some interesting topics within hydrogen production and the effect of excess production capacity combined with storage, which we could not include in this thesis.

We found excess production capacity and storage to be a beneficial combination under some circumstances. However, the uncertainty of electricity prices could make long-term

scheduling challenging. An interesting topic would be to explore strategies on how plants with excess production capacity and storage could schedule production based on the day-ahead prices. Historical data could suggest a general production schedule today. Additionally, a plant could adjust today's production schedule based on day-ahead prices. Higher prices or fewer fluctuations tomorrow might influence today's production. Thus, exploring if the proposed strategies in this thesis would yield prosperous results, also when the future electricity prices are unknown to the system. A possibility could also be to implement a training and test set of electricity price data, compare the results of a given system size and investigate how or if the results differ substantially in some direction compared to the findings in this thesis.

It is also a need to determine a long-term, economic equilibrium of the energy generation mix. Hence, another interesting research question would be how a renewable energy producer, combined with water electrolysis, hydrogen storage, and fuel-cells, has to choose between different strategies. The strategy could consist of three possibilities, in which a renewable energy producer could either (1) sell electricity directly, (2) produce hydrogen at low-cost electricity and use fuel-cells to convert back to electricity for sale at peak hours, or (3) produce hydrogen at low-cost electricity and sell the hydrogen as a commodity. The establishment of a long-term equilibrium would be of importance to determine the economic viability of future technologies.

We also mentioned the possibility of exploiting flexible hydrogen production to provide grid balancing in the future. However, the topic can be explored in further detail in terms of socioeconomic benefits or competitiveness compared to batteries.

Lastly, it could be of interest to perform a detailed sensitivity analysis for a similar model to better understand the importance of the different parameters on the cost of hydrogen production, especially in regards to how they affect the possibilities of overproduction and storage of H_2 . If other researchers are to perform a sensitivity analysis on important parameters in a similar case, we believe that the effects of changing efficiency should be investigated, as this has a great significance on the production costs, which again is the most consequential effect on LCOH. Other possible parameters to perform a sensitivity analysis for are electrolyzer CAPEX – along with the scaling exponent for electrolyzer equipment; Storage CAPEX – mainly underground storage together with investigating

possibilities for economy of scale for underground storage and how even larger underground facilities can affect the LCOH for large production plants; and possibly an even more detailed scenario analysis of the electricity prices – in which it could be interesting to test if the distribution of the cheap and expensive hours within a day, week, month, or year, affect the results.

8 Conclusion

Throughout the thesis, we have performed steps in developing a multi-period optimization model to schedule hydrogen production from alkaline water electrolysis across the system's lifetime. The purpose was to determine the most cost-efficient combination of production and storage capacity to minimize overall costs by exploiting electricity price fluctuations and avoid production during peak hours. A scenario analysis, represented by different time horizons, was performed to establish the current and future potential for excess production capacity combined with two different storage methods – tanks or underground.

The strategy of investing in excess production capacity to concentrate hydrogen production to hours of low-cost electricity proved costly. In many short and medium-term cases, it did not lead to overall cost reductions. Nevertheless, increased electricity price fluctuations and lower capital expenditure makes flexible hydrogen production schedules more attractive.

The results showed that it was preferable to invest in storage capacity in all scenarios. However, only some excess production capacity, combined with storage, was necessary to shave the most prominent electricity price peaks. Given a flat delivery commitment of 40 tonnes H₂/day, increasing the storage capacity from 0 to 3,000 kg led to a decrease in LCOH of 0.79% in a future scenario. Increasing the daily production capacity to 60 tonnes and combining it with 30 tonnes of storage, thus achieving the maximal amount of flexibility, increased the LCOH by 2.25%. Achieving such a large degree of production flexibility, without a substantial increase in overall costs, can lead to the possibility for a water electrolysis plant to gain additional revenues through other channels, such as providing grid balancing or by acting as insurance directly to renewable energy generators, using excess energy during hours of overproduction.

The optimal option, across all scenarios, was found when underground storage was combined with excess production capacity. A 6.8% increase in production capacity alone led to a decrease in LCOH of 0.3%. When assuming a different cost structure for grid fees, a 36% increase in production capacity led to a decrease in LCOH of 1.85% in the same scenario.

References

- Abe, J., Popoola, A., Ajenifuja, E., and Popoola, O. (2019). Hydrogen energy, economy and storage: Review and recommendation. *International Journal of Hydrogen Energy*, 44(29):15072 – 15086.
- Adam Christensen (2020). Assessment of Hydrogen Production Costs from Electrolysis: United States and Europe. Technical report, The International Council on Clean Transportation.
- AEN (2020). Priser og betalbare tjenester (rates and payable services). Accessed 21.11.2020 from <https://www.aenett.no/kundeforhold/kundebetingelser/kundebetingelser-bedriftskunde/tariffer-og-betalbare-tjenester/>.
- Ahluwalia, R., Papadias, D., Peng, J.-K., and Roh, H. (2019). System level analysis of hydrogen storage options. Accessed 07.12.2020 from https://www.hydrogen.energy.gov/pdfs/review19/st001_ahluwalia_2019_o.pdf.
- AMPL (2020). AMPL API. Accessed 03.02.2021 from <https://ampl.com/products/api/>.
- Berk, J. and DeMarzo, P. (2017). *Corporate Finance, Global Edition*. Pearson Education.
- Bray, N. (2017). Space applications of hydrogen and fuel cells. Accessed 08.12.2020 from <https://www.nasa.gov/content/space-applications-of-hydrogen-and-fuel-cells>.
- Brynolf, S., Taljegard, M., Grahn, M., and Hansson, J. (2018). Electrofuels for the transport sector: A review of production costs. *Renewable and Sustainable Energy Reviews*, 81:1887 – 1905.
- Buttler, A. and Spliethoff, H. (2018). Current status of water electrolysis for energy storage, grid balancing and sector coupling via power-to-gas and power-to-liquids: A review. *Renewable and Sustainable Energy Reviews*, 82:2440 – 2454.
- Caglayan, D. G., Weber, N., Heinrichs, H. U., Linßen, J., Robinius, M., Kukla, P. A., and Stolten, D. (2020). Technical potential of salt caverns for hydrogen storage in europe. *International Journal of Hydrogen Energy*, 45(11):6793 – 6805.
- Castetter, T. (2019). Hydrogen fuel cell forklifts: An alternative energy solution. Accessed 08.12.2020 from <https://www.toyotaforklift.com/blog/hydrogen-fuel-cell-forklifts-an-alternative-energy-solution>.
- Crotogino, F. (2016). Chapter 19 - traditional bulk energy storage—coal and underground natural gas and oil storage. In Letcher, T. M., editor, *Storing Energy*, pages 391 – 409. Elsevier, Oxford.
- Dagdougui, H., Sacile, R., Bersani, C., and Ouammi, A. (2018). Chapter 4 - hydrogen storage and distribution: Implementation scenarios. In Dagdougui, H., Sacile, R., Bersani, C., and Ouammi, A., editors, *Hydrogen Infrastructure for Energy Applications*, pages 37 – 52. Academic Press.
- Damodaran, A. (2020). Cost of capital by industry sector; europe. Accessed 11.12.2020

- from
<http://pages.stern.nyu.edu/~adamodar/>.
- De-León Almaraz, S. and Azzaro-Pantel, C. (2017). Chapter 4 - design and optimization of hydrogen supply chains for a sustainable future. In Scipioni, A., Manzardo, A., and Ren, J., editors, *Hydrogen Economy*, pages 85 – 120. Academic Press.
- DNV GL (2019). Produksjon og bruk av hydrogen i norge. Published January 2019.
- Ereev, S. Y. and Patel, M. (2012). Standardized cost estimation for new technology (scent) - methodology and tool. *Journal of Business Chemistry*, 9:31–48.
- EU Commission (2020). A hydrogen strategy for a climate-neutral europe. Accessed 27.11.2020 from
https://ec.europa.eu/energy/sites/ener/files/hydrogen_strategy.pdf.
- European Commission (2016). The EU Emission Trading System (EU ETS).
- Forskrift om særavgifter (2001). For-2001-12-11-1451. Accessed 7.12.2020 from
<https://lovdata.no/dokument/SF/forskrift/2001-12-11-1451>.
- Gorre, J., van Leeuwen, C., and Ortloff, F. (2019). Report on the optimal time profile and operation of the conversion technology during a representative year, in the perspective of the available storage capacities. Accessed 12.12.2020 from
<https://ec.europa.eu/research/participants/documents/downloadPublic?documentIds=080166e5c1ae5cb2&appId=PPGMS>.
- Hanan Luss (1982). Operations research and capacity expansion problems: A survey. *Operations Research*, 30(5):907 – 947.
- Houchins, C. and James, B. (2017). Hydrogen storage system cost analysis: Summary of fy 2017 activities sponsorship and acknowledgements. Technical report, Strategic Analysis, Inc.
- Houmøller, A. P. (2017). Chapter 5 - scandinavian experience of integrating wind generation in electricity markets. In Jones, L. E., editor, *Renewable Energy Integration (Second Edition)*, pages 55 – 68. Academic Press, Boston, second edition edition.
- Hydrogen Europe (2017). Hydrogen applications. Accessed 08.12.2020 from
<https://www.hydrogeneurope.eu/hydrogen-applications>.
- IEA (2019). The Future of Hydrogen: Seizing Today’s Opportunities. Published June 2019.
- IRENA (2019). Hydrogen: A renewable energy perspective. Published September 2019.
- Kane, M. (2020). Hydrogen fuel cell car sales in 2019 improved to 7,500 globally. Accessed 08.12.2020 from
<https://insideevs.com/news/397240/hydrogen-fuel-cell-sales-2019-7500-globally/>.
- Kaut, M., Flatberg, T., and Ortiz, M. M. (2019). The hyopt model: Input data and the mathematical formulation. Accessed 1.12.2020 from
<https://sintef.brage.unit.no/sintef-xmlui/handle/11250/2643389>.
- Keçebaş, A., Kayfeci, M., and Bayat, M. (2019). Chapter 9 - electrochemical hydrogen

- generation. In Calise, F., D'Accadia, M. D., Santarelli, M., Lanzini, A., and Ferrero, D., editors, *Solar Hydrogen Production*, pages 299 – 317. Academic Press.
- Khalilpour, K. R. (2019). Chapter 5 - interconnected electricity and natural gas supply chains: The roles of power to gas and gas to power. In Khalilpour, K. R., editor, *Polygeneration with Polystorage for Chemical and Energy Hubs*, pages 133–155. Academic Press.
- Kharel, S. and Shabani, B. (2018). Hydrogen as a long-term large-scale energy storage solution to support renewables. *Energies*, 10:1–17.
- Kotzur, L., Markewitz, P., Robinius, M., and Stolten, D. (2018). Time series aggregation for energy system design: Modeling seasonal storage. *Applied Energy*, 213:123 – 135.
- Kruck, O., Crotogino, F., Prelicz, R., and Rudolph, T. (2013). Overview on all known underground storage technologies for hydrogen: Assessment of the potential, the actors and relevant business cases for large scale and seasonal storage of renewable electricity by hydrogen underground storage in europe. <http://hyunder.eu/>.
- Kuckshinrichs, W., Ketelaer, T., and Koj, J. (2017). Economic Analysis of Improved Alkaline Water Electrolysis. *Frontiers in Energy Research*, 5:1.
- Larrosa, J., Oliveras, A., and Rodriguez-Carbonell, E. (2020). Mixed integer linear programming: Combinatorial problem solving (cps).
- Le Duigou, A., Bader, A.-G., Lanoix, J.-C., and Nadau, L. (2017). Relevance and costs of large scale underground hydrogen storage in france. *International Journal of Hydrogen Energy*, 42(36):22987 – 23003.
- Ligen, Y., Vrubel, H., and Girault, H. (2020). Energy efficient hydrogen drying and purification for fuel cell vehicles. *International Journal of Hydrogen Energy*, 45(18):10639 – 10647.
- Lord, A. S., Kobos, P. H., and Borns, D. J. (2014). Geologic storage of hydrogen: Scaling up to meet city transportation demands. *International Journal of Hydrogen Energy*, 39(28):15570 – 15582.
- Makridis, S. S. (2016). Hydrogen storage and compression. <https://arxiv.org/ftp/arxiv/papers/1702/1702.06015.pdf>.
- Matute, G., Yusta, J., Beyza, J., and Correas, L. (2020). Multi-state techno-economic model for optimal dispatch of grid connected hydrogen electrolysis systems operating under dynamic conditions. *International Journal of Hydrogen Energy*.
- Matute, G., Yusta, J., and Correas, L. (2019). Techno-economic modelling of water electrolyzers in the range of several mw to provide grid services while generating hydrogen for different applications: A case study in spain applied to mobility with fcevs. *International Journal of Hydrogen Energy*, 44(33):17431 – 17442.
- Mayyas, A. and Mann, M. (2019). Manufacturing competitiveness analysis for hydrogen refueling stations. *International Journal of Hydrogen Energy*, 44(18):9121 – 9142.
- Mayyas, A., Wei, M., and Levis, G. (2020). Hydrogen as a long-term, large-scale energy storage solution when coupled with renewable energy sources or grids with dynamic

- electricity pricing schemes. *International Journal of Hydrogen Energy*, 45(33):16311 – 16325.
- Mazloomi, K. and Gomes, C. (2012). Hydrogen as an energy carrier: Prospects and challenges. *Renewable and Sustainable Energy Reviews*, 16:3024–3033.
- Michalski, J., Bünger, U., Crotogino, F., Donadei, S., Schneider, G.-S., Pregger, T., Cao, K.-K., and Heide, D. (2017). Hydrogen generation by electrolysis and storage in salt caverns: Potentials, economics and systems aspects with regard to the german energy transition. *International Journal of Hydrogen Energy*, 42(19):13427 – 13443. Special Issue on The 21st World Hydrogen Energy Conference (WHEC 2016), 13-16 June 2016, Zaragoza, Spain.
- Ministry of Climate and Enviroment (2020). Slutterm seg på europeisk satsing på hydrogen. Accessed 10.12.2020 from <https://www.regjeringen.no/no/aktuelt/slutterm-seg-til-europeisk-satsing-pa-hydrogen/id2790732/>.
- Ministry of Finance (2019). Skattesatser 2020 (tax rates 2020). Accessed 7.12.2020 from <https://www.regjeringen.no/no/tema/okonomi-og-budsjett/skatter-og-avgifter/skattesatser-2020/id2671009/>.
- Møller, K. T., Jensen, T. R., Akiba, E., and wen Li, H. (2017). Hydrogen - a sustainable energy carrier. *Progress in Natural Science: Materials International*, 27(1):34 – 40. SI-HYDROGEN STORAGE MATERIALS.
- NEL (2019). Nel hydrogen electrolyzers: The world’s most efficient and reliable electrolyzers. Accessed 04.12.2020 from <https://nelhydrogen.com/wp-content/uploads/2020/03/Electrolyzers-Brochure-Rev-C.pdf>.
- NEL (2020). Atmospheric ALkaline Electrolyzer. Accessed 10.10.2020 from <https://nelhydrogen.com/product/atmospheric-alkaline-electrolyser-a-series/>.
- Nguyen, T., Abdin, Z., Holm, T., and Mérida, W. (2019). Grid-connected hydrogen production via large-scale water electrolysis. *Energy Conversion and Management*, 200:112108.
- Nord Pool (2020). Day-ahead market. Accessed 15.12.2020 from <https://www.nordpoolgroup.com/the-power-market/Day-ahead-market/>.
- Norges Bank (2020). Inflasjon. Accessed 25.11.2020 from <https://www.norges-bank.no/tema/pengepolitikk/Inflasjon/>.
- NVE (2016). The wacc-model. Accessed 17.11.2020 from <https://www.nve.no/norwegian-energy-regulatory-authority/economic-regulation/the-wacc-model/>.
- NVE (2019). Nettleie (grid fee). Accessed 21.11.2020 from <https://www.nve.no/stromkunde/nettleie/>.
- NVE (2020a). Langsiktig kraftmarksanalyse 2020-2040: Mer fornybar kraftproduksjon gir mer væravhengige kraftpriser. Published October 2020.

- NVE (2020b). Utkobbar tariff. Accessed 19.01.2021 from <https://www.nve.no/reguleringsmyndigheten/nettjenester/nettleie/nettleie-for-forbruk/utkobbar-forbruk/>.
- Pedroso, R. and Picheta, R. (2021). Oxygen shortage forces evacuation of 60 premature babies from amazon city. Accessed 22.01.2021 from <https://edition.cnn.com/2021/01/15/americas/brazil-amazon-coronavirus-evacuation-intl/index.html>.
- Pellow, M., Emmott, C., Barnhart, C., and Benson, S. (2015). Hydrogen or batteries for grid storage? a net energy analysis. *Energy Environ. Sci.*, 8.
- Poncelet, K. (2018). *Long-term energy-system optimization models - Capturing the challenges of integrating intermittent renewable energy sources and assessing the suitability for descriptive scenario analyses*. PhD thesis, Arenberg Doctoral School, Faculty of Engineering Science.
- Proost, J. (2019). State-of-the art capex data for water electrolyzers, and their impact on renewable hydrogen price settings. *International Journal of Hydrogen Energy*, 44(9):4406 – 4413. European Fuel Cell Conference & Exhibition 2017.
- Rashid, M., Naseem, H., Kaloofa al Mesfer, M., and Danish, M. (2015). Hydrogen production by water electrolysis: A review of alkaline water electrolysis, pem water electrolysis and high temperature water electrolysis. *International Journal of Engineering and Advanced Technology*, 4(3):81.
- Rösler, H., van der Zwaan, B., Keppo, I., and Bruggink, J. (2014). Electricity versus hydrogen for passenger cars under stringent climate change control. *Sustainable Energy Technologies and Assessments*, 5:106 – 118.
- Schulte Beerbühl, S., Fröhling, M., and Schultmann, F. (2015). Combined scheduling and capacity planning of electricity-based ammonia production to integrate renewable energies. *European Journal of Operational Research*, 241(3):851 – 862.
- Sheffield, J., Martin, K., and Folkson, R. (2014). 5 - electricity and hydrogen as energy vectors for transportation vehicles. In Folkson, R., editor, *Alternative Fuels and Advanced Vehicle Technologies for Improved Environmental Performance*, pages 117 – 137. Woodhead Publishing.
- Shiva Kumar, S. and Himabindu, V. (2019). Hydrogen production by pem water electrolysis – a review. *Materials Science for Energy Technologies*, 2(3):442 – 454.
- Siemens Gamesa (2020). Siemens gamesa and siemens energy to unlock a new era of offshore green hydrogen production. Accessed 13.01.2021 from <https://www.siemensgamesa.com/newsroom/2021/01/210113-siemens-gamesa-press-release-siemens-energy-agreement-green-hydrogen>.
- Statnett (2020). Langsiktig markedsanalyse: Norden og Europa 2020-2050. Published October 2020.
- Steilen, M. and Jörissen, L. (2015). Chapter 10 - hydrogen conversion into electricity and thermal energy by fuel cells: Use of h₂-systems and batteries. In Moseley, P. T. and Garche, J., editors, *Electrochemical Energy Storage for Renewable Sources and Grid Balancing*, pages 143 – 158. Elsevier, Amsterdam.

- Tarkowski, R. (2019). Underground hydrogen storage: Characteristics and prospects. *Renewable and Sustainable Energy Reviews*, 105:86 – 94.
- Urbanucci, L. (2018). Limits and potentials of mixed integer linear programming methods for optimization of polygeneration energy systems. *Energy Procedia*, 148:1199 – 1205. ATI 2018 - 73rd Conference of the Italian Thermal Machines Engineering Association.
- U.S. Department of energy (2015). Energy efficiency & renewable energy: Fuel cell technologies office. Accessed 19.01.2021 from https://www.energy.gov/sites/prod/files/2015/11/f27/fcto_fuel_cells_fact_sheet.pdf.
- Vogl, V., Åhman, M., and Nilsson, L. J. (2018). Assessment of hydrogen direct reduction for fossil-free steelmaking. *Journal of Cleaner Production*, 203:736 – 745.
- Wolff, G. and Feuerriegel, S. (2019). Emissions trading system of the european union: Emission allowances and epeex electricity prices in phase iii. *Energies*, 12:2894.
- Yates, J., Daiyan, R., Patterson, R., Egan, R., Amal, R., Ho-Baille, A., and Chang, N. L. (2020). Techno-economic analysis of hydrogen electrolysis from off-grid stand-alone photovoltaics incorporating uncertainty analysis. *Cell Reports Physical Science*, 1(10):100209.
- Zacharia, R. and Rather, S. U. (2015). Review of solid state hydrogen storage methods adopting different kinds of novel materials. *Journal of Nanomaterials*, 2015:1–18.
- Ziazi, R., Mohammadi, K., and Goudarzi, N. (2017). Techno-economic assessment of utilizing wind energy for hydrogen production through electrolysis.

Appendix

A1 Figures

A1.1 Statnett mentions

Statnett publish a long term market analysis report every 2 years, in which mentions of the word hydrogen have increased from 13 to 238 in the latest reports.

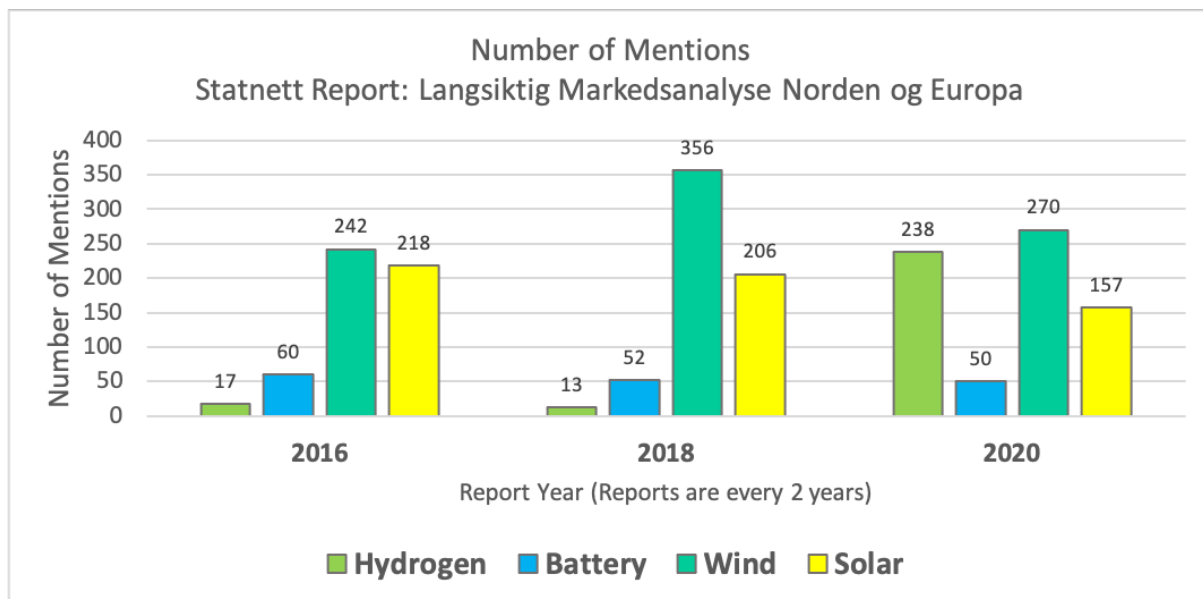


Figure A1.1: Greensight AS' overview of mentions in Statnett reports.

A2 Data

A2.1 Statnett estimates

Table A2.1: Statnett estimations for future electricity price in Nordic regions. Published 26.10.2020 in Statnetts's long term market analysis.

		Electricity prices in the Nordic countries by area [€/MWh]:			
		2020	2025	2030	2040
Sørøst-Norge (NO1)	Basis	29.00	33.00	36.00	40.00
Sørvest-Norge (NO2)	Basis	28.00	34.00	36.00	39.00
Midt-Norge (NO3)	Basis	28.00	28.00	33.00	39.00
Nord-Norge (NO4)	Basis	27.00	25.00	31.00	38.00
Vest-Norge (NO5)	Basis	29.00	35.00	37.00	41.00
Svergie Nord (SE2)	Basis	28.00	26.00	30.00	38.00
Svergie Sør (SE3)	Basis	30.00	31.00	35.00	42.00
Danmark	Basis	29.00	35.00	40.00	41.00

A2.2 NVE estimates

Table A2.2: NVE estimations for future electricity price in Nordic regions. Published 28.10.2020 in NVE's long term power market analysis.

		Electricity prices in Norway by area [øre/kWh]:				
Scenario	NO1	NO2	NO3	NO4	NO5	
B2022	39.33	39.78	36.76	33.37	38.65	
B2025	43.63	44.01	41.40	36.88	43.45	
B2030	41.09	41.98	36.98	34.23	40.58	
B2040	43.02	42.51	40.19	35.39	42.41	
L2022	30.65	30.96	28.68	25.84	30.11	
L2025	32.19	32.45	30.40	26.88	32.03	
L2030	28.26	28.89	25.31	23.44	27.89	
L2040	25.97	25.62	24.10	21.14	25.56	
H2022	45.81	46.40	42.31	38.19	44.90	
H2025	51.03	51.50	48.25	43.03	50.79	
H2030	47.83	48.96	42.88	39.65	47.23	
H2040	50.47	49.88	47.16	41.51	49.76	

A3 Parameter comparison

Table A3.1: Overview of alkaline water electrolysis costs and parameters drawn from different studies, reports and organisations. Published year is used in cases where year of estimation is not specified.

Parameter	Value	Year	Comment	Reference
Elec CAPEX	500 - 1400 \$/kW	Today	-	IEA (2019)
Elec CAPEX	400 - 850 \$/kW	2030	-	IEA (2019)
Elec CAPEX	200 - 700 \$/kW	Long term	-	IEA (2019)
Elec CAPEX	800 - 1500 €/kW	2018	-	Buttler and Spliethoff (2018)
Elec CAPEX	571 - 1268 \$/kW	2020	-	Adam Christensen (2020)
Elec CAPEX	830 €/kW	2017	-	Matute et al. (2019)
Elec CAPEX	600 €/kW	2025	-	Matute et al. (2019)
Elec CAPEX	682 - 886 \$/kW	2020	At 1000 kW	Yates et al. (2020)
Elec CAPEX	1100 €/kW	2018	-	Brynnolf et al. (2018)
Elec CAPEX	400-900 €/kW	Future	-	Brynnolf et al. (2018)
Elec CAPEX	840 \$/kW	Today	-	IRENA (2019)
Elec CAPEX	200 \$/kW	Future	-	IRENA (2019)
Elec CAPEX	€1 million/tonne	Today	Correspondence	Greensight AS
Storage cost (tank)	333 \$/kg	2020	US DOE goal	Abe et al. (2019)
Storage cost (tank)	300 \$/kg	2025	US DOE goal	Abe et al. (2019)
Storage cost (tank)	266 \$/kg	Ultimate	US DOE goal	Abe et al. (2019)
Storage cost (tank)	438 \$/kg	2018	-	Kharel and Shabani (2018)
Storage cost (tank)	397 - 557 €/kg	2019	-	Mayyas and Mann (2019)
Storage cost (tank)	276 - 453 €/kg	2017	-	Houchins and James (2017)
Storage cost (tank)	€500 000/1.1 tonne	Today	Correspondence	Greensight AS
Storage cost (underground)	7.02 €/kg	2013	Green Fields Design (salt cavern)	Kruck et al. (2013)
Storage cost (underground)	33.08 €/kg	2014	Derived from CAPEX and capacity	Lord et al. (2014)
Storage cost (underground)	0.1 - 10 €/kg	2017	From "The use of hydrogen as a massive electricity storage means" by ALPHEA	Le Duigou et al. (2017)

Table A3.2: Continuation of Table A3.1.

Parameter	Value	Year	Comment	Reference
Efficiency	63 - 70%	Today	LHV (stack)	IEA (2019)
Efficiency	65 - 71%	2030	LHV (stack)	IEA (2019)
Efficiency	70 - 80%	Long term	LHV (stack)	IEA (2019)
Efficiency	63 - 71%	2018	LHV (stack)	Buttler and Spliethoff (2018)
Efficiency	51 - 60%	2018	LHV (system)	Buttler and Spliethoff (2018)
Efficiency	70%	2020	LHV (stack)	Adam Christensen (2020)
Efficiency	80%	2050	LHV (stack)	Adam Christensen (2020)
Efficiency	52 kWh/kg	2017	System	Matute et al. (2019)
Efficiency	50 kWh/kg	2017	System	Matute et al. (2019)
Efficiency	50 - 58 kWh/kg	2020	System	Yates et al. (2020)
Efficiency	62%	2019	HHV (stack)	Nguyen et al. (2019)
Efficiency	43-69%	2018	LHV (system)	Brynnolf et al. (2018)
Efficiency	50-74%	2030	LHV (system)	Brynnolf et al. (2018)
Efficiency	46 - 50 kWh/kg	Today	Correspondence	Greensight AS
Efficiency	44 - 48 kWh/kg	2025	Correspondence	Greensight AS
Efficiency	43 - 47 kWh/kg	2030	Correspondence	Greensight AS
Efficiency	3 kWh/kg	Today	Correspondence	Greensight AS
Efficiency	2.9 kWh/kg	2025	Correspondence	Greensight AS
Efficiency	2.7 kWh/kg	2030	Correspondence	Greensight AS
Compression (350-380 bar)	60 000 - 90 000 hours	Today	-	IEA (2019)
Compression (350-380 bar)	90 000 - 100 000 hours	2030	-	IEA (2019)
Compression (350-380 bar)	100 000 - 150 000 hours	Long term	-	IEA (2019)
Stack lifetime	55 000 - 120 000 hours	2018	-	Buttler and Spliethoff (2018)
Stack lifetime	75 000 hours	2020	-	Adam Christensen (2020)
Stack lifetime	80 000 hours	2017	-	Matute et al. (2019)
Stack lifetime	80 000 hours	2025	-	Matute et al. (2019)
Stack lifetime	70 000 - 90 000 hours	2020	-	Yates et al. (2020)
Stack lifetime	80 000 hours	2019	-	Nguyen et al. (2019)
Stack lifetime	60 000 - 90 000 hours	2018	-	Brynnolf et al. (2018)
Stack lifetime	90 000 - 100 000 hours	2030	-	Brynnolf et al. (2018)
Stack lifetime	Approx. 10 years	Today	Correspondence	Greensight AS

Table A3.3: Continuation of Table A3.2.

Parameter	Value	Year	Comment	Reference
Stack replacement cost	380 €/kW	2017	-	Matute et al. (2019)
Stack replacement cost	270 €/kW	2025	-	Matute et al. (2019)
Stack replacement cost	35 - 45%	2020	Of capital cost	Yates et al. (2020)
Stack replacement cost	340 \$/kW	2019	-	Nguyen et al. (2019)
Stack replacement cost	50%	2018	Of capital cost	Brynnolf et al. (2018)
Stack replacement cost	35 - 40%	Today	Correspondence	Greensight AS
OPEX	2 - 3%	2018	Yearly	Buttler and Spliethoff (2018)
OPEX	13.6 - 20.5 \$/kW	2020	Yearly	Matute et al. (2019)
OPEX	2 - 5%	2018 and 2030	-	Brynnolf et al. (2018)
OPEX	3%	Today	Correspondence	Greensight AS
Minimum utilization	10%	Today	Maximum 110%	IEA (2019)
Minimum utilization	20%	2018	Maximum 100%	Buttler and Spliethoff (2018)
Minimum utilization	10%	2017/2025	-	Matute et al. (2019)
Minimum utilization	3 - 8%	2019	-	Nguyen et al. (2019)
Minimum utilization	30% (20 - 40%)	2018	-	Brynnolf et al. (2018)
Minimum utilization	10 - 20%	2030	-	Brynnolf et al. (2018)
Minimum utilization	15%	Today	Correspondence	Greensight AS
Degradation	0.1 - 0.5%	2020	Yearly	Yates et al. (2020)
Degradation	0.25 - 1.5%	2018	Yearly	Buttler and Spliethoff (2018)
Degradation	0.7 - 1.2%	Today	Correspondence	Greensight AS

A4 CAPEX specifications in scenarios 1-5

A4.1 Scenario 1

Capital expenditure for alkaline electrolyzer equipment today is in the range of 850-2,628 k€/tonne daily production capacity, depending on system size (CAPEX: 425-1,190 €/kW, spec. energy. cons: 48-53 kWh/kg) (IEA, 2019). Table A4.1 illustrates CAPEX for different capacities in scenario 1.

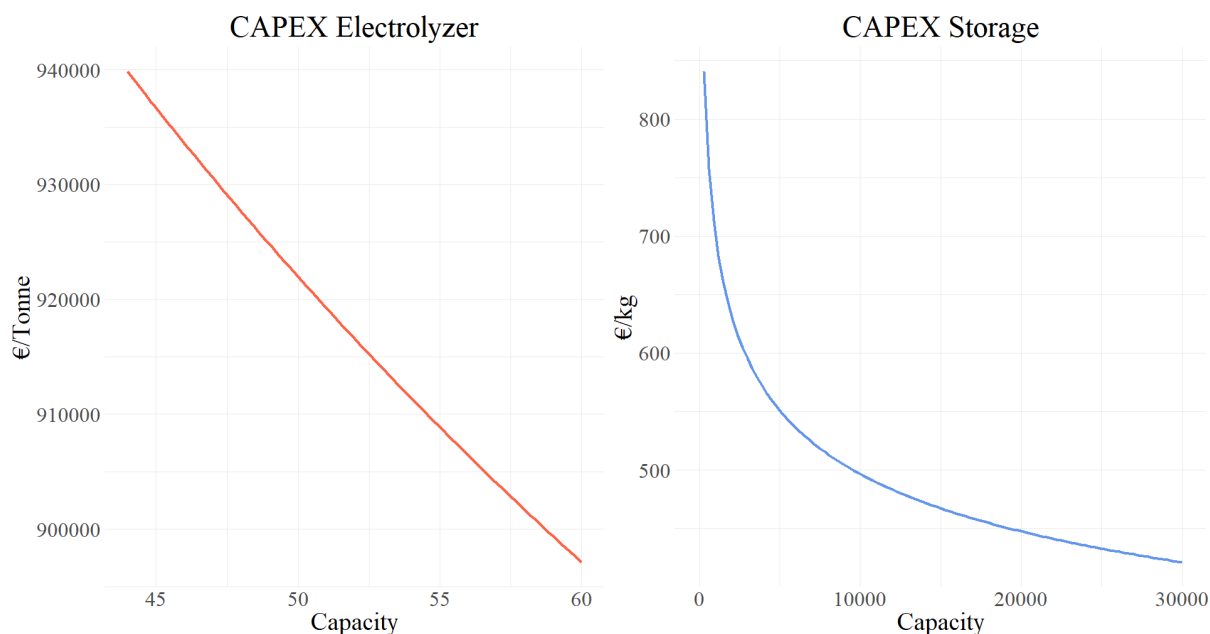


Figure A4.1: Electrolyzer and storage CAPEX based on system size in scenario 1.

A4.2 Scenario 2

Capital expenditure for alkaline electrolyzer equipment today is expected to be in the range of 666-1,536 k€/tonne daily production capacity in 2030 (CAPEX: 340-723 €/kW, spec. energy. cons: 47-51 kWh/kg) (IEA, 2019). Figure A4.2 illustrates CAPEX for different capacities in scenario 2.

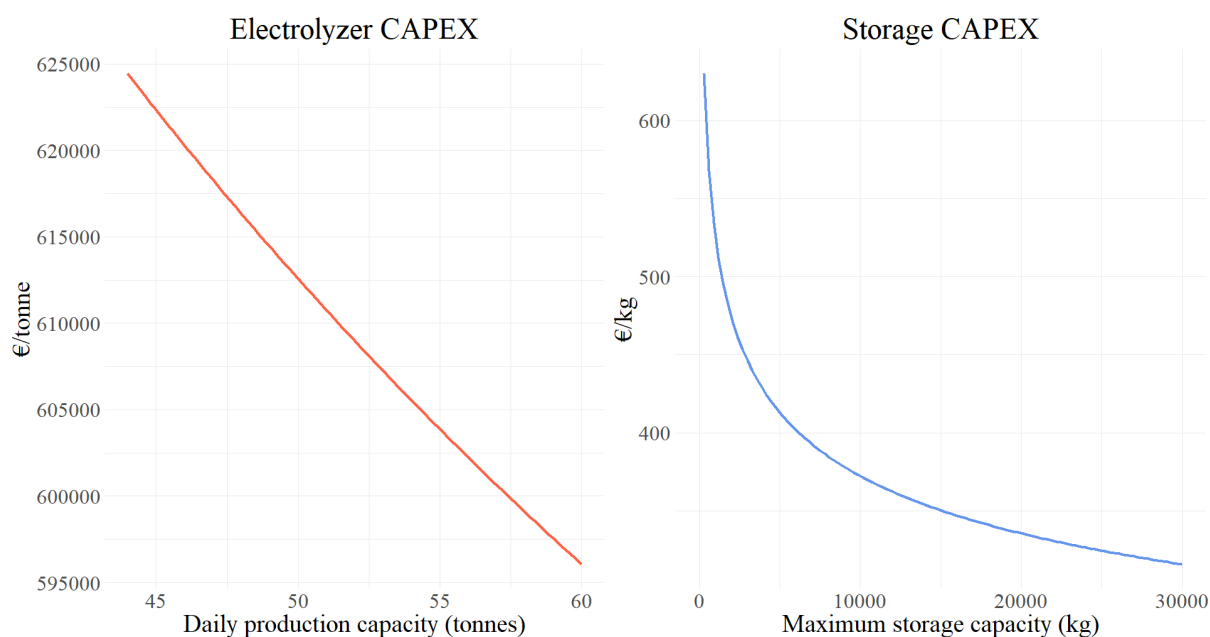


Figure A4.2: Electrolyzer and storage CAPEX based on system size in scenario 2.

A4.3 Scenario 3

Capital expenditure for alkaline electrolyzer equipment today is expected to be in the range of 298-1,190 k€/tonne daily production capacity in the long term (CAPEX: 170-595 €/kW, spec. energy. cons: 42-48 kWh/kg) (IEA, 2019). Figure A4.3 illustrates CAPEX for different capacities in scenario 3.

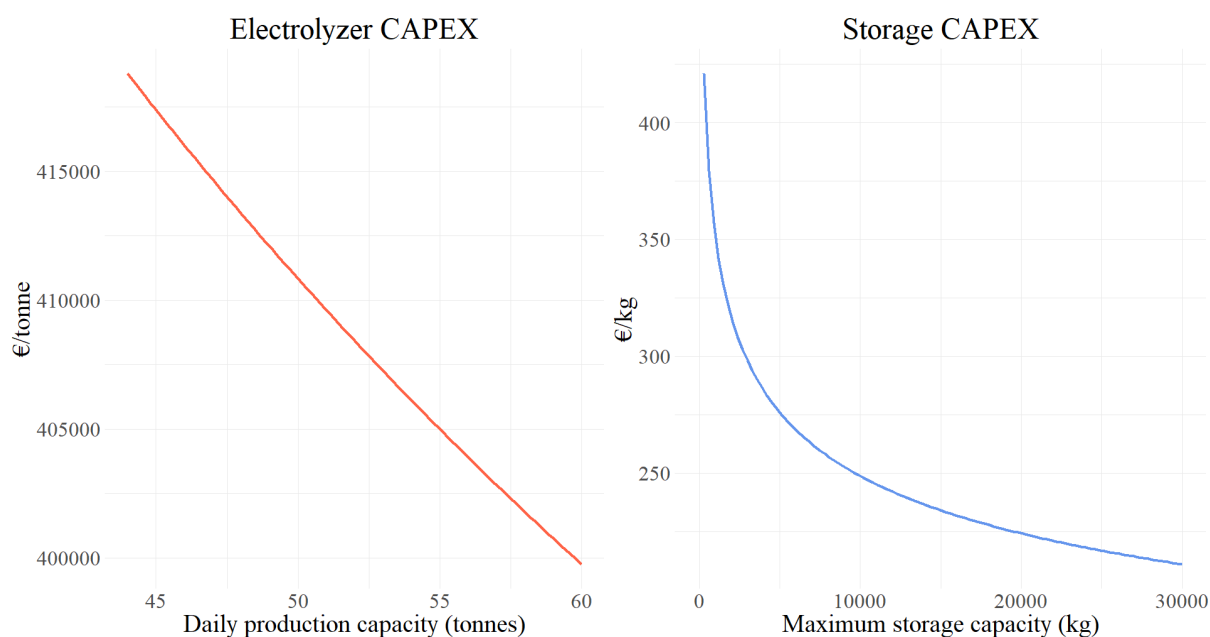


Figure A4.3: Electrolyzer and storage CAPEX based on system size in scenario 3.

A4.4 Scenario 4

Capital expenditure in scenario 4 is the same as in scenario 2.

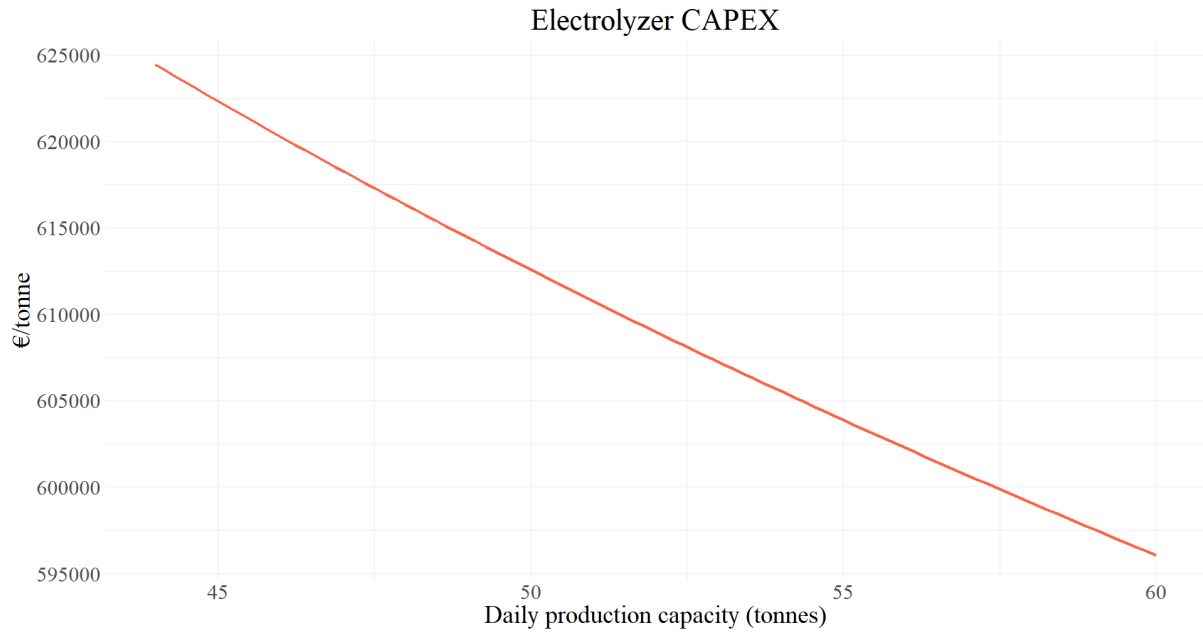


Figure A4.4: Electrolyzer CAPEX based on system size in scenario 4.

A4.5 Scenario 5

Capital expenditure in scenario 5 is the same as in scenario 3.

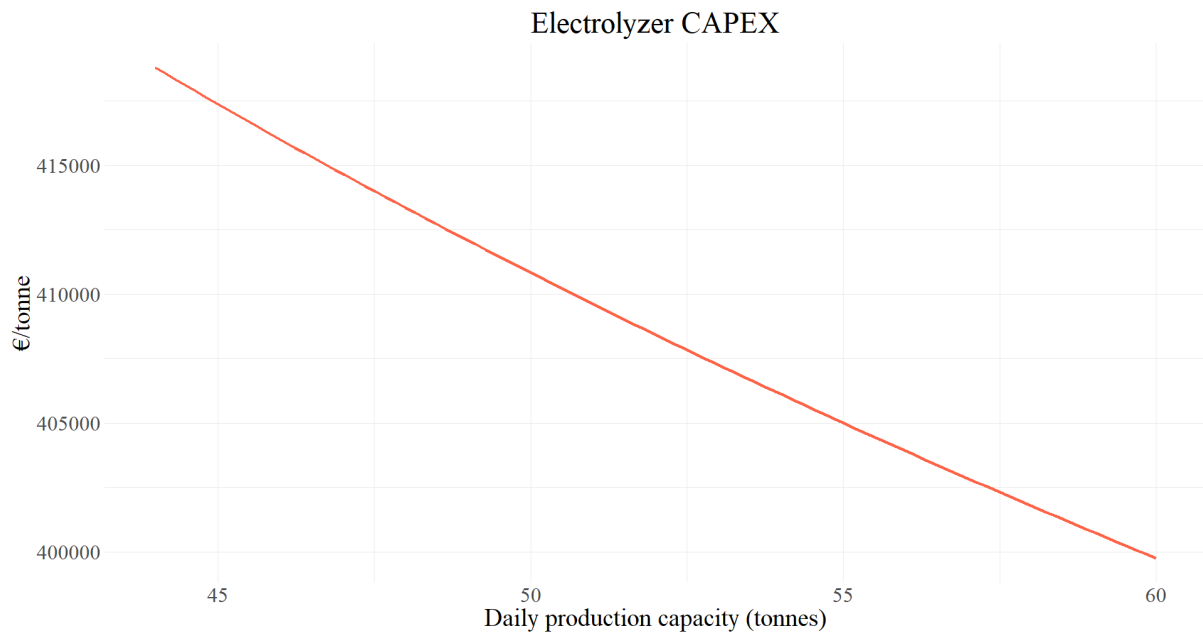


Figure A4.5: Electrolyzer CAPEX based on system size in scenario 5.

A5 LCOH when neglecting grid fees in scenarios 1-5

The following tables presents LCOH in scenarios 1-5 when grid fees are neglected. Each column in a table represent production capacity (tonne) while each row represent storage capacity (kg).

A5.1 Scenario 1

Table A5.1: LCOH (€/kg) in scenario 1 (neglecting grid fees).

	44	46	48	50	52	54	56	58	60
0	2.732	2.750	2.769	2.787	2.805	2.824	2.842	2.859	2.877
3000	2.717	2.722	2.731	2.741	2.754	2.769	2.784	2.800	2.817
6000	2.726	2.729	2.734	2.741	2.749	2.759	2.769	2.781	2.793
9000	2.736	2.737	2.742	2.748	2.756	2.764	2.774	2.783	2.794
12000	2.747	2.746	2.750	2.756	2.763	2.772	2.780	2.790	2.800
15000	2.757	2.756	2.759	2.764	2.771	2.779	2.788	2.797	2.807
18000	2.768	2.766	2.768	2.773	2.779	2.787	2.796	2.805	2.814
21000	2.779	2.777	2.778	2.782	2.788	2.795	2.803	2.812	2.821
24000	2.789	2.787	2.788	2.791	2.796	2.803	2.811	2.820	2.829
27000	2.799	2.797	2.798	2.801	2.806	2.812	2.819	2.828	2.837
30000	2.809	2.807	2.808	2.811	2.815	2.821	2.828	2.836	2.845

A5.2 Scenario 2

Table A5.2: LCOH (€/kg) in scenario 2 (neglecting grid fees).

	44	46	48	50	52	54	56	58	60
0	2.390	2.403	2.415	2.427	2.439	2.451	2.462	2.474	2.486
3000	2.379	2.381	2.385	2.391	2.399	2.408	2.418	2.428	2.439
6000	2.385	2.385	2.387	2.391	2.395	2.400	2.406	2.413	2.420
9000	2.392	2.391	2.393	2.396	2.400	2.404	2.409	2.415	2.421
12000	2.400	2.398	2.399	2.402	2.406	2.410	2.414	2.420	2.425
15000	2.409	2.405	2.406	2.408	2.411	2.416	2.420	2.425	2.431
18000	2.417	2.413	2.413	2.414	2.417	2.421	2.426	2.431	2.436
21000	2.425	2.421	2.420	2.421	2.424	2.428	2.432	2.437	2.442
24000	2.432	2.429	2.427	2.428	2.430	2.434	2.438	2.443	2.448
27000	2.440	2.436	2.435	2.435	2.437	2.44	2.444	2.449	2.454
30000	2.448	2.444	2.442	2.443	2.444	2.447	2.450	2.455	2.460

A5.3 Scenario 3

Table A5.3: LCOH (€/kg) in scenario 3 (neglecting grid fees).

	44	46	48	50	52	53	54	56	58	60
0	2.145	2.153	2.161	2.169	2.176	2.180	2.184	2.192	2.200	2.208
3000	2.125	2.121	2.120	2.121	2.124	2.126	2.129	2.134	2.140	2.147
6000	2.127	2.121	2.118	2.116	2.115	2.114	2.114	2.115	2.117	2.12
9000	2.131	2.123	2.120	2.117	2.116	2.115	2.115	2.115	2.115	2.116
12000	2.136	2.127	2.122	2.119	2.118	2.117	2.117	2.116	2.117	2.117
15000	2.141	2.131	2.125	2.122	2.120	2.120	2.119	2.119	2.119	2.119
18000	2.146	2.136	2.129	2.125	2.123	2.122	2.122	2.121	2.121	2.121
21000	2.151	2.141	2.134	2.129	2.126	2.126	2.125	2.124	2.124	2.124
24000	2.156	2.146	2.139	2.134	2.130	2.129	2.128	2.127	2.127	2.127
27000	2.161	2.151	2.143	2.138	2.134	2.133	2.132	2.130	2.130	2.130
30000	2.166	2.156	2.148	2.143	2.139	2.137	2.136	2.134	2.133	2.133

A5.4 Scenario 4

Table A5.4: LCOH (€/kg) in scenario 4 (neglecting grid fees).

	44	46	48	50	52	54	56	58	60
500,000	2.358	2.352	2.350	2.351	2.352	2.355	2.358	2.361	2.365

A5.5 Scenario 5

Table A5.5: LCOH (€/kg) in scenario 5 (neglecting grid fees).

	44	46	48	50	52	54	56	58	60
500,000	2.103	2.090	2.081	2.076	2.072	2.069	2.067	2.065	2.064